

Copyright  
by  
Paul Blanton Kilgore  
2022

**The Dissertation Committee for Paul Kilgore Certifies that this is the approved  
version of the following dissertation:**

**Heterologous Prime-Boost strategies using live-attenuated and  
viral vector vaccines to combat pneumonic plague**

**Committee:**

---

Ashok Chopra, PhD, CSc, Mentor, Chair

---

Vladimir Motin, PhD

---

Johnny Peterson, PhD

---

Yingzi Cong, PhD

---

Matthieu Gagnon, PhD

---

Jason Rosenzweig, PhD

---

**Heterologous Prime-Boost strategies using live-attenuated and viral  
vector vaccines to combat pneumonic plague**

**by**

**Paul Blanton Kilgore, B.S.**

**Dissertation**

Presented to the Faculty of the Graduate School of

The University of Texas Medical Branch

in Partial Fulfillment

of the Requirements

for the Degree of

**Doctor of Philosophy**

**The University of Texas Medical Branch**

**July 2022**

## **Dedication**

To my friends, family, and dog who provided friendship and support along the way. This endeavor would not have been possible without them.

## **Acknowledgements**

I would like to thank Dr. Ashok Chopra for his patience, guidance, and support throughout my graduate studies in his lab. I would like to thank my committee members: Dr. Vladimir Motin, Dr. Johnny Peterson, Dr. Yingzi Cong, Dr. Matthieu Gagnon, and Dr. Jason Rosenzweig for their advice and input during my committee meetings. I would especially like to thank Dr. Motin for providing the recombinant plague antigens used in the investigation of individual antibody titers. I would like to thank Dr. Jian Sha for help designing and performing the studies. I would also like to thank the other members of the Chopra lab both past and present for encouragement and help with the experiments involved in these studies. I would also like to thank the Microbiology and Immunology program director Dr. Lynn Soong and coordinator Aneth Zertuche for guidance and assistance whenever I needed it during my graduate studies. I would like to thank the McLaughlin Foundation and T32 Biodefence Training Grant for providing funding support. Lastly, I would like to thank my friends and family for providing encouragement during this journey.

# **Heterologous Prime-Boost strategies using live-attenuated and viral vector vaccines to combat pneumonic plague**

Publication No. \_\_\_\_\_1\_\_\_\_\_

Paul Blanton Kilgore, PhD

The University of Texas Medical Branch, 2022

Supervisor: Ashok K. Chopra

Mice immunized with a 2-dose strategy utilizing either 2-doses of an adenovirus vector (Ad5-YFV) or a heterologous strategy utilizing Ad5-YFV and a live-attenuated (LMA) vaccine were evaluated for protective efficacy against pneumonic plague. A single immunization event giving both Ad5-YFV and LMA at once was also tested as a potential strategy for use during an outbreak when quick protective immunity is desired. While the Ad5-YFV vaccine harbors a fusion cassette of three genes encoding YscF, F1, and LcrV, LMA represents a mutant of parental *Yersinia pestis* CO92 deleted for genes encoding Lpp, MsbB, and Ail. Ad5-YFV and LMA were either administered simultaneously (1-dose regimen) or 21 days apart in various order and route of administration combinations (2-dose regimen). The 2-dose regimen induced robust immune responses to provide full protection to animals against parental CO92 and its isogenic F1 (CAF<sup>-</sup>)-deletion mutant challenges during both short- and long-term studies. While all of these approaches were completely protective, differences in the immune phenotype of these mice were observed based on which vaccine was given first. Mice intranasally (i.n.) immunized with Ad5-YFV first followed by LMA (i.n. or intramuscularly [i.m.]) had higher T- and B- cell

proliferative responses and LcrV antibody titers than those in mice vaccinated with LMA (i.n. or i.m.) first ahead of Ad5-YFV (i.n.) during the long-term study. Mice immunized with Ad5-YFV first had the highest levels of T and B-cell replication. Mice immunized first with LMA had the strongest Th17 phenotypes. In addition, when Ad5-YFV was given as the first dose, mice had a Th1 favored response while when LMA was given first, a more balanced phenotype of Th1, Th2, and Th17 responses were seen. There are different advantages in vaccine administration based on the different combinations as well. The 2-dose vaccination strategy would be ideal for regions where plague is endemic and yearly outbreaks occur like in Madagascar. An intranasal only administration strategy eliminates the use of needles. The simultaneous administration strategy would be ideal for use in an outbreak response scenario where high levels of protection generated in the shortest time would be ideal.

# TABLE OF CONTENTS

|   |     |
|---|-----|
| List of Figures .....   | ix  |
| List of Abbreviations .....   | xii |
| Chapter 1 Introduction .....  | 1   |
| Virulence Factors .....   | 1   |
| Transmission of Plague.....   | 4   |
| Clinical Course of Disease.....   | 4   |
| Epidemiology of Plague.....   | 5   |
| Vaccines and Treatment.....   | 6   |
| Previously Developed Vaccines in our Lab.....   | 7   |
| Chapter 2: Materials and Methods .....  | 11  |
| Bacterial strains and vaccines .....  | 11  |
| Animals .....   | 12  |
| Iron-overload studies .....   | 12  |
| Rag1 KO mice studies .....  | 13  |
| Heterologous vaccination and challenge studies .....  | 13  |
| Antibody titer analysis .....   | 15  |
| T-cell phenotypes.....  | 15  |
| Cell proliferation and cytokine production.....   | 16  |
| Statistical Analysis.....   | 17  |
| Chapter 3: A new generation needle- and adjuvant-free trivalent plague vaccine<br>utilizing adenovirus-5 nanoparticle platform.....       | 18  |
| Introduction.....   | 18  |
| Results.....  | 21  |
| A 2-dose rAd5-YFV trivalent needle free vaccination regimen provides<br>complete protection to mice against plague.....                   | 21  |
| The rAd5-YFV trivalent vaccine elicits better humoral immune<br>response than the rAd5-LcrV monovalent vaccine.....                       | 24  |
| The rAd5-YFV trivalent vaccine induces better cell-mediated immune<br>response compared to that of the rAd5-LcrV monovalent vaccine ..... | 27  |



|  |     |
|--|-----|
| The rAd5-YFV trivalent vaccination regimen induces a sustained protective immune response .....  | 33  |
| The rAd5-YFV trivalent vaccination regimen elicits strong cytokine and chemokine production in the long-term study .....   | 37  |
| Discussion .....   | 40  |
| Chapter 4: Combinatorial Viral Vector-Based and Live Attenuated Vaccines without an Adjuvant to Generate Broader Immune Responses to Effectively Combat Pneumonic Plague ..... | 51  |
| Introduction.....  | 51  |
| Results.....   | 52  |
| Virulence and immunogenic characterization of the LMA vaccine candidate in iron over loaded conventional and or in immunocompromised mice.....                                 | 52  |
| Strong immune responses were elicited in conventional mice by heterologous vaccination with either a 1- or 2-dose (prime-boost) regimen .....                                  | 58  |
| Robust immune response was sustained in conventional mice with a 2-dose regimen vaccination during a long-term study .....   | 63  |
| Conventional mice vaccinated with the 2-dose regimen were fully protected from CO92 and CAF <sup>-</sup> challenges during a long-term study ....                              | 66  |
| Characterization of mice splenic cytokine and chemokine profiles in response to vaccination and CO92 challenge .....   | 71  |
| Discussion .....   | 77  |
| Chapter 5: Conclusion and Future Direction .....   | 85  |
| References.....  | 87  |
| Vita .....   | 105 |

## List of Figures

|  |           |
|--|-----------|
| <b>Figure 1: Type Three Secretion System Structure(6).....</b>   | <b>3</b>  |
| <b>Figure 2: Survival analysis and subsequent protection conferred by high doses of the <math>\Delta lpp \Delta msbB \Delta ail</math> triple mutant of <i>Y. pestis</i> CO92 in a pneumonic plague mouse model.....</b> | <b>9</b>  |
| <b>Figure 3. Schematic depicting the amino acid sequence of YFV fusion protein in Ad5 vector.....</b>  | <b>19</b> |
| <b>Figure 4. T-cell mediated immune response in mice elicited by immunization with the rAd5-YFV vaccine alone or in combination with rYFV. .</b>   | <b>20</b> |
| <b>Figure 5: Protection and immune responses in mice immunized with 1 or 2 doses of the rAd5-YFV vaccine.....</b>  | <b>22</b> |
| <b>Figure 6: Animal protection conferred by immunization of mice with rAd5-YFV or rAd5-LcrV vaccines.....</b>  | <b>23</b> |
| <b>Figure 7: Antibody responses generated in mice immunized with rAd5-YFV or rAd5-LcrV vaccines.....</b>   | <b>25</b> |
| <b>Figure 8: Cell proliferation and IFN<math>\gamma</math> production in mice immunized with either rAd5-YFV or the rAd5-LcrV vaccines. ....</b>   | <b>27</b> |
| <b>Figure 9. Splenocyte cytokine and chemokine profiles in mice immunized with either rAd5-YFV or rAd5-LcrV vaccines.....</b>  | <b>32</b> |

|  |           |
|--|-----------|
| <b>Figure 10: Long-term protection and antibody titers in mice immunized with 2 doses of the rAd5-YFV vaccine. ....</b>                        | <b>34</b> |
| <b>Figure 11: Cell proliferation and IFN<math>\gamma</math> production in mice immunized with rAd5-YFV vaccine during long-term study.....</b> | <b>36</b> |
| <b>Figure 12: Splenocyte cytokine and chemokine profiles from the rAd5-YFV vaccine- immunized mice during a long-term study.....</b>           | <b>40</b> |
| <b>Figure 13: Iron-overload condition does not restore virulence of the LMA vaccine.....</b>   | <b>54</b> |
| <b>Figure 14. Parental <i>Y. pestis</i> CO92 causes clinical disease in Rag1 KO mice. ...</b>  | <b>55</b> |
| <b>Figure 15: Attenuation and immunologic characterization of LMA vaccine in Rag1 KO mice. ....</b>  | <b>57</b> |
| <b>Figure 16: Short-term heterologous vaccination study with conventional mice. ....</b>   | <b>60</b> |
| <b>Figure 17: Humoral and cell-mediated immune responses during short-term heterologous vaccination study.....</b>                             | <b>62</b> |
| <b>Figure 18: Antibody responses during long-term heterologous prime-boost vaccination study.....</b>  | <b>65</b> |
| <b>Figure 19: T- and B-cell proliferation in response to heterologous prime-boost vaccination during long-term study. ....</b>                 | <b>66</b> |
| <b>Figure 20: Heterologous prime-boost vaccinations provide protection to immunized mice in long-term study.....</b>                           | <b>67</b> |

|  |           |
|--|-----------|
| <b>Figure 21. No significant differences in F1-V specific serum IgA are observed in vaccinated mice before and after infection.....</b>          | <b>69</b> |
| <b>Figure 22: T-cell responses to CO92 challenge during long-term heterologous prime-boost vaccination study.....</b>                            | <b>70</b> |
| <b>Figure 23: Splenocyte proinflammatory and anti-proinflammatory responses during long-term heterologous prime-boost vaccination study.....</b> | <b>72</b> |
| <b>Figure 24: Splenocyte Th1/Th2/Th17 cytokine responses during long-term heterologous prime-boost vaccination study.....</b>                    | <b>75</b> |
| <b>Figure 25: Splenocyte chemokine responses during long-term heterologous prime-boost vaccination study.....</b>                                | <b>77</b> |

## List of Abbreviations

|                  |  |
|------------------|--|
| FDA              | Food and Drug Administration   |
| CDC              | Centers for Disease Control and Prevention   |
| Ail              | Attachment and invasion locus  |
| T3SS             | Type Three Secretion System  |
| <i>Y. pestis</i> | <i>Yersinia pestis</i>   |
| Kb               | Kilobase pairs   |
| C                | Celsius  |
| Ymt              | Murine Toxin   |
| CAF1             | Capsule antigen fraction 1   |
| F1               | Capsule antigen fraction 1   |
| h                | hours  |
| pgm              | pigmentation locus   |
| LMA              | <i>Y. pestis</i> CO92 $\Delta$ <i>lpp</i> $\Delta$ <i>msbB</i> $\Delta$ <i>ail</i> |
| YFV              | YscF F1 LcrV   |
| TLR-2            | Toll like receptor 2   |
| LPS              | lipopolysaccharide   |
| TLR-4            | Toll like receptor 4   |
| CFU              | Colony Forming Units   |
| LD50             | Lethal Dose 50%  |
| WT               | Wildtype   |
| i.n.             | intranasal   |
| p.i.             | post-infection   |
| hpi              | hours post-infection   |
| dpi              | days post-infection  |
| Th1              | T helper type 1  |
| TH2              | T helper type 2  |
| TH17             | T helper type 17   |
| CD4              | Cluster of differentiation 4   |
| CD8              | Cluster of differentiation 8   |
| IL-17            | Interleukin 17   |
| Ad5              | Adenovirus type 5  |
| i.m.             | intramuscular  |
| GNL              | Galveston National Lab   |
| UTMB             | University of Texas Medical Branch   |
| v.p.             | viral particles  |
| mL               | milliliter   |
| CD-293           | Cluster of differentiation 293   |
| BSL3             | Biosafety level 3  |
| HIB              | Heart Infusion Broth   |
| rpm              | revolutions per minute   |
| $\mu$ L          | microliter   |

|               |   |
|---------------|---|
| ABSL-3        | Animal biosafety level 3                                  |
| µg            | microgram   |
| i.p.          | intraperitoneal   |
| n             | group size  |
| PBS           | phosphate buffered saline                                 |
| SBA           | sheeps blood agar   |
| PFU           | plague forming units                                      |
| BALF          | bronchoalveolar lavage fluid                              |
| µm            | micrometer  |
| ELISA         | enzyme linked immunosorbent assay                         |
| ng            | nanogram  |
| F1-V          | F1 LcrV fusion protein                                    |
| rF1           | recombinant F1  |
| rLcrV         | recombinant LcrV  |
| r YscF        | recombinant YscF  |
| DPBS          | Dulbecco's modified phosphate buffered saline             |
| HRP           | horseradish peroxidase                                    |
| Min           | minute  |
| IgG           | Immunoglobulin G  |
| IgA           | Immunoglobulin A  |
| N             | Normal  |
| TMB           | 3,3',5,5'-Tetramethylbenzidine                            |
| PMA           | phorbol 12-myristate 13-acetate                           |
| IFN $\gamma$  | Interferon gamma  |
| BrdU          | bromodeoxyuridine   |
| ANOVA         | analysis of variance                                      |
| SDS-PAGE      | Sodium dodecyl sulfate polyacrylamide gel electrophoresis |
| WHO           | World Health Organization                                 |
| TPP           | Target product profile                                    |
| s.c.          | subcutaneous  |
| OD            | optical density   |
| IL-1 $\alpha$ | Interleukin 1 alpha                                       |
| IL-1 $\beta$  | Interleukin 1 beta  |
| IL-6          | Interleukin 6   |
| IL-4          | Interleukin 4   |
| GM-CSF        | Granulocyte-macrophage colony-stimulating factor          |
| IL-13         | Interleukin 13  |
| Lux           | luciferase  |
| CD19          | Cluster of differentiation 19                             |
| CD38          | Cluster of differentiation 38                             |
| TNF- $\alpha$ | Tumor necrosis factor alpha                               |
| IL-10         | Interleukin 10  |
| IL-12         | Interleukin 12  |
| IL-13         | Interleukin 13  |
| IL-5          | Interleukin 5   |
| G-CSF         | Granulocyte colony-stimulating factor                     |

|               |  |
|---------------|--|
| CXCL1         | C-X-C Motif Chemokine Ligand 1   |
| RANTES        | Regulated upon Activation, Normal T Cell Expressed and Presumably Secreted Chemokine |
| MCP1          | Macrophage Chemoattractant Protein-1   |
| CCL4          | Chemokine (C-C motif) Ligand 4   |
| CCL2          | Chemokine (C-C motif) Ligand 2   |
| US            | United States  |
| NHP           | Non-human primate  |
| MIP1 $\alpha$ | Macrophage inflammatory protein alpha  |
| MIP1 $\beta$  | Macrophage inflammatory protein beta   |
| DC            | Dendritic cell   |
| KO            | Knock out  |
| RAG1          | Recombination activating gene 1  |
| CAF-          | Capsular antigen fraction 1 knockout   |
| CD3           | Cluster of differentiation 3   |
| BCG           | Bacille Calmette-Guérin  |
| TB            | Tuberculosis   |
| HIV           | Human immunodeficiency virus   |
| COVID-19      | Coronavirus disease 2019   |
| mRNA          | messenger ribonucleic acid   |
| SARS-CoV-2    | severe acute respiratory syndrome coronavirus 2                                      |
| TRM           | resident memory T cells  |
| S-FLU H1N1    | signal minus influenza vaccine   |

## Chapter 1 Introduction

Sections of the following chapter was reproduced with permission from:

Kilgore PB, Sha J, Hendrix EK, Motin VL, Chopra AK. Combinatorial Viral Vector-Based and Live Attenuated Vaccines without an Adjuvant to Generate Broader Immune Responses to Effectively Combat Pneumonic Plague. *mBio*. 2021 Dec 21;12(6):e0322321. doi: 10.1128/mBio.03223-21. Epub 2021 Dec 7. PMID: 34872353; PMCID: PMC8649767.

Kilgore, P. B., Sha, J., Andersson, J. A., Motin, V. L., & Chopra, A. K. (2021). A new generation needle- and adjuvant-free trivalent plague vaccine utilizing adenovirus-5 nanoparticle platform. *Npj Vaccines*, 6(1). <https://doi.org/10.1038/s41541-020-00275-3>

*Yersinia pestis*, the causative agent of plague, is a Gram-negative gammaproteobacteria that has been responsible for three major pandemics throughout human history resulting in over 200 million deaths(1). There are endemic regions for plague throughout the world including the Western United States, Madagascar, and China, making eradication unlikely. There are three different forms of plague: bubonic, septicemic, and pneumonic. The first form is generally caused from the bite of an infected flea or exposure through a break in the skin. Pneumonic plague is caused by inhalation of the bacterium. Both forms can then disseminate through the body to cause septicemic plague. Plague can be effectively treated through administration of antibiotics; however, due to the quick progression of pneumonic plague and to be effective, antibiotic treatment must be given within 24 hours of symptoms (2). There are currently no FDA-approved vaccines to prevent plague in the United States(3, 4). Due to these reasons, *Yersinia pestis* has been classified as a Tier-1 select agent by the Centers for Disease Control and Prevention (CDC).

### VIRULENCE FACTORS



*Yersinia pestis* has a variety of virulence factors encoded both on the chromosome as well as on three virulence plasmids. The attachment invasion locus (Ail) is a chromosomally encoded gene that plays a variety of roles during infection. During infection, ail helps with the delivery of type three secretion system (T3SS) effector proteins. It also helps inhibit inflammation during infection to allow *Y. pestis* to evade the innate immune system early during infection. In addition, ail also serves as an adherence and invasions factor as well as providing serum resistance to complement to promote bacterial survival during infection(5).

*Y. pestis* has three virulence plasmids: the 70Kb pCD1, 110Kb pMT1, and 9.6Kb pPCP-1(1). Each of these plasmids encodes important virulence factors. The T3SS is encoded on pCD1. The T3SS is only expressed at 37°C and not at 28°C when *Y. pestis* resides in the flea vector. Components such as LcrV and YscF which compose the needle-tip and barrel structure respectively of the T3SS (**Fig. 1**) are encoded on pCD1 as well as the effector proteins that are exported through the T3SS(6). These effectors known as

YOPS (yersinia outer proteins) help down regulate the host innate immune response during infection to prevent effective activation of the innate immune system(7).

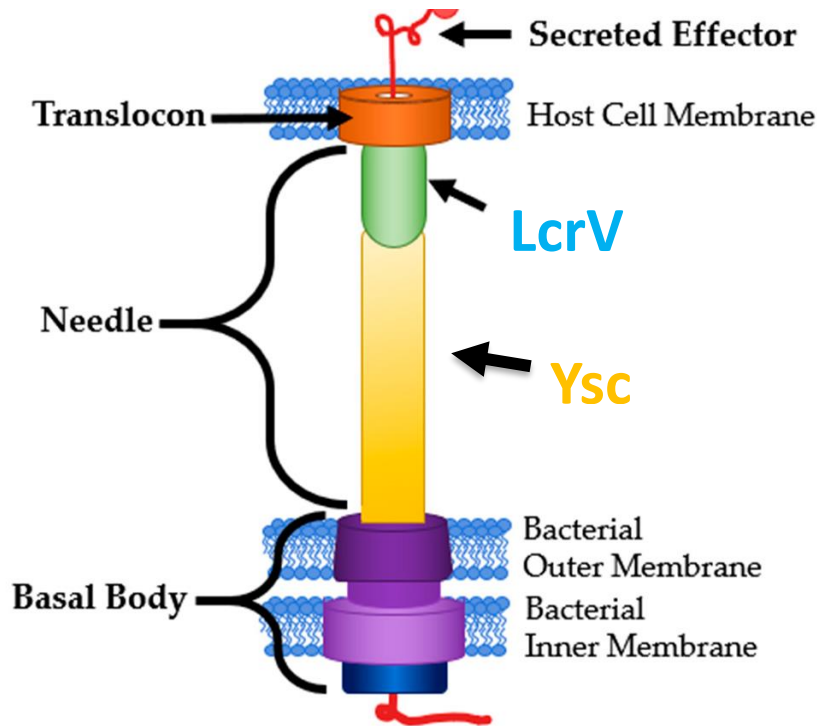


**Figure 1: Type Three Secretion System Structure(6)**

The above figure was reproduced with permission from:

Hotinger JA, May AE. 2020. Antibodies Inhibiting the Type III Secretion System of Gram-Negative Pathogenic Bacteria.

Antibodies 9:35.

The largest virulence plasmid, pMT1, encodes virulence factors important for both flea colonization and human infection. Murine Toxin (Ymt), a phospholipase plays an important role during the flea colonization step of the *Y. pestis* lifecycle(8). Ymt protects *Y. pestis* inside the flea gut and promotes colonization in the flea midgut(8). Also encoded on pMT1 is the protein capsule CAF1 or F1. This protein capsule is only expressed at 37°C similar to the T3SS. F1 is an important antibody target and helps prevent phagocytosis of *Y. pestis* by immune cells during infection(9). It is important to note that while F1 is an

important virulence factor, deletion of F1 does not significantly attenuate *Y. pestis* infection(10). Importantly, strains of *Y. pestis* have been detected that have naturally lost F1 in nature(11).

The last and smallest virulence plasmid, pPCP-1 encodes Pla, plasminogen activator protease. This protease is important for dissemination of *Y. pestis* by cleaving plasmin found in fibrin clots(12). This is important for both pneumonic and bubonic plague as it helps promote dissemination. Deletion of Pla is significantly attenuating(13).

### **TRANSMISSION OF PLAGUE**

Plague is maintained in the environment through a rodent flea vector system. An epizootic cycle exists where plague will infect fleas which will then feed on small rodents such as marmots or prairie dogs which will become infected and be fed on by fleas to maintain plague in the environment(14). This is characterized by large die offs of rodents in areas since most rodent populations are very susceptible to plague. When *Y. pestis* infects a flea, it will colonize the midgut of the flea and form a biofilm blocking the digestive tract of the flea. This will starve the flea, making it aggressively seek out a meal from a mammal. The flea will then bite the mammal and infect it with *Y. pestis*(15).

Rarely, infected fleas can bite humans transmitting bubonic plague or humans can encounter infected or deceased mammals from plague and acquire bubonic plague through a break in the skin(15). Activities such as cleaning animal carcasses for food preparation or poaching has also been known to be a possible way to transmit plague(16). This has been documented with plague infected marmots in China led to several outbreaks there(16). Inhalation of *Y. pestis* either from infected people or from the environment leads to primary pneumonic plague.

### **CLINICAL COURSE OF DISEASE**

The primary forms of plague are bubonic and pneumonic. Bubonic plague usually makes up most cases(1). There have been notable exceptions though such as the 2017 epidemic in Madagascar which was mostly pneumonic plague(17, 18). Bubonic plague has a longer course of disease and a lower case fatality rate. This makes it easier to treat with antibiotics. During bubonic plague, the bacteria is inoculated into the skin either by the bite of an infected flea or some other break in the skin allowing entry. From there, *Y. pestis* moves to the lymph nodes where it will start replicating for several days(19). During this time, symptoms such as fever and chills can occur. Replication in the lymph nodes leads to enlargement and inflammation of the lymph nodes, leading the formation of bubos which are characteristic of bubonic plague(1). These are painful and can become necrotic. *Y. pestis* can then disseminate from the lymphatic system to the blood stream leading to septicemic plague or to the lungs leading to pneumonic plague. Untreated bubonic plague is fatal in up to 60% of untreated cases however the relatively slow course of disease compared to pneumonic plague allows for antibiotic treatment which is effective(1).

Pneumonic plague occurs when *Y. pestis* is inhaled either from the environment or from other persons that have pneumonic plague. The possibility of person-to-person transmission of pneumonic plague makes it a much higher public health issue than bubonic plague(2). During the first 24 hours of pneumonic plague infection, *Y. pestis* downregulates the innate immune system leading to silent replication within the lungs and no symptoms called the preinflammatory phase(20). From 24 hours to 48 hours post infection the pro inflammatory phase occurs. The bacteria begin to disseminate and a huge increase of neutrophil recruitment to the lungs and production of pro-inflammatory cytokines occurs(21). This is when symptoms start to be noticed such as a high fever and chills. If treatment is not started within 24 hours of symptom onset, pneumonic plague is fatal in almost 100% of cases(2). Death usually occurs by 72 hours post infection(2).

## **EPIDEMIOLOGY OF PLAGUE**

Plague is found across the world in every continent except Antarctica and Oceania. Plague has been documented in 33 countries worldwide(1, 15). In the United States, *Y. pestis* is most found in the Western United States particularly around the four corners region(1). Outside the United States, plague hotspots have been documented in Peru, Democratic Republic of Congo, Madagascar, and China with minor outbreaks being reported in the last 5 years(15). Madagascar experienced the most significant recent epidemic of plague in 2017(17, 18). This outbreak was noticeable in that there were over 2000 cases. Madagascar experiences yearly outbreaks of plague however the 2017 epidemic occurred earlier than usual and was composed of mostly pneumonic cases which was significant from a public health perspective due to the possibility for person-to-person transmission and high mortality rate compared to bubonic plague. Over 75% of cases were pneumonic plague and ~200 people died leading to a mortality rate of 8.6% even when prophylactic use of antibiotics were used widely during the outbreak with millions of doses of levofloxacin being administered(17, 18, 22).

#### **VACCINES AND TREATMENT**

Plague is susceptible to a variety of antibiotics such as aminoglycosides, fluoroquinolones, and tetracyclines(23). There have been isolated antibiotic resistant strains of plague identified during outbreaks however most strains remain susceptible to antibiotic treatment(24). Due to the slower disease course of bubonic plague, antibiotic treatment is very effective. The limited treatment window for pneumonic plague makes prompt initiation of treatment very important since if antibiotics are not given within 24 hours of symptom onset, antibiotic treatment will not be effective(23). As was seen during the Madagascar outbreak in 2017, the case fatality rate remained significant even when antibiotics were used. Since vaccines can be given before an outbreak occurs, they provide a more ideal tool to control pneumonic plague.

Early plague vaccines were developed in the United States to try and control plague however none of them are currently in use due to some poor characteristics. A heat-inactivated vaccine was developed for use by the United States army however this vaccine was quite reactive and only protected against bubonic plague and not pneumonic plague(1). Due to these characteristics, it is no longer used(25).

Outside the United States in Russia, former members of the Soviet Union, and China, a live-attenuated plague vaccine called EV76 is used to control plague(26). This live-attenuated vaccine is based on mutations in the pigmentation locus (pgm) that interfere with the ability of *Y. pestis* to acquire iron(27). This vaccine is effective against preventing both bubonic and pneumonic plague however it is quite reactogenic and would not be approved for use in the United States. It is also not safe in certain immunocompromised populations such as those with hemochromatosis(28). This was seen with a laboratory acquired infection occurred in an individual with hemochromatosis using a similar strain that was fatal. This is because hemochromatosis leads to high iron levels in the body which can complement the attenuating mutation.

There have been extensive studies with subunit plague vaccines(25). These vaccines rely on purified F1 and LcrV plague antigens either administered together or as a fusion protein. These have been shown to be very effective in mice and cynomolgus macaque studies. Studies in African green monkeys however, showed variable protection. These subunit vaccines have undergone phase 1 and 2 clinical trials however have not moved forward(29–33).

A variety of subunit, live-attenuated, and vector-based vaccines have all be studied in animal models and shown to be effective however none of these vaccines have moved past the pre-clinical development phase(25, 26).

#### **PREVIOUSLY DEVELOPED VACCINES IN OUR LAB**

In our laboratory, we have developed two types of plague vaccine candidates, namely LMA and Ad5-YFV. The live-attenuated vaccine LMA is a triple deletion mutant of *Y. pestis* CO92 in which genes encoding Braun lipoprotein (Lpp), an acyltransferase (MsbB), and the attachment invasion locus (Ail), were deleted (34). While Lpp activates pro-inflammatory cascade by binding to toll-like receptor 2 (TLR-2) (35, 36), MsbB adds lauric acid to the lipid A moiety of lipopolysaccharide (LPS), which triggers TLR-4 signaling (37, 38). Ail, in addition to promoting attachment and invasion of *Y. pestis* to the host, provides serum resistance to the organism (34, 39). LMA is highly attenuated. When  $3.4 \times 10^6$  CFU was administered intranasally (equivalent to 6,800 LD<sub>50</sub> of WT *Y. pestis* CO92), all mice survived and 70% of the mice were protected when rechallenged with wildtype *Y. pestis* three weeks after the initial infection (**Fig. 2**).

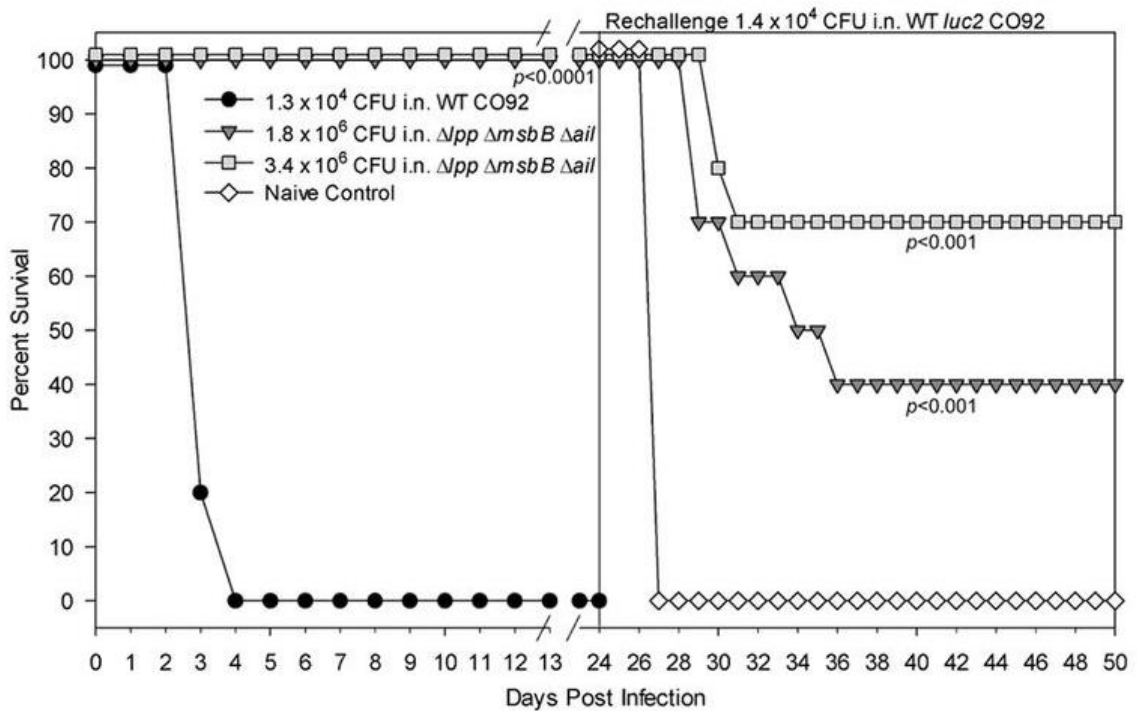


**Figure 2: Survival analysis and subsequent protection conferred by high doses of the  $\Delta lpp \Delta msbB \Delta ail$  triple mutant of *Y. pestis* CO92 in a pneumonic plague mouse model.**

Female Swiss Webster mice (5 to 10 per group) were infected with various doses of the  $\Delta lpp \Delta msbB \Delta ail$  triple mutant or  $1.3 \times 10^4$  CFU of WT *Y. pestis* CO92 by the i.n. route. Surviving mice with age-matched naive animals were then rechallenged on day 24 p.i. with  $1.4 \times 10^4$  CFU of the WT CO92 *luc2* strain. Statistically significant *P* values are for comparisons to the WT CO92-infected mice in the initial challenge or to naive control mice during the WT CO92 *luc2* rechallenge.(34)

The above figure was reproduced with permission from:

Tiner BL, Sha J, Kirtley ML, Erova TE, Popov VL, Baze WB, van Lier CJ, Ponnusamy D, Andersson JA, Motin VL, Chauhan S, Chopra AK. 2015. Combinational Deletion of Three Membrane Protein-Encoding Genes Highly Attenuates *Yersinia pestis* while Retaining Immunogenicity in a Mouse Model of Pneumonic Plague. *Infection and Immunity* 83:1318–1338.

The Ad5-YFV is a replication deficient adenovirus type 5 vector-based vaccine containing genes for three plague antigens: fraction 1 capsule-like antigen F1, tip protein of the T3SS LcrV, and YscF that forms the barrel structure of T3SS needle (40). Using a prime-boost immunization regimen (21 days apart), both vaccines when used individually, elicited robust humoral and cell-mediated immune responses in animals and conferred 100% protection against lethal *Y. pestis* CO92 challenge (41, 42). Importantly, each of these vaccines has its own unique characteristics. Notably, we observed a significant induction of CD4<sup>+</sup> IL-17<sup>+</sup>-producing T-cells in LMA vaccine-immunized mice (42, 43). IL-17 production is an important correlate of protection against plague in the absence of protective antibodies (44, 45). However, such a T-cell population was not detected in animals immunized with the Ad5-YFV vaccine (41). Further, the Th1 immune response was favored after vaccination of mice with the Ad5-YFV vaccine over Th2, possibly due to the Ad5 vector used, while the Th2 immune response was favored after immunization of animals with the LMA vaccine (41, 43). In our past studies, the Ad5-YFV vaccine was



always delivered intranasally (i.n.), while the LMA vaccine was administered by the i.m. or the i.n. route (34, 40–43).

## Chapter 2: Materials and Methods

The following chapter was reproduced with permission from:

Kilgore PB, Sha J, Hendrix EK, Motin VL, Chopra AK. Combinatorial Viral Vector-Based and Live Attenuated Vaccines without an Adjuvant to Generate Broader Immune Responses to Effectively Combat Pneumonic Plague. *mBio*. 2021 Dec 21;12(6):e0322321. doi: 10.1128/mBio.03223-21. Epub 2021 Dec 7. PMID: 34872353; PMCID: PMC8649767.

### **BACTERIAL STRAINS AND VACCINES**

A fully virulent human pneumonic plague isolate, the parental *Y. pestis* strain (CO92), was obtained from BEI Resources (Manassas, VA). The F1-negative strain (CAF<sup>-</sup>) was created in our laboratory by deletion of partial *cafIA* and most of the *cafI* gene from CO92. The mutant strain retained its virulence in both pneumonic and bubonic plague animal models (10). The live-attenuated vaccine candidate (LMA) is a triple deletion mutant of CO92 in which genes encoding Lpp, MsbB, and Ail, were deleted (34). The KIM/D27 strain of *Y. pestis* deleted for the pigmentation locus required for iron acquisition from the host was used in an iron-overload experiment performed in mice (46). The Ad5-YFV is a human replication-defective adenovirus type 5 vector-based vaccine containing genes for three plague antigens: F1, LcrV, and YscF (40). All studies involving *Y. pestis* were performed in Tier 1 select agent laboratories at UTMB in the Galveston National Laboratory (GNL), Galveston, TX.

A large batch of Ad5-YFV vaccine [ $1 \times 10^{16}$  virus particles (v.p.)/batch, aliquoted in 1 ml at  $1 \times 10^{12}$  v.p. and stored at  $-80^{\circ}\text{C}$ ] was prepared from a 20-liter suspension culture of HEK293 cells in a chemically defined, protein-free CD-293 medium. The vaccine was purified at the Baylor College of Medicine Vector Development Laboratory and by our company partner in collaboration with Lonza, Houston, TX, under good laboratory practice

conditions. This batch of vaccine was used for our subsequent studies in mice and non-human primates (40, 41). Likewise, a large batch of the LMA vaccine (2-liters) was prepared under a highly regulated quality control system in GNL biosafety level 3 (BSL-3) suite, by growing in Heart Infusion Broth (HIB) overnight at 28°C as a shake flask culture (180 rpm). The culture was centrifuged, washed with HIB, and resuspended to 1/20<sup>th</sup> the original volume. The culture was aliquoted (500 µl, ~1x10<sup>9</sup> colony forming units [CFU]/ml) with 25% glycerol and stored at -80°C. Titers of the vaccines were confirmed before and after each inoculation, and the same batches of the vaccines were used throughout our earlier and these studies (34, 42).

#### **ANIMALS**

Outbred Swiss-Webster (female) and inbred C57BL6 Rag1 Knockout (KO, lacking mature T- and B- cells, male and female)) mice (6-8 weeks) were purchased from Jackson Laboratory (Bar Harbor ME). All experiments were conducted in the animal biosafety level 3 (ABSL-3) facility at UTMB in the GNL. Studies were ethically performed under an approved Institutional Animal Care and Use Committee protocol.

#### **IRON-OVERLOAD STUDIES**

Swiss-Webster mice (n=5/group) were injected with 75 µg of ferrous chloride (FeCl<sub>2</sub>·4H<sub>2</sub>O, Sigma-Aldrich Inc., St. Louis, MO) by the intraperitoneal (i.p.) route (46) and then challenged i.n. with either the KIM/D27 strain or the LMA vaccine strain (2x10<sup>5</sup>-5x10<sup>6</sup> CFU/50 µl). A similar number of untreated mice (without FeCl<sub>2</sub>·4H<sub>2</sub>O) were also infected and served as controls. The animals were observed for body weight loss, other clinical signs of the disease (ruffled fur, hunched back, lethargy, lack of grooming, sunken

eyes, squinting of eyes with ocular and or nasal discharge, open-mouth breathing, gasping for air), and morbidity over a period of 14 days.

### **RAG1 KO MICE STUDIES**

Rag1 KO mice (n=10, males or females) were infected with 4 LD<sub>50</sub> of CO92 by either i.n. or i.m. routes and observed for morbidity and mortality. For inbred mice, 1 LD<sub>50</sub>=10 or 100 colony-forming units (CFU) when delivered by the i.m. or the i.n. route, respectively. Lungs, liver, and spleen were excised from moribund mice and homogenized in 1-2 mL of phosphate-buffered saline (PBS). Homogenates were 10-fold serially diluted and plated on sheep blood agar (SBA) plates to quantify bacterial load. For the LMA vaccine studies, Rag1 KO mice (10 for each infection route) were infected with 2.0 x 10<sup>6</sup> CFU by either the i.n. or the i.m. route. A cohort of 10 mice (5 from each infection route) was sacrificed on day 5 post-infection (p.i.), and bacterial loads in spleen and at the initial infection sites (lungs or the muscle) were determined as described above. The remaining 10 mice were observed for signs of disease for 28 days, and the survivors were then i.n. challenged with 6 LD<sub>50</sub> of CO92. On day 3 post-challenge, mice were bled to collect serum, and lungs from 5 moribund animals were excised on day 4 to quantify bacterial load.

### **HETEROLOGOUS VACCINATION AND CHALLENGE STUDIES**

Swiss-Webster mice were immunized with Ad5-YFV and LMA vaccines in either a 1- or 2-dose regimens. In a 1-dose regimen, both Ad5-YFV and LMA were delivered simultaneously, while in a 2-dose regimen, Ad5-YFV and LMA vaccines were administered 21 days apart in various order and route combinations. Mice receiving PBS

were used as controls. The vaccination doses were  $1.2 \times 10^{10}$  plaque forming units (PFU)/40  $\mu$ L for Ad5-YFV and  $2.0 \times 10^6$  CFU/50  $\mu$ L for the LMA vaccine (41, 42).

For short-term studies, the immunized and naïve control mice (n=8-10) were retro-orbitally bled on day 21 after the last dose of immunization. The animals were then i.n. challenged with 100 LD<sub>50</sub> of CO92 or CAF<sup>-</sup> mutant on day 24 after completion of the vaccination course. For Swiss-Webster mice, 1 LD<sub>50</sub>=500 CFU of CO92 or CAF<sup>-</sup> by the i.n. route (10, 47). In a separate experiment, mice (n=5) were similarly immunized with various combinations as described above; however, the group in which LMA and Ad5-YFV vaccines were administered simultaneously *via* the i.n. route was excluded because of interference in generating immune responses and reduced animal protection after bacterial challenge (see results). On day 21 after completion of the immunization course, mice were euthanized, and spleens collected for the evaluation of cell-mediated immunity.

For long-term studies, mice were immunized with the 2-dose regimen only, and animals receiving PBS were used as controls. Blood and spleens were collected from 5 mice in each immunized and control group on day 63 (42 days after last immunization dose), and the rest of mice were challenged with 100 LD<sub>50</sub> of either CO92 or its CAF<sup>-</sup> strain on day 105 (84 days after last immunization dose). On day 3 post challenge with CO92, organs (spleen, lungs, and liver) were collected from all moribund animals to quantify bacterial load, and spleens were also excised from 5 alive animals (after euthanization) of each group. At the end of the experiment, bronchoalveolar lavage fluid (BALF), spleen and lungs or muscle were collected from all the surviving animals. The isolated sera and BALFs were filtered using 0.1  $\mu$ m filter cartridges (Millipore Sigma Life Science Center, Burlington, MA) and sterility confirmed before performing subsequent experiments at a

lower biocontainment level. The collected organs were either used for quantitation of the bacterial load or for the evaluation of cell-mediated immunity.

#### **ANTIBODY TITER ANALYSIS**

Antibody titers were measured by performing indirect Enzyme-linked immunosorbent assay (ELISA) (41). Briefly, MaxiSorp ELISA plates (NUNC, Rochester, NY) were coated with 100 ng of recombinant fusion protein (rF1-V) (BEI Resources) or individual plague antigens rF1, rLcrV, or rYscF in carbonate buffer (100  $\mu$ L) at 4°C overnight. Non-coated antigens were removed with 3 washes of Dulbecco's PBS (DPBS) with 0.05% Tween 20. Plates were then blocked with 1% powdered milk (EMD Chemicals Inc., Gibbstown, NJ) in DPBS for 1 h at room temperature. After 3 more washes, sera or BALFs were 2-fold serially diluted and incubated for 1-h at room-temperature. Plates were again washed 3 times and then horseradish peroxidase (HRP)-conjugated secondary anti-mouse antibodies for IgG, IgG1, IgG2a or IgA (Southern Biotech, Birmingham, AL), diluted at 1:8000, were added and incubated for 1 h at room temperature. Plates were washed 3 times and then 100  $\mu$ L of TMB (3,3',5,5'-Tetramethylbenzidine) substrate was added for 5-15 min at room temperature. Colorimetric reaction development was stopped using 2N H<sub>2</sub>SO<sub>4</sub>. Absorbance was then measured at 450 nm using a Versamax tunable microplate reader (Molecular Devices San Jose, CA).

#### **T-CELL PHENOTYPES**

Spleens collected from both immunized and control mice were smashed and passed through a 70  $\mu$ m cell strainer to obtain single cell suspension in RPMI 1640 cell culture medium. Splenocytes were then seeded into 24 well tissue culture plates at a density of 2.0

x 10<sup>6</sup> cells/well. Four wells/mouse/plate were treated with ionomycin (750 ng/mL, calcium ionophore), PMA (phorbol 12-myristate 13-acetate, protein kinase C activator, 50 ng/mL), and Brefeldin A (5 µg/mL) for 5 h at 37° C in a 5% CO<sub>2</sub> incubator. Stimulation of splenocytes with PMA and ionomycin leads to activation of several intracellular signaling pathways, bypassing the T cell membrane receptor complex, resulting in strong T cell activation and production of a variety of cytokines. Splenocytes were then blocked with anti-mouse CD16/32 antibodies (BioLegend, San Diego, CA) followed by staining with Fixable Viability Dye eFluor™ 506 (eBioscience, San Diego, CA) and APC anti-mouse CD3e (eBioscience), PE/Dazzle 594 anti-mouse CD4 (BioLegend), FITC anti-mouse CD8 (BioLegend) for CD3, CD4, and CD8 T-cell surface markers, respectively. Cells were then permeabilized for intracellular staining with PerCP/Cy5.5 anti-mouse interferon (IFN)-γ, PE/Cy7 anti-mouse IL-17A (BioLegend), and analyzed by flow cytometry.

#### **CELL PROLIFERATION AND CYTOKINE PRODUCTION**

To measure T- and B- cell proliferation, bromodeoxyuridine (BrdU), a thymidine analog, incorporation method was used. Briefly, the isolated splenocytes were seeded in duplicate 24 well tissue culture plates (1.0 x 10<sup>6</sup> cells/well) and stimulated with rF1-V fusion protein (100 µg/ml) for 72 h at 37°C. The BrdU (BD Bioscience, San Jose, CA) was then added into the wells of one of the plates at a final concentration of 10 µM during the last 18 h of incubation with rF1-V to be incorporated into newly synthesized DNA of the splenocytes (48, 49).

Subsequently, the BrdU-labeled splenocytes were surface stained for T-cell (CD3e-APC; eBioscience) and B-cell (CD19-eFluor450, ThermoFisher Scientific, Grand Island, NY) markers after blocking with anti-mouse CD16/32 antibodies (BioLegend). Cells were

then permeabilized and treated with DNase to expose BrdU epitopes followed by anti-BrdU-FITC and 7-AAD (7-amino-actinomycin D) staining by using BD Pharmingen FITC BrdU Flow Kit (San Jose, CA). The splenocytes were then subjected to flow cytometry, and data analyzed as we previously described (43). The percent of BrdU positive cells in CD3 and CD19 positive populations were calculated using FACSDiva software.

To assess cytokine production, cell supernatants were collected from a duplicate plate above after stimulation with rF1-V (100  $\mu$ g/ml) for 72 h at 37°C. For these studies, we used *Y. pestis* specific antigens for stimulation to confirm flow cytometry data. Cytokines in the supernatants were then measured by using Bio-Plex Pro Mouse Cytokine 23-plex Assay (Biorad Laboratories, Hercules, CA) following the manufacturer's standard protocol.

## **STATISTICAL ANALYSIS**

One-way or Two-way analysis of variance (ANOVA) with Tukey's post hoc test or the Student's t-test was used for data analysis. We used Kaplan-Meier with log-rank (Mantel-Cox) test for animal studies, and P values of  $\leq 0.05$  were considered significant for all the statistical tests used. The number of animals per group is described in each figure and two biological replicates were performed. All in vitro studies were performed in triplicates.



# Chapter 3: A new generation needle- and adjuvant-free trivalent plague vaccine utilizing adenovirus-5 nanoparticle platform

The following chapter was reproduced with permission from:

Kilgore, P. B., Sha, J., Andersson, J. A., Motin, V. L., & Chopra, A. K. (2021). A new generation needle- and adjuvant-free trivalent plague vaccine utilizing adenovirus-5 nanoparticle platform. *Npj Vaccines*, 6(1). <https://doi.org/10.1038/s41541-020-00275-3>

## INTRODUCTION

We have previously developed a replication-defective human adenovirus-5 (Ad5) vector-based vaccine containing three *Y. pestis* antigens and included: YscF which constitutes needle of the T3SS, the capsule protein F1, and the T3SS component and effector LcrV(40). The vaccine was designated as rAd5-YFV. **Figure 3** depicts amino acid sequence of the rAd5-YFV construct. The details for generating rAd5-YFV trivalent- and rAd5-LcrV monovalent- vaccines, expression of the corresponding genes encoding LcrV and YFV (as determined by SDS-PAGE and Western blot analysis using LcrV antibodies, as well as ELISA by coating plates with individual YscF, F1, and LcrV antigens), were provided in our earlier paper(40).

```
MANFSGFTKGTDIADLDAVAQTLKKPADDANKAVNDSIAALKDKPDNPALLADLQHSINKWSVIYNINST
IVRSMKDLMOGILQKFPGGGSGGGSGGGGSADLTASTTATATLVEPARITLTYKEGAPITIMDNGNID
TELLVGTTLTGGYKTGTTSTSVNFTDAAGDPMYLTFTSQDGNNHQFTTKVIGKDSRDFDISPKVNGENLV
GDDVVLATGSQDFVRSIGSKGGKLAAGKYTDAVTVTVSNQGGGSGGGSGGGGSMIRAYEQNPQHFI
DLEKVRVEQLTGHGSSVLEELVQLVKDKNIDISIKYDPRKDSEVFANRVITDDIELLKKILAYFLPEDAI
LKGGHYDNQLQNGIKRVKEFLESSPNTQWELRAFMAVMHFSLTADRIDDDILKVIIVDSMNHGHDARSKLR
EELAELTAELKIYSVIQAEINKHLSSSGTINIHDKSNLMDKNLYGYTDEEIFKASAEYKILEKMPQTTI
QVDGSEKKIVSIKDFLGSNKRTGALGNLKNYSYNKDNNELSHFATTCSDKSRPLNDLVSQKTTQLSDI
TSRFNSAIEALNRFIQKYDSVMQRLLDDTSGK
```

**Figure 3. Schematic depicting the amino acid sequence of YFV fusion protein in Ad5 vector.**

YcsF (yellow), F1 (gray) and LcrV (cyan) were connected by a flexible linker of 3 GGGGS sequences (bold and red). The construction of rAd5-YFV and rAd5-LcrV has been detailed in our earlier paper<sup>24</sup>.

The rAd5-YFV vaccine was initially tested either as a single dose alone ( $8.0 \times 10^9$  virus particles [v.p] intranasally [i.n.] or intramuscularly [i.m.]) or followed by a booster of purified recombinant trivalent fusion antigen (rYFV) administered i.m. after 15 days of the first vaccine dose in a prime-boost strategy. One dose of the rAd5-YFV vaccine (delivered i.n.) offered significant protection (60%) in a pneumonic plague mouse model when challenged with  $\sim 100$  LD<sub>50</sub> of *Y. pestis* CO92. However, a rYFV protein boost was needed to achieve complete protection in both mouse as well as non-human primate models at much higher challenge doses of aerosolized *Y. pestis* CO92 (Fig. 4)(40).

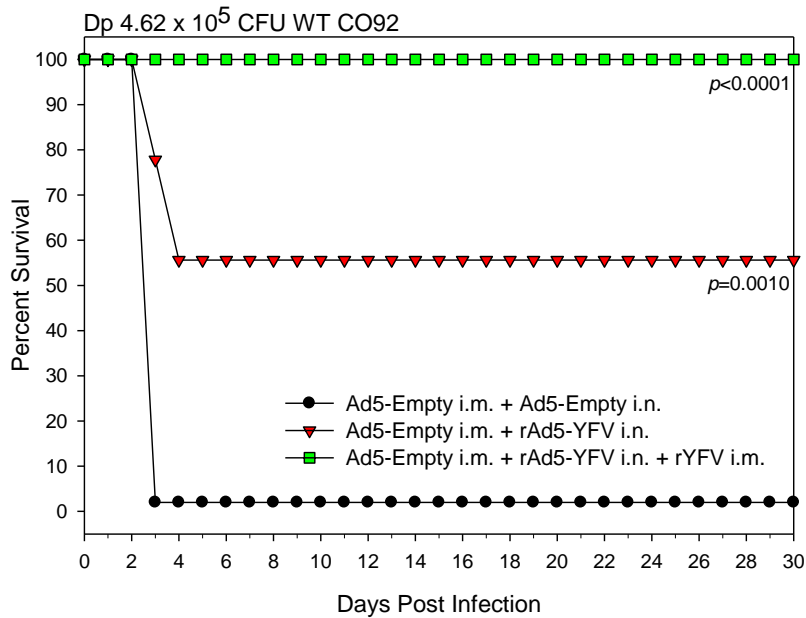


**Figure 4. T-cell mediated immune response in mice elicited by immunization with the rAd5-YFV vaccine alone or in combination with rYFV.**

PreAd mice (n = 10 to 25) were either i.n. immunized with  $8 \times 10^9$  v.p./40  $\mu$ l of rAd5-YFV alone or in combination with 10  $\mu$ g of rYFV (emulsified 1:1 in alum adjuvant) i.m. The immunizations occurred 2 weeks apart. After 15 days postimmunization, 20 mice from each immunized group and 10 from the control group were aerosol challenged with WT CO92 at a Dp of  $4.62 \times 10^5$  CFU. The P values are in comparison to the negative-control group or between groups (as indicated by the arrow) and are based on Kaplan-Meier curve analysis.

The above figure was reproduced with permission from:

Sha J, Kirtley ML, Klages C, Erova TE, Telepnev M, Ponnusamy D, Fitts EC, Baze WB, Sivasubramani SK, Lawrence WS, Patrikeev I, Peel JE, Andersson JA, Kozlova E V., Tiner BL, Peterson JW, McWilliams D, Patel S, Rothe E, Motin VL, Chopra AK. 2016. A Replication-Defective Human Type 5 Adenovirus-Based Trivalent Vaccine Confers Complete Protection against Plague in Mice and Nonhuman Primates. *Clinical and Vaccine Immunology* 23:586–600.

Recently, the World Health Organization (WHO) has released preferred target product profile (TPP) of plague vaccines(50). The recommendations included a needle-free vaccine that should not be administered in more than 2 doses, and the vaccine should generate long-lasting immune responses. In this study, we evaluated our rAd5-YFV vaccine delivered in 1- or 2- doses (21 days apart) by the i.n. route without a boost of the rYFV fusion protein. Subsequently, we compared rAd5-LcrV monovalent and rAd5-YFV trivalent vaccines in a short term study (challenge on day 45 of the study, 24 days [ $\sim$ 3 weeks] after the 2<sup>nd</sup> vaccination dose), and a long term study (challenge on day 105 of the study, 85 days [ $\sim$ 12 weeks] after the 2<sup>nd</sup> vaccination dose) for their efficacies. Robust humoral, mucosal, and cell-mediated immune responses were observed in mice immunized with the rAd5-YFV vaccine using a 2-dose vaccination regimen. The animals were fully protected from challenge with either parental *Y. pestis* CO92 or its isogenic F1 mutant in bubonic and pneumonic plague mouse models, with complete clearing of the pathogen. Furthermore, our data suggested that the T3SS needle structure protein YscF might be an

important component in the rAd5-YFV vaccine formulation, especially against F1-negative *Y. pestis* CO92 challenge.

## RESULTS

### **A 2-dose rAd5-YFV trivalent needle free vaccination regimen provides complete protection to mice against plague**

We have previously shown that a single dose administration of the rAd5-YFV vaccine ( $8.0 \times 10^9$  v.p.) by the i.n. route to mice provided complete protection against bubonic plague (subcutaneous, s.c., challenge), while 60% protection was achieved against pneumonic plague (i.n. challenge)(40). Similar levels of protection were observed even when pre-existing immunity to Ad5 vector was induced in mice prior to vaccination(40). Further, immunization of animals with the Ad5 vector alone did not influence humoral- and cell- mediated immune responses(40).

To improve efficacy of the rAd5-YFV vaccine against pneumonic plague, our first attempt was to increase the i.n. immunization dose from  $8.0 \times 10^9$  v.p. to  $1.2 \times 10^{10}$  v.p., and use vaccination regimen of either 1 dose or 2 doses in mice (**Fig. 5a&b**). As shown in **Fig. 5c**, animals immunized with 2-doses of the rAd5-YFV vaccine were completely protected (100%) compared to when animals received 1-dose of the vaccine (88% protection). In these experiments, animals were challenged ~3 weeks post last immunization dose (**Fig. 5b**). Further, while immune response analysis showed a similar percentage of CD8<sup>+</sup> IFN $\gamma$ <sup>+</sup> T-cells between these two groups of immunized mice (**Fig. 5e**), a significantly higher percentage of CD4<sup>+</sup> IFN $\gamma$ <sup>+</sup> T-cell population was noted when animals were immunized with 2-doses of the vaccine over the 1-dose vaccination group (**Fig. 5d**). These data indicated that a better T-cell immune response was elicited with a 2-dose vaccination regimen.

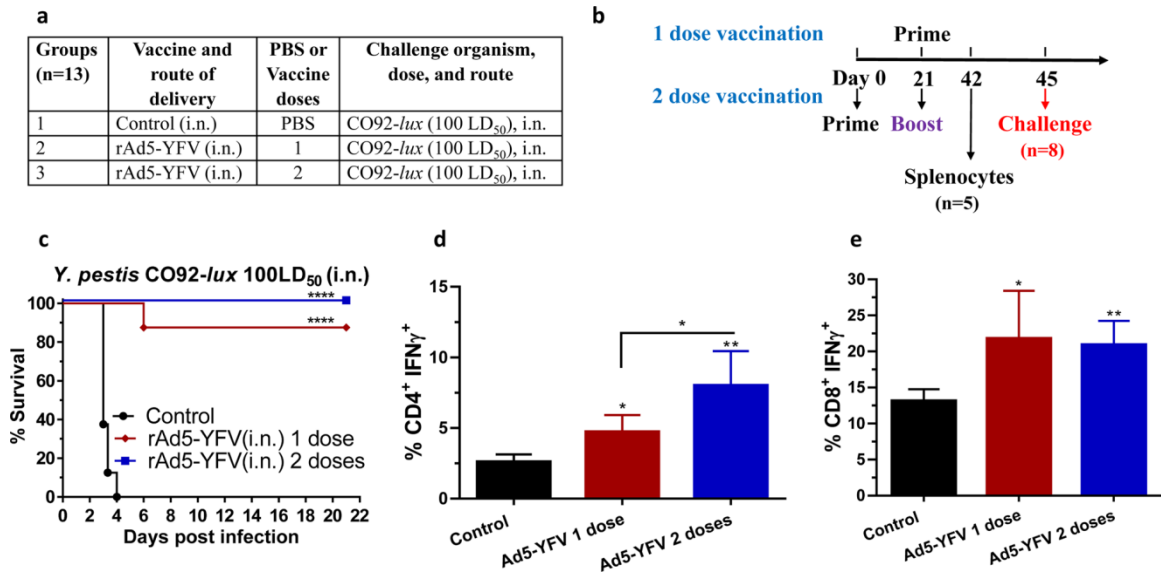


**Figure 5: Protection and immune responses in mice immunized with 1 or 2 doses of the rAd5-YFV vaccine.**

Female Swiss-webster mice (n=13/group) were immunized (i.n.) with either 1 or 2 doses (21 days apart) of rAd5-YFV vaccine ( $1.2 \times 10^{10}$  v.p.), and animals administered PBS served as controls (a). Vaccination scheme is depicted in panel b. Twenty-four days after the final vaccination, 8 mice from each group were i.n. challenged with 100 LD<sub>50</sub> ( $5 \times 10^4$  CFU/40  $\mu$ L) of *Y. pestis* CO92-*lux*, and the survival of animals plotted (c). P values were calculated using Kaplan-Meier analysis with log-rank (Mantel-Cox) test for animal survival. Spleens were harvested from the 5 remaining unchallenged mice in each group and splenocytes stimulated with PMA and Ionomycin. Brefeldin A was added to prevent secretion of cytokines. Splenocytes were then stained for T-cell surface markers CD3, CD4, and CD8, followed by intracellular IFN $\gamma$  staining. Percent of CD4<sup>+</sup> IFN $\gamma$ <sup>+</sup> (d) and CD8<sup>+</sup> IFN $\gamma$ <sup>+</sup> (e) T-cells were analyzed by flow cytometry and the data expressed as the arithmetic means  $\pm$  standard deviations. P values were calculated using a one-way ANOVA with Tukey *post hoc* test to compare multiple groups or student t-test to compare 1 dose of Ad5-YFV vaccine to control in panel e. Asterisks above columns represent comparison to the control

group, while horizontal bars represent differences between test groups. \*P<0.05, \*\*P<0.01, \*\*\*\* P<0.0001. Two biological replicates were performed, and data plotted.

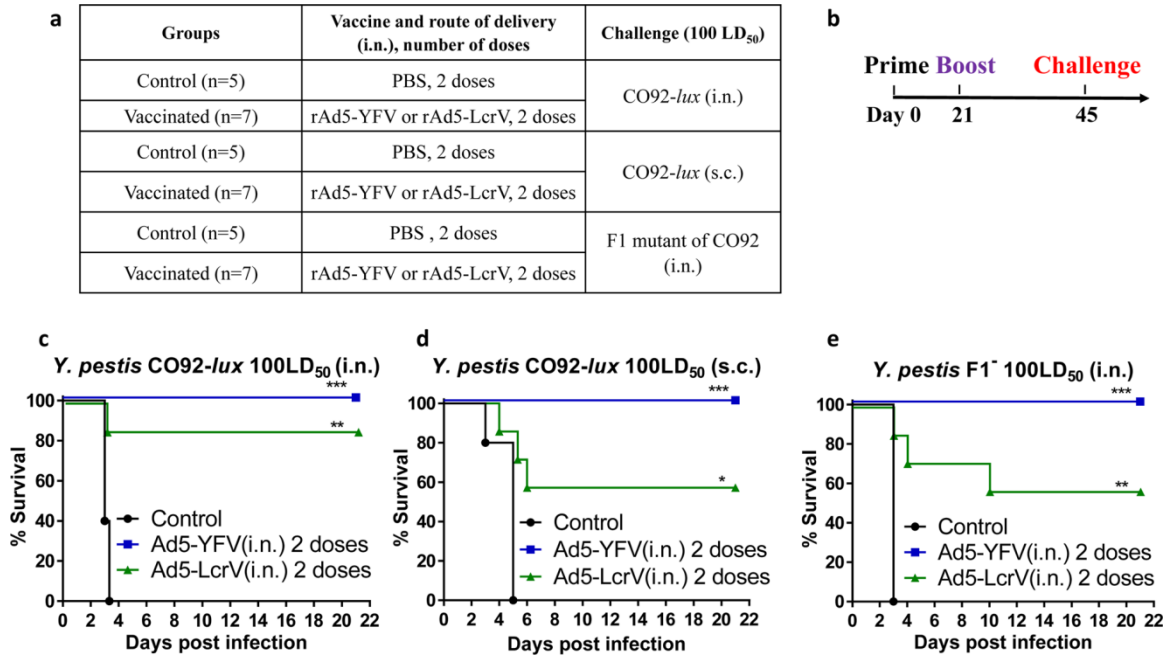


**Figure 6: Animal protection conferred by immunization of mice with rAd5-YFV or rAd5-LcrV vaccines.**

Mice (n=5-7/group) were immunized (i.n.) twice 21 days apart with either 1.2x 10<sup>10</sup> v.p. of rAd5-YFV or rAd5-LcrV vaccines, with mice receiving PBS served as controls (a). After 24 days post second immunization, animals were challenged with 100 LD<sub>50</sub> of *Y. pestis* CO92-*lux* (b) by either i.n. route (c) or s.c. route (d) or by *Y. pestis* CO92 F1-negative strain via the i.n. route (e). The percent of animal survival was then plotted. P values were calculated using Kaplan-Meier analysis with log-rank (Mantel-Cox) test. Asterisks represent comparison to the control group. \*P<0.05, \*\*P<0.01, \*\*\*P<0.001. Two biological replicates were performed, and data plotted.

To further evaluate the 2-dose immunization strategy with the rAd5-YFV vaccine, we included the F1-minus CO92 strain in addition to the parental CO92 for challenge

studies. The capsular antigen F1 is one of the three immunogens in the rAd5-YFV vaccine, and F1-negative strains of *Y. pestis* exist in nature that are fully virulent. Thus, with the F1-minus CO92 challenge, the protection conferred by the rAd5-YFV vaccine is only dependent on antibodies to LcrV and YscF. Therefore, for comparison, we also included the monovalent vaccine rAd5-LcrV in the study to assess the role of YscF in the rAd5-YFV vaccine when challenging immunized mice with the F1-minus CO92 strain. As expected, both trivalent and monovalent vaccines provided protection to immunized mice albeit to varying degrees (**Fig. 6**). Various animal groups and the timeline for vaccination and challenge have been provided in **Fig. 6a&b**. When mice were challenged with the parental *Y. pestis* CO92 strain, we observed complete protection (100%) in the rAd5-YFV vaccine-immunized group, and an impressive 86% protection in the rAd5-LcrV vaccinated group, in a pneumonic plague mouse model (**Fig. 6c**). The efficacy of the rAd5-LcrV monovalent vaccine was decreased in a bubonic challenge model with only a 57% protection rate, while the rAd5-YFV trivalent vaccine provided 100% protection (**Fig. 6d**). Importantly, when the immunized mice were challenged with the F1-minus *Y. pestis* CO92 strain in a pneumonic plague model, the rAd5-YFV trivalent vaccine still conferred complete protection to mice, while the rAd5-LcrV monovalent vaccine provided only 57% protection (**Fig. 6e**).

### **The rAd5-YFV trivalent vaccine elicits better humoral immune response than the rAd5-LcrV monovalent vaccine**

We measured antibody titers to F1 and V in the sera of mice immunized with both the trivalent and monovalent vaccines using a most commonly used purified rF1-V fusion protein as the source of antigen. Various animal groups and the timeline for vaccination

have been provided in **Fig. 7a&b**. A significant increase in anti-F1-V IgG antibody titers was noted after the second dose of rAd5-YFV vaccine. Importantly, the trivalent vaccine mounted significantly higher anti-F1-V IgG antibody titers compared to the rAd5-LcrV monovalent vaccine after 2-doses of the vaccination regimen (**Fig. 7c**).

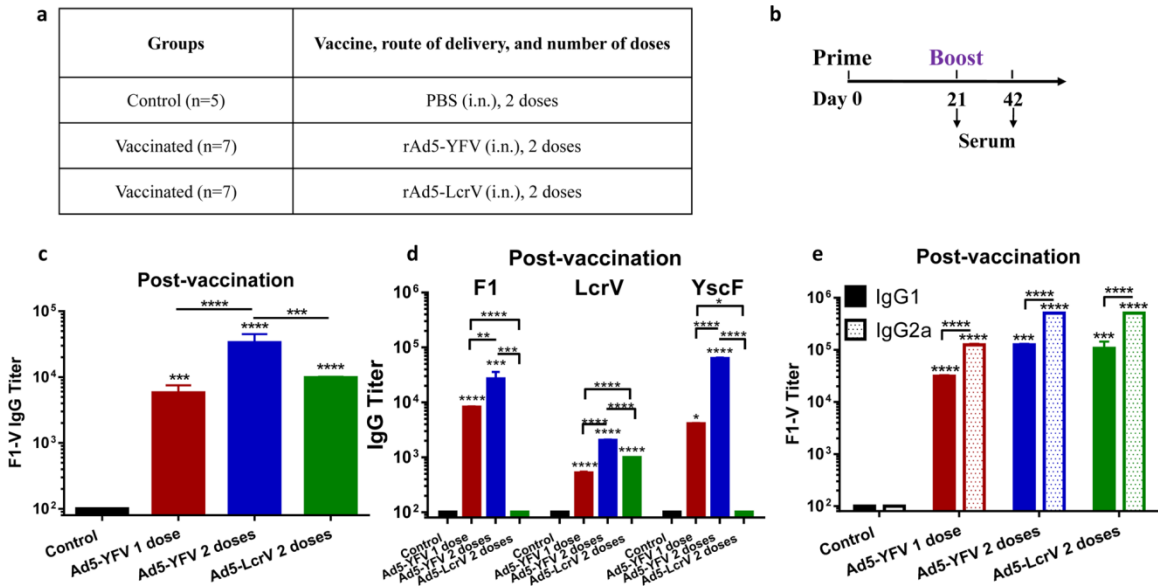


**Figure 7: Antibody responses generated in mice immunized with rAd5-YFV or rAd5-LcrV vaccines.**

Mice (n=5-7/group) were immunized (i.n.) twice 21 days apart with  $1.2 \times 10^{10}$  v.p. of rAd5-YFV or rAd5-LcrV vaccines, with animals that received PBS served as controls (a&b). Serum was collected on day 21 after the first dose as well as after the second dose of immunization (day 42) (b). The IgG antibody titers to F1-V fusion protein (c) or to each individual antigen F1, LcrV, and YscF (d), as well as the IgG1 and IgG2a isotype titers to F1-V fusion protein (e), were measured by ELISA. The geometric mean of each sample  $\pm$  standard deviations was used for data plotting. P values were calculated using a one-way or two-way ANOVA with Tukey's *post hoc* test to compare multiple groups or Student's t-test to compare 2 groups. Asterisks above columns represent comparison to the control group, while horizontal bars represent differences between test groups. \*P<0.05, \*\*P<0.01, \*\*\*P<0.001, \*\*\*\*P<0.0001. Two biological replicates were performed, and data plotted.



To further profile the antibody titers, we measured IgG antibodies against the individual antigens (F1, LcrV, and YscF). We observed the same boosting effect on antibody production with significant increases in IgG titers against all 3 antigens after the second dose of the rAd5-YFV vaccine (**Fig. 7d**). As expected, no antibodies against F1 or YscF were detected in sera from mice vaccinated with the rAd5-LcrV monovalent vaccine. Further, antibody levels against LcrV were lower in mice vaccinated with 2 doses of the rAd5-LcrV monovalent vaccine than in mice that had been administered 2 doses of the rAd5-YFV trivalent vaccine (**Fig. 7d**). Interestingly, the antibody titer to YscF was the highest in the rAd5-YFV trivalent vaccine group of mice followed by antibody titers to F1 and then LcrV, indicating variation in immunogenicity and/or epitopes of the 3 antigens that were exposed in the rAd5-YFV vaccine (**Fig. 7d**). Some variations in the IgG titers in **Figs. 7c&d** could be reflective of antigens that were used to coat the microtiter plates and/or avidity of the antibodies to F1-V or individual F1, LcrV, and YscF antigens. Further, since antibody levels to F1 were higher than that of LcrV (**Fig. 7d**), it is expected that antibody titers to F1-V (**Fig. 7c**) would be similar to that of F1 titers observed in **Fig. 7d**.

Regarding isotypes of antibodies generated to F1-V, slight increases in both IgG1 and IgG2a titers were observed after the second dose of the rAd5-YFV trivalent vaccine (**Fig. 7e**). Both rAd5-YFV trivalent- and rAd5-LcrV monovalent- vaccines generated similar levels of IgG1 and IgG2a against F1-V (**Fig. 7e**) although the OD<sub>450nm</sub> readings were higher for the rAd5-YFV trivalent vaccine than that of the rAd5-LcrV monovalent vaccine at a given dilution, without overall affecting the antibody titers. Further, significantly higher levels of IgG2a compared to that of IgG1 indicated a stronger Th1-biased immune response that was generated by both the vaccines (**Fig. 7e**).

## The rAd5-YFV trivalent vaccine induces better cell-mediated immune response compared to that of the rAd5-LcrV monovalent vaccine

We then compared cell-mediated immune responses generated by the trivalent versus the monovalent rAd5 vaccine. This was accomplished by measuring specific T- and B- cell proliferation in response to rF1-V stimulation (*ex-vivo*) post-immunization as well as in response to *Y. pestis* infection (*in vivo*) on day 3 post-challenge of mice (**Fig. 8a&b**). The proliferation of immune cells was evaluated by measuring bromodeoxyuridine (BrdU) incorporation in dividing cells.

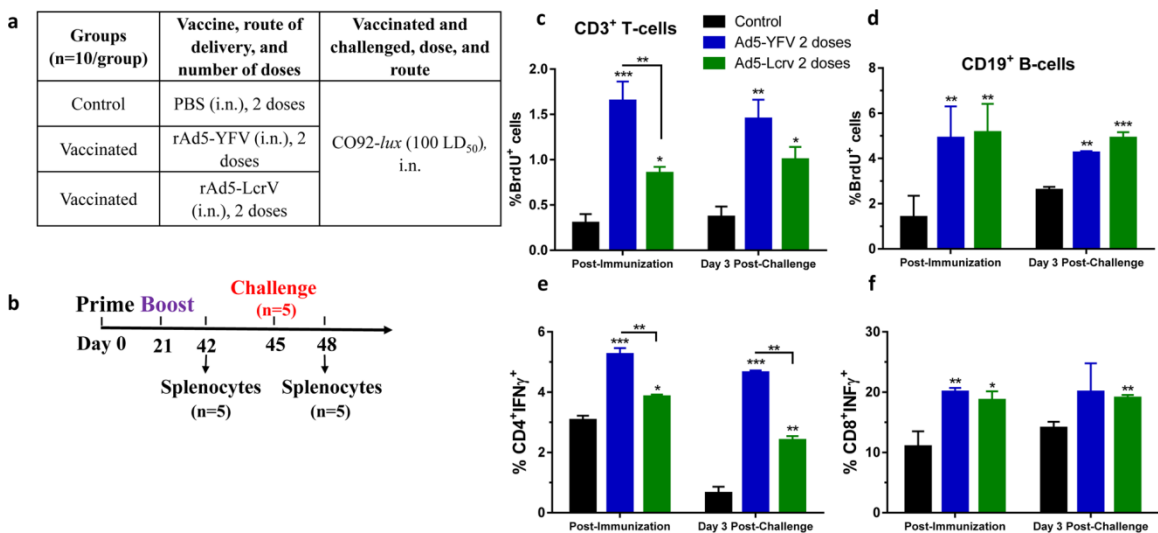


**Figure 8: Cell proliferation and IFN $\gamma$  production in mice immunized with either rAd5-YFV or the rAd5-LcrV vaccines.**

Mice (n=10/group) were immunized (i.n.) twice 21 days apart with indicated vaccines as described in panel a. Splens were harvested from mice (n=5) either 21 days after the second vaccination dose or on day 3 post i.n. challenge with 100 LD<sub>50</sub> of *Y. pestis* CO92-*lux* (b). For cell proliferation study after the second vaccination dose, splenocytes were stimulated with rF1-V (100  $\mu$ g/ml) for 72 h at 37°C, and then 10  $\mu$ M BrdU was added during the last 18 h of incubation with the recombinant protein. For post-challenge time point, mice (n=5) was i.n. challenged on day 24 after immunization (day 45 of the study) with *Y. pestis* CO92-*lux* (b), and 1mg/100  $\mu$ L BrdU was i.p. injected daily into mice for 3 days. On day 3 p.i., splens were harvested after 1 h of last BrdU injection. The harvested splenocytes were then stained for T- and B- cell surface markers (CD3 and CD19) as well as for incorporated BrdU, and analyzed by flow cytometry. The percent of BrdU

incorporation in CD3 (c) or CD19 (d) positive cells was plotted. For IFN $\gamma$  studies (e and f), splenocytes were first stimulated with PMA and Ionomycin. Brefeldin A was added to prevent secretion of cytokines. Cells were then stained with T-cell surface markers CD3, CD4, and CD8 followed by intracellular IFN $\gamma$  staining. Percentage of CD4<sup>+</sup> IFN $\gamma$ <sup>+</sup> (e) and CD8<sup>+</sup> IFN $\gamma$ <sup>+</sup> cells (f). P values were calculated using a one-way ANOVA with Tukey *post hoc* test to compare multiple groups or student t-test to compare rAd5-LcrV CD8<sup>+</sup>IFN $\gamma$ <sup>+</sup> T-cells to control during post-challenge time point. Asterisks above columns represent comparison to the control group, while horizontal bars represent differences between test groups. \*P<0.05, \*\*P<0.01, \*\*\*P<0.001. Two biological replicates were performed, and data plotted.

As shown in **Fig. 8c**, we observed higher T-cell proliferation in rAd5-YFV trivalent vaccine-immunized mice than that in the rAd5-LcrV monovalent vaccinated animals during both post-immunization and post-challenge. On the other hand, both rAd5-YFV trivalent- and rAd5-LcrV monovalent- vaccine immunized mice had a similar level of B-cell proliferation, although their proliferation levels were significantly higher compared to their respective controls (**Fig. 8d**). Our earlier studies have convincingly shown that Ad5 vector- and rAd5-YFV- vaccinated mice did not contribute to any non-specific cellular immune responses, including T-cell proliferation(40). The cellular immune responses were only triggered after stimulating T-cells with *Y. pestis* specific antigens.

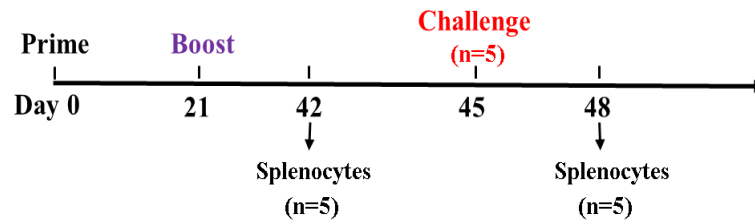
To further investigate the T-cell response, interferon gamma (IFN $\gamma$ ) production was measured by flow cytometry both during post-immunization and at 3-day post-challenge with parental *Y. pestis* CO92 in mice (**Fig. 8b**). CD4<sup>+</sup> T-cells from the rAd5-YFV trivalent vaccine-immunized mice had a significantly higher percentage of IFN $\gamma$  producing cells compared to the respective control, as well as to the rAd5-LcrV monovalent vaccine-immunized animals (**Fig. 8e**). There was no difference in percentage of CD8<sup>+</sup> IFN $\gamma$ <sup>+</sup> T-cells between rAd5-YFV trivalent and rAd5-LcrV monovalent vaccine-immunized mice,

but their percentages were increased in both the vaccinated groups as compared to their respective control groups of mice (**Fig. 8f**). No non-specific IFN $\gamma$  production was noted when T-cells from the Ad5 vector- and rAd5-YFV- vaccinated mice remained unpulsed, but significantly higher levels of IFN $\gamma$  was produced when T-cells were pulsed with rF1-V, based on ELISpot(40).

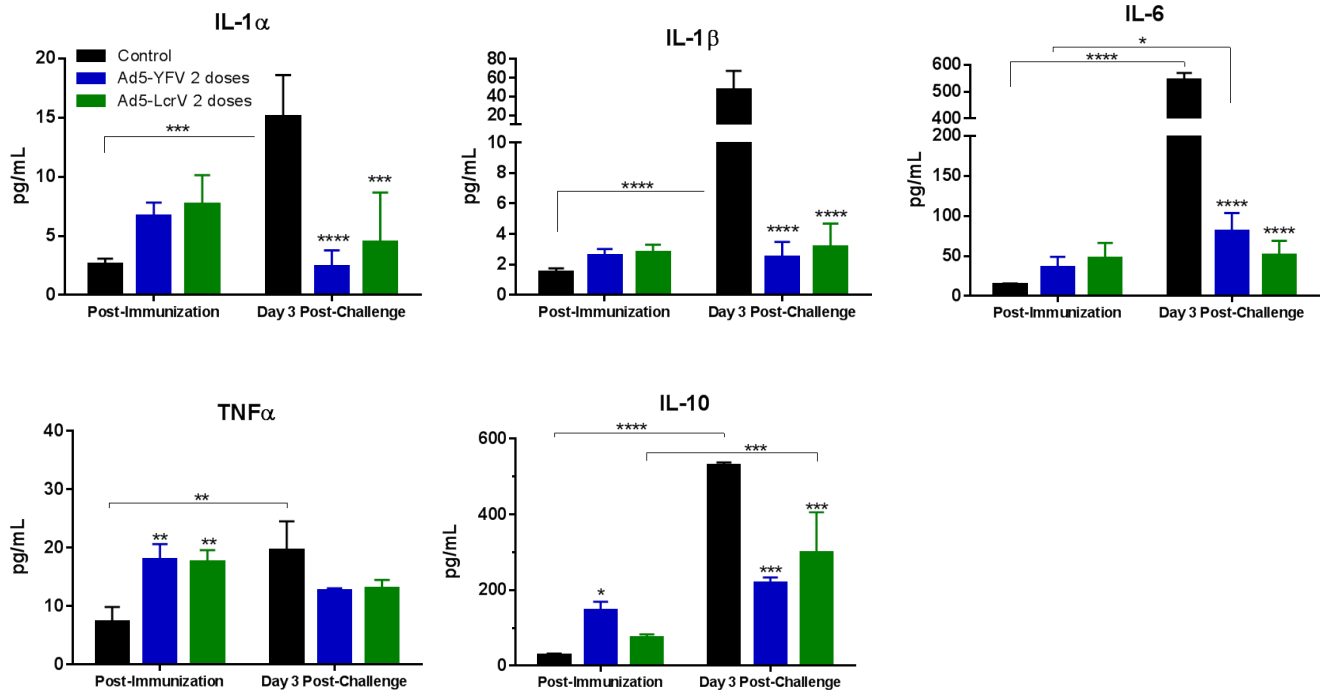
a

| Groups (n=10/group) | Vaccine, route of delivery, and number of doses | Vaccinated and challenged, dose, and route     | Cytokine analysis post immunization and post challenge by Bioplex |
|---------------------|---|--|---|
| Control             | PBS (i.n.), 2 doses                             | CO92- <i>lux</i> (100 LD <sub>50</sub> ), i.n. | Pro-inflammatory, Th1, Th2, and chemokines                        |
| Vaccinated          | rAd5-YFV (i.n.), 2 doses                        |  |   |
| Vaccinated          | rAd5-LcrV (i.n.), 2 doses                       |  |   |

b



c



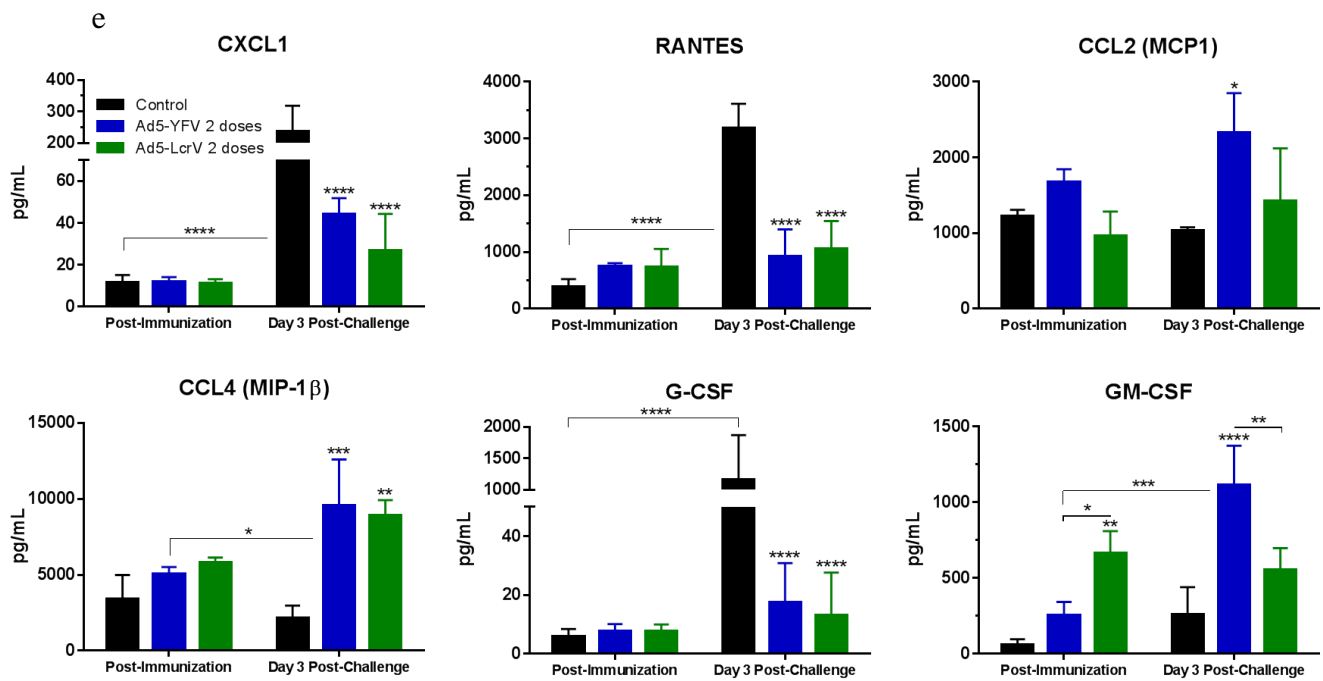
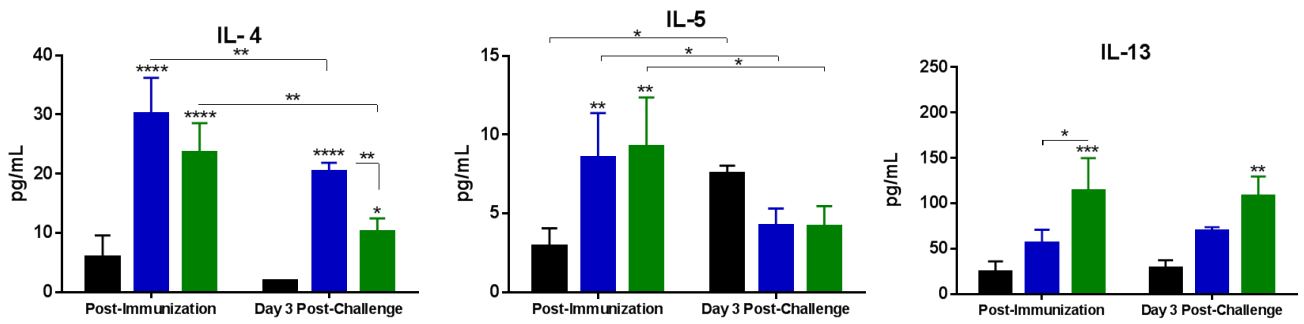
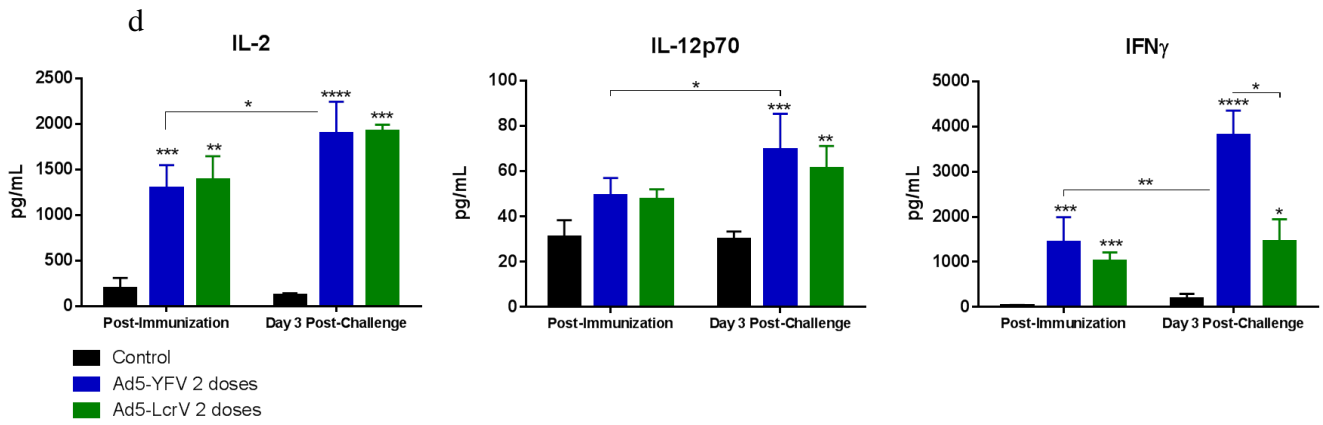


**Figure 9. Splenocyte cytokine and chemokine profiles in mice immunized with either rAd5-YFV or rAd5-LcrV vaccines.**

Mice (n=10/group) were immunized (i.n.) twice 21 days apart with  $1.2 \times 10^{10}$  v.p. of rAd5-YFV or rAd5-LcrV vaccines, with animals receiving PBS served as controls (a). Twenty-one days after the second vaccination dose or on day 3 post-challenge, spleens were harvested from mice (n=5/group/time point) and stimulated with purified F1-V (100  $\mu\text{g}/\text{mL}$ ) for 3 days (b). The cytokines in the culture supernatants were analyzed by using Bioplex-23 assay and expressed as the arithmetic means  $\pm$  standard deviations. The proinflammatory and anti-proinflammatory cytokines were listed in (c), while the Th1 and Th2 cytokines were displayed in (d), and the chemokines as well as colony stimulating factors are presented in (e). P values were calculated using a two-way ANOVA with Tukey post hoc test to compare multiple time-points or One-way ANOVA with Tukey post hoc test to compare groups within the same time-point. Asterisks above columns represent comparison to the control group, while horizontal bars represent differences between test groups. \*P<0.05, \*\*P<0.01, \*\*\*P<0.001, \*\*\*\* P<0.0001. Two biological replicates were performed, and data plotted.

We also measured cytokine and chemokine production in the splenocyte culture supernatants (**Fig. 9a&b**). Compared to the respective controls (**Fig. 9c-e**), the overall mouse cytokines and chemokines induced by either rAd5-YFV trivalent or rAd5-LcrV monovalent vaccine immunizations were similar in terms of their trends and levels. Significantly higher levels of pro-inflammatory cytokines IL-1 $\alpha$ , IL-1 $\beta$ , and IL-6 were observed in control mice during infection. However, their levels remained low in either rAd5-YFV trivalent or rAd5-LcrV monovalent vaccinated animals both during immunization and post challenge (**Fig. 9c**). Significantly higher amounts of IFN $\gamma$ , IL-4, and GM-CSF were observed in the rAd5-YFV trivalent vaccine-immunized mice when compared to animals vaccinated with the rAd5-LcrV monovalent vaccine in response to infection (**Fig. 9d&e**). On the other hand, IL-13 and GM-CSF levels were substantially elevated in the rAd5-LcrV monovalent vaccinated mice (prior to infection) as compared to animals that were immunized with the rAd5-YFV trivalent vaccine (**Fig. 9d&e**).

### **The rAd5-YFV trivalent vaccination regimen induces a sustained protective immune response**

To assess the long-term protective immune responses, the immunized mice were challenged 85 days (12 weeks) after immunization (**Fig. 10a&b**), and the progression of infection monitored by whole body *in vivo* imaging. As shown in **Fig. 10c** at day 3 post infection (p.i.), a strong bioluminescence detected in the challenged control mice was indicative of *Y. pestis* CO92-*lux* (with the luciferase gene) dissemination. However, the rAd5-YFV-immunized and challenged animals did not exhibit any bioluminescence at day 3 p.i., indicating clearing of the pathogen. All control mice in both *Y. pestis* CO92-*lux* and its F1-minus strain challenged groups went to moribund stage on day 3 p.i., while 100% of the rAd5-YFV-immunized ones survived from the challenges (**Fig. 10d&e**), correlating with non-detectable number of *Y. pestis* CO92-*lux* on day 3 p.i. (**Fig. 10c&f**). Furthermore, animal mortality was correlated with high numbers of plague bacilli present in multiple organs (lungs, liver, and spleen) of moribund control mice on day 3 p.i., while no *Y. pestis* was detected in the organs of rAd5-YFV-immunized and challenged mice neither on day 3 p.i. (**Fig. 10c**, based on bioluminescence) nor on day 28 p.i., based on standard bacterial plate counts (**Fig. 10f**).



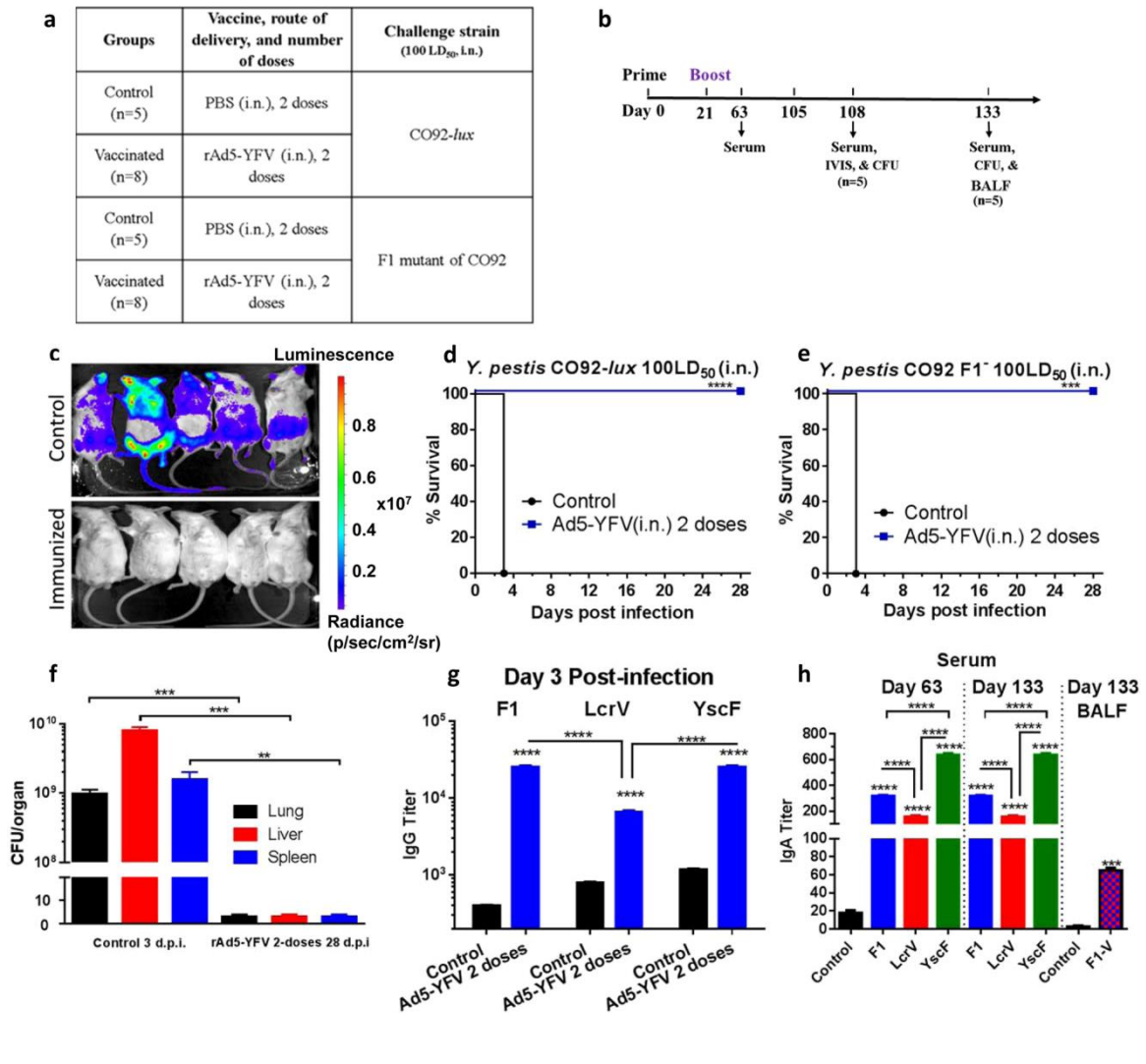


**Figure 10: Long-term protection and antibody titers in mice immunized with 2 doses of the rAd5-YFV vaccine.**

Mice (n=5-8/group) were immunized (i.n.) twice 21 days apart with  $1.2 \times 10^{10}$  v.p. of the rAd5-YFV vaccine, with animals receiving PBS served as controls (Fig. 5a). Eighty-four days (day 105 of study) after last vaccination, mice were i.n. challenged with 100 LD<sub>50</sub> ( $5 \times 10^4$  CFU/40  $\mu$ L) of *Y. pestis* CO92-*lux* or *Y. pestis* CO92 F1-minus strain (Fig. 5b). The progression of infection in *Y. pestis* CO92-*lux* challenged mice was monitored by IVIS, and representative images of mice with a heat map of bacterial burden from lowest (violet) to highest (red) at day 3 p.i. are shown (Fig. 5c). The percent of animal survival was plotted (d) for the *Y. pestis* CO92-*lux* challenge or (e) for its F1 minus strain challenge. The actual bacterial loads in moribund control mice at day 3 p.i., and in the rAd5-YFV immunized mice at day 28 p.i. is displayed in panel f. On day 3 p.i., serum was collected from each group, and F1, LcrV, and YscF specific IgG titers were determined by ELISA (g). On days 63, and 133 (Fig. 5b), serum was examined for F1, LcrV, and YscF specific IgA titers by ELISA (Fig. 5h). At 28 days post-challenge, BALF was collected from mice in the *Y. pestis*

CO92-*lux* challenged cohort and F1-V specific IgA titers were determined by ELISA (Fig. 5h). P values were calculated using Kaplan-Meier analysis with log-rank (Mantel-Cox) test for animal survival. One-way or two-way ANOVA with Tukey's *post hoc* test to compare multiple groups or Student's t-test to compare 2 groups. Asterisks above columns represent comparison to the control group, while horizontal bars represent differences between test groups. \*P<0.05, \*\*P<0.01, \*\*\*P<0.001, \*\*\*\* P<0.0001. Two biological replicates were performed, and data plotted.

We also observed that immunized mice maintained high IgG antibody titers to F1, LcrV, and YscF in sera on day 3 p.i. with *Y. pestis* CO92-*lux* (compare Fig. 7d and Fig. 10g). We also measured serum IgA levels against all 3 antigens on days 63 and 133 (Fig. 10b). As noted in Fig. 10h, higher IgA antibody titers were noted against F1 and YscF, with relatively lower IgA titers to LcrV, data which matched IgG antibody titers (Fig. 10g). After 28 days post challenge (day 133), a significantly higher IgA titers to F1-V were also detected in the broncho-alveolar lavage fluid (BALF) collected from the rAd5-YFV-immunized mice that survived the *Y. pestis* CO92-*lux* infection when compared to BALF collected from the uninfected control animals (Fig. 10h).

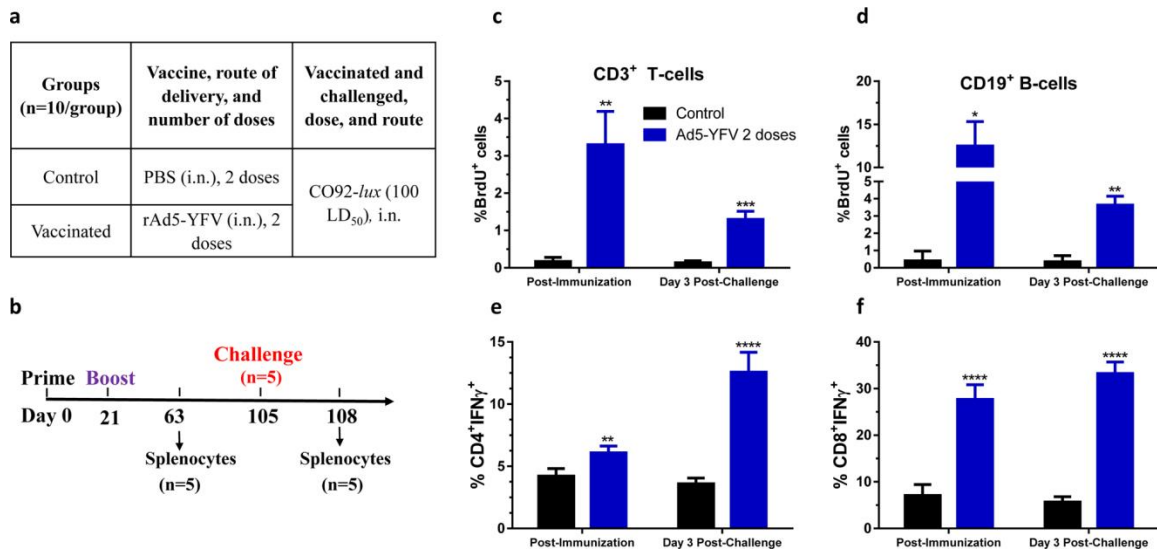


**Figure 11: Cell proliferation and IFN $\gamma$  production in mice immunized with rAd5-YFV vaccine during long-term study.**

Mice (n=10/group) were immunized (i.n.) twice 21 days apart with rAd5-YFV vaccine (a). Forty-two days after the second vaccination (day 63 of the study), spleens were harvested from mice (n=5) and also on day 3 post-challenge with *Y. pestis* CO92-*lux* (b). For cell proliferation study after the second vaccination, mouse splenocytes were stimulated with rF1-V and treated with BrdU for the post-vaccination time point (n=5) as described in panel b. For the post-challenge time point, mice (n=5) was i.n. challenged on day 85 after immunization (day 105 of the study) with *Y. pestis* CO92-*lux*, and i.p. injected with BrdU (b). On day 3 p.i., spleens were harvested and splenocytes were then stained for T- and B-cell surface markers (CD3 and CD19) as well as for incorporated BrdU, and analyzed by flow cytometry. The percent of BrdU incorporation in CD3 (c) or CD19 (d) positive cells was plotted. For IFN $\gamma$  studies (e and f), splenocytes were stimulated with PMA, Ionomycin, and Brefeldin A. Cells were then stained with T-cell surface markers CD3, CD4, and CD8 followed by intracellular IFN $\gamma$  staining. Percentage of CD4<sup>+</sup> IFN $\gamma$ <sup>+</sup> (e) and CD8<sup>+</sup> IFN $\gamma$ <sup>+</sup> cells (f) were shown. Student's t-test was used to determine statistical significance between T-cell population from control and rAd5-YFV vaccinated groups. Asterisks above columns represent comparison to the control group. \*P<0.05, \*\*P<0.01, \*\*\*P<0.001, \*\*\*\*P<0.0001. Two biological replicates were performed, and data plotted.

We also observed that the rAd5-YFV immunized mice (**Fig. 11a&b**) had significantly higher levels of proliferating T-cells (**Fig. 11c**) and B-cells (**Fig. 11d**) post-immunization as well as on day 3 post-challenge with *Y. pestis* CO92 as compared to their appropriate controls (**Fig. 11a**). Similarly, the rAd5-YFV vaccinated mice had higher percentages of CD4<sup>+</sup> IFN $\gamma$ <sup>+</sup> T-cells (**Fig. 11e**) and CD8<sup>+</sup> IFN $\gamma$ <sup>+</sup> T-cells (**Fig. 11f**) compared

to their respective controls (**Fig. 11a**) both at post-immunization and post-challenge of vaccinated mice.

### **The rAd5-YFV trivalent vaccination regimen elicits strong cytokine and chemokine production in the long-term study**

We measured cytokine and chemokine production by splenocytes on day 63 post-immunization and day 3 post-challenge with parental *Y. pestis* CO92 strain (**Fig. 12a&b**). Based on our earlier studies(43), we have shown that with the live-attenuated plague vaccines, significant levels of CD19<sup>+</sup> CD38<sup>+</sup> IgG memory B cells could be detected until day 63. However, by day 84, the percentage of these memory B cells were similar to that of the control. Similarly, percentage of CD4<sup>+</sup> T cells producing IL-17 remained high until day 63, declining to that of control by day 84. Based on these data, we chose to examine cytokines/chemokines on day 63 post immunization(43).

In response to rAd5-YFV vaccination, the overall cytokines and chemokines in mice were either elevated or remained at compatible levels to those of control mice prior to infection (**Fig. 12a&b**). However, significant changes in cytokine and chemokine levels were observed during infection of immunized mice.

More specifically, the pro-inflammatory cytokines (IL-1 $\alpha$ , IL-1 $\beta$ , IL-6 and TNF- $\alpha$ ), as well as an anti-inflammatory cytokine IL-10, all were elevated in challenged control mice (**Fig. 12c-g**), but were generally unchanged in immunized mice in response to CO92 challenge (**Fig. 12c-g**). In contrast, cytokines related to a Th1-immune response [IL-2, IL-12(p70), and IFN $\gamma$ ] were significantly elevated in immunized mice, while these cytokines remained almost unchanged in control mice in response to an infection (**Fig. 12h-j**). On

the other hand, the Th2-immune response cytokines (IL-4, IL-5, and IL-13) were induced in vaccinated mice compared to control animals. However, they either significantly subsided (IL-4 and IL-5) or maintained at a similar level (IL-13) in immunized mice in response to an infection with CO92 (**Fig. 12k-m**). It is important to note that vaccinated and challenged animals still had higher levels of IL-4 and IL-13 compared to challenged control mice (**Fig. 12k&m**).

For the chemokines and G-CSF (**Fig.12n-r**), a similar level was observed in both control and immunized mice except for GM-CSF (**Fig. 12s**) which was significantly higher in immunized mice than in controls. However, in response to an infection, the levels of CXCL1, RANTES and G-CSF were significantly higher in challenged control mice (**Fig. 12n,o&r**). In contrast, MCP1 and CCL4 were elevated in immunized and infected mice (**Fig. 12p&q**), while GM-CSF (**Fig. 12s**) remained at high levels in both immunized as well as in immunized and challenged mice.

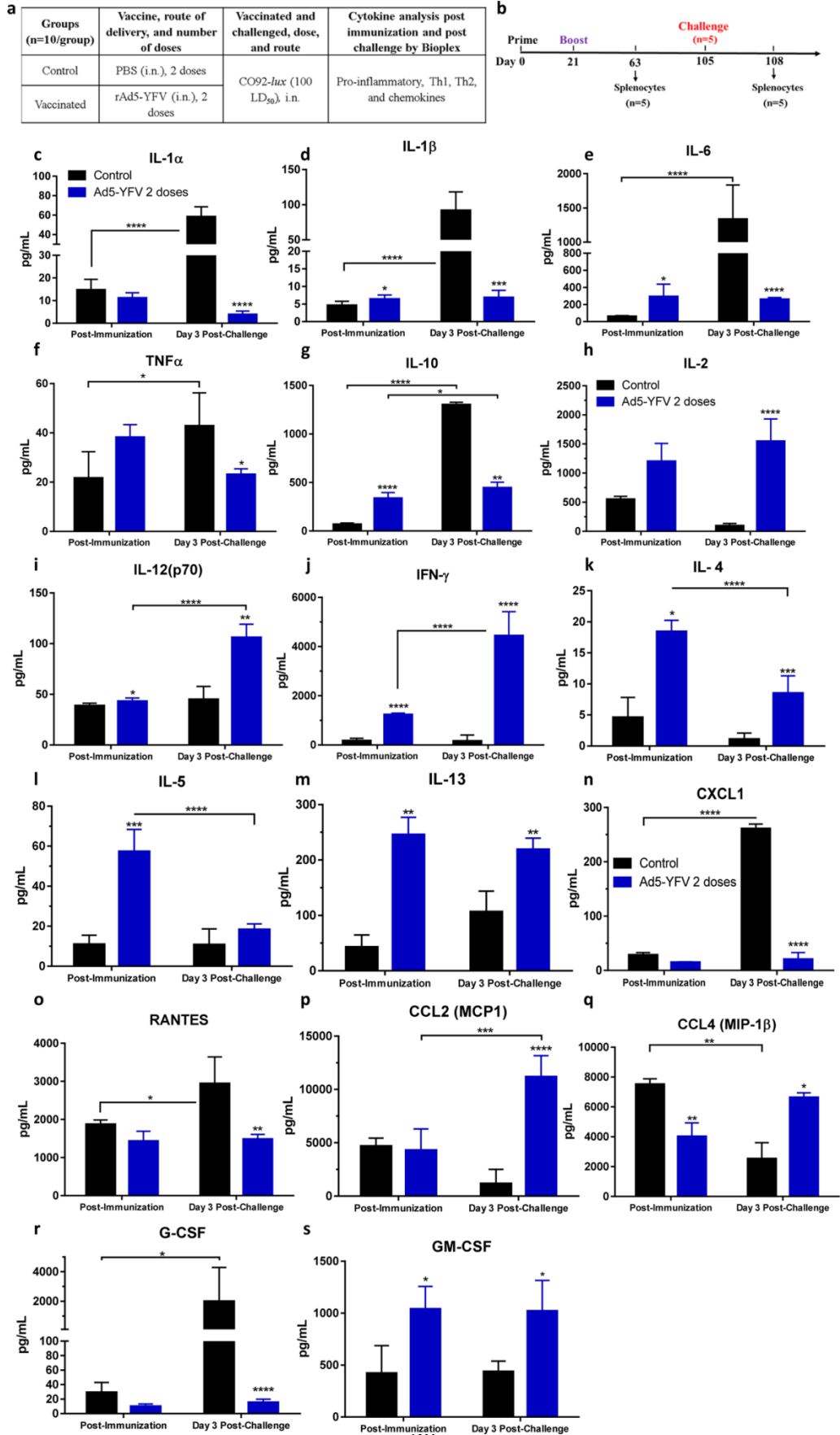


**Figure 12: Splenocyte cytokine and chemokine profiles from the rAd5-YFV vaccine-immunized mice during a long-term study.**

Mice (n=10/group) were immunized (i.n.) twice 21 days apart with  $1.2 \times 10^{10}$  v.p. of rAd5-YFV vaccine or rAd5-LcrV vaccine, with animals receiving PBS served as controls (Fig. 7a). Forty-two days after the second vaccination dose or on day 3 post-challenge, spleens were harvested from mice (n=5/group/time point) and stimulated with purified F1-V (100  $\mu\text{g/mL}$ ) for 3 days (b). The cytokines in the culture supernatants were analyzed by using Bioplex-23 assay and expressed as the arithmetic means  $\pm$  standard deviations. The proinflammatory and anti-proinflammatory cytokines were listed in panel Fig. 7c-g, while the Th1 and Th2 cytokines were displayed in panels h-m, and the chemokines as well as colony stimulating factors are presented in panels n-s. P values were calculated using a two-way ANOVA with Tukey *post hoc* test to compare multiple time-points or student t-test to compare 2 groups within the same time-point. Asterisks above columns represent comparison to the control group, while horizontal bars represent differences between test groups. \*P<0.05, \*\*P<0.01, \*\*\*P<0.001, \*\*\*\* P<0.0001. Two biological replicates were performed, and data plotted.

**DISCUSSION**

In the aftermath of the 2017-2018 pneumonic plague outbreak in Madagascar, the WHO released a TPP outlining the desired characteristics of a successful plague vaccine(50). These characteristics included: no more than 2-dose regimen, durability of protection, needle-free administration, universal coverage against all plague-causing strains, and stability during storage(50). This outbreak of 2017-2018 seemed to mirror the third pandemic, which first established plague in Madagascar(14), and served as a reminder to proactively react to prevent future plague outbreaks(14).

Considering number of plague cases and deaths reported to WHO from 33 countries, including the US between 2013-2018 (a case fatality rate of 17.5%), necessitates the development of new generation plague vaccines. Further, the recent finding that amoebae can serve as reservoirs for the plague bacterium is alarming(14). Finally, the natural cellular immune response to pneumonic plague is not well understood, and to date, no phase III clinical trials have been conducted on any of the plague vaccines. Therefore,

our study is timely to test a new generation plague vaccine in mice, and study in depth the immune responses.

As alluded to in our earlier paper(40), we preferred to use Ad5 vector for developing plague vaccine because of its i) well characterized viral genome and the capability of integrating multiple genes; ii) the use of Ad5 vector for gene therapeutic applications in humans; iii) broad tropism infecting a variety of dividing and non-dividing cells; iv) ability of adenoviruses to effectively present transgene products to antigen presenting cells *in vivo* to promote rapid and robust humoral and cellular immune responses; v) preferential induction of Th1-type immune responses, alleviating Th2-mediated eosinophil-related immunopathology; vi) ability of adenoviruses to replicate to high titers in tissue culture cells; vii) low biocontainment requirements for producing adenoviral vaccines, viii) can be applied systemically as well as through mucosal surfaces, and adenoviruses are relative thermostable to facilitate their clinical use; ix) inexpensive production, x) no need for an adjuvant, and the vaccine can be delivered as aerosol mist stimulating potent and long-lasting humoral- and cell- mediated immune responses, and xi) plug and play platform to develop multivalent/multicomponent vaccines.

Ad5 vector was also used in evaluating the efficacy of monovalent Ad5-F1 and Ad5-LcrV vaccines in a pneumonic plague mouse model using only the parental *Y. pestis* CO92 strain; however, the vaccines were administered by the i.m. route(51). Further, we noted that while 1 dose of the rAd5-LcrV monovalent vaccine ( $8 \times 10^9$  v.p.) provided only 20% protection to mice in a pneumonic plague mouse model when administered by the i.n. route, no protection was observed when delivered by the i.m. route at 90 LD<sub>50</sub> of CO92, in spite of high antibody titers(40). Our studies also showed that i.n. administration of the



vaccine bypasses pre-existing antibodies to Ad5 vector to provide protection to animals(40). Although Ad5 is the most prevalent serotype to which humans are exposed to, it induces minimal innate pro-inflammatory cytokine responses compared to other adenoviral serotypes used as vaccine vectors(52).

Our 2-dose rAd5-YFV intranasal vaccination strategy essentially fulfills WHO's TPP. The currently developed plague vaccines which underwent phase I and II clinical trials are based on F1 and V proteins mixed with alum(53) or flagellin(33) adjuvants. These vaccines induce a strong humoral response against both F1 and V antigens and have been shown to be efficacious in mouse and some non-human primate models of pneumonic plague. For example, consistent protection was observed in cynomolgus macaques; however, in African green monkeys, inconsistency in protection (0-75%) was noted in multiple studies(3, 54, 55). The precise mechanism(s) for the lack of consistent protection has not been determined; however, humoral responses generated were similar for both non-human primate (NHP) models. It has been hypothesized that cell-mediated immune responses might be needed for complete protection in African green monkeys(3), which are not adequately developed by the F1-V-based subunit vaccines.

While F1 and V are important antigens for plague vaccine development, there are some concerns that highlight the importance of including other plague immunogens to a potential universal plague vaccine. F1 capsule has been shown to be important for *Y. pestis* to resist phagocytosis during infection(56). Strains of *Y. pestis* that lack F1, are still fully virulent in both pneumonic and bubonic models of disease albeit with a longer disease course seen during bubonic infection(10). Bio-sampling studies have estimated that naturally occurring F1-negative *Y. pestis* strains could be as prevalent as 10-16%(11).

Likewise, LcrV is a polymorphic protein which contains hypervariable regions within the COOH-terminal half where protective residues have been identified(57). Studies have shown that vaccination with LcrV from different clades than the LcrV present in the challenge strain do not offer cross-protection during *Y. pseudotuberculosis* infection(57). This scenario presents a situation where a potential outbreak strain of *Y. pestis* could avoid protection offered by a F1-V-based subunit vaccine.

In some earlier studies(54), the efficacy of F1-V-based subunit vaccines against challenge with F1-negative *Y. pestis* strain at 11 weeks post immunization, were reported. Likewise, the efficacy of a mutated *Y. pseudotuberculosis* strain expressing the gene encoding Caf1 when administered orally in mice against evoking bubonic and pneumonic plague was published(58). In this study, we have evaluated efficacy of the rAd5-YFV vaccine (administered by the i.n. route) for the duration of 15 weeks of immunization, and also after challenge with F1-negative *Y. pestis* strain in a pneumonic plague model.

Our rAd5-YFV vaccine potentially could alleviate the issue of infection with either F1-negative *Y. pestis* strains or those harboring LcrV variants by the inclusion of a third antigen YscF, another component of the T3SS(59). During parental *Y. pestis* CO92 pneumonic challenge, we observed slightly decreased protection (86%) by the monovalent rAd5-LcrV vaccine compared to 100% protection provided by the rAd5-YFV trivalent vaccine (Fig. 6c). The decrease in protection was even more pronounced (57% versus 100%) in a bubonic plague model (Fig. 6d). Furthermore, during F1-negative *Y. pestis* intranasal challenge, monovalent rAd5-LcrV vaccination only provided 57% protection, while the trivalent rAd5-YFV vaccination still conferred 100% protection (Fig. 6e). The higher level of protection conferred by rAd5-YFV immunization, especially against the

F1-negative *Y. pestis*, could be contributed to the additional antigen YscF, as the F1 component in both vaccine (rAd5-LcrV and rAd5-YFV)-immunized mice would not have a role. However, we draw this conclusion with caution as LcrV epitopes might possibly be differentially exposed in Ad5-LcrV versus Ad5-YFV vaccines which could afford better protection against infection with the latter vaccine. Such studies would be elaborated in the future.

In retrospect, we would prefer to have generated rAd5-FV vaccine as well. However, since we generated F1<sup>-</sup> mutant of *Y. pestis* CO92(10), we did not feel the necessity to develop rAd5-FV vaccine. We reasoned that infecting Ad5-LcrV-immunized animals with F1<sup>-</sup> mutant of *Y. pestis* CO92 would provide the needed information for this study. We selected YscF as studies have shown that vaccination of mice with this T3SS needle structure protein provided protection to mice against subcutaneous injection with the encapsulated *Y. pestis* CO92(60), and against an intravenously injected pigmentation locus-negative *Y. pestis* KIM strain(59). In addition, we have also shown that serum from animals immunized with *Y. pestis* CO92 reacted strongly with YscF based on our proteomics studies (unpublished data). Therefore, we hypothesized that the protective antigen YscF could be used in combination with F1 and LcrV to formulate a more effective new generation trivalent rAd5-YFV vaccine.

The rAd5-YFV vaccine elicited stronger immune responses in mice compared to that of rAd5-LcrV vaccine. First, a much higher antibody titers were observed in mice immunized with the rAd5-YFV vaccine, and the higher antibodies were not only to the F1-V fusion protein but also to each individual antigen (F1, LcrV and YscF) (Fig. 7c&d). We noted relatively higher IgG1 and IgG2a titers with both rAd5-YFV and rAd5-LcrV

vaccines compared to IgG titers (Fig. 7). Biologically, it should not be the case; however, it is not uncommon and could be reflective of binding affinity and specificity of the secondary antibodies that were used. Indeed, higher levels of IgG subclasses over IgG titers have been reported in other studies as well(59, 61–63). Overall, both the trivalent and monovalent vaccines generated a stronger Th1 response based on IgG2a antibody titers (ratio of IgG2a/IgG1 >1)(64). IgG1 and IgG2a have a differential role in animal protection against various infections(65, 66).

We observed significantly higher levels of T-cell proliferation in rAd5-YFV vaccine-immunized mice than those in rAd5-LcrV vaccinated animals when splenocytes were stimulated *ex-vivo* with F1-V antigen and labeled with BrdU (Fig. 8c). A similar trend was also seen when BrdU was injected during challenge of immunized mice and proliferation measured 72 h post-infection *in vivo* (Fig. 8c). Likewise, we also observed a significantly increased population of CD4<sup>+</sup> IFN $\gamma$ <sup>+</sup> T-cells both post-immunization as well as post-challenge when vaccination occurred with rAd5-YFV over rAd5-LcrV vaccine (Fig. 8e). Furthermore, substantially higher amounts of IFN $\gamma$  and IL-4 were produced in the splenocyte supernatants of rAd5-YFV vaccine-immunized mice than those from rAd5-LcrV vaccinated animals in response to an infection (Fig. 9e). These data further highlighted the advantage of rAd5-YFV over rAd5-LcrV as a plague vaccine candidate.

It has been reported that F1-V-based subunit vaccines adjuvanted with alum bias the immune response towards Th2 based on antibody isotyping(55, 67). In contrast, both rAd5-LcrV and rAd5-YFV vaccination generated strong Th1 and Th2 immune responses and were more biased towards Th1 based on the IgG2a/IgG1 antibody ratio, as well as the cytokine profile with overall higher magnitude of Th1 cytokines over Th2 cytokines (Figs.

7e and Fig. 9d). A Th1-biased response is usually correlated with robust cell-mediated immunity that might be needed for complete protection in African green monkeys against pneumonic plague.

A single dose of the rAd5-YFV vaccine provided impressive but incomplete protection (88%) in mice after challenge with parental CO92 (Fig. 5c). We noted a significant increase in anti-F1-V IgG antibody titers after the second dose of rAd5-YFV vaccine administration (Fig. 7). This boosting effect was also observed in the cell-mediated immune response, as increased levels of antigen specific CD4<sup>+</sup> IFN $\gamma$ <sup>+</sup> T-cells were observed in mice immunized with 2 doses of the rAd5-YFV vaccine compared to a single vaccine dose (Fig. 5d). While these data suggested that 2 doses of vaccine were needed to confer complete protection, 1 dose of the rAd5-YFV vaccine could be given during an outbreak emergency response scenario where there is not enough time to complete a full vaccination regimen as outlined in the TPP developed by the WHO(50).

The TPP also stipulated that a viable vaccine should confer protection for at least 2 years in a reactive vaccination scenario and at least 5-10 years for an ideal preventative use scenario(50). We detected high levels of antigen specific antibody titers in the rAd5-YFV vaccine-immunized mice on day 3 post-challenge which was 88 days (~13 weeks) after last immunization (challenge day 108). These data suggested that 2 doses of the rAd5-YFV vaccine induced a sustained immune response in mice (Fig. 10g-h). It is difficult to correlate duration of protection in mouse models to length of protection that may be generated in humans due to a nonlinear relationship between life stages in mice and humans(68). However, we did not observe a downward trend in antibody titers noted in

other vaccine studies at similar time points when using 1- or 2- doses of the F1+V based subunit vaccines(69, 70).

We also observed significant levels of F1, LcrV, and YscF specific IgA antibodies in the serum of vaccinated mice that survived 4 weeks of challenge compared to the control (Fig. 10h). While we did not measure IgA antibodies in the lungs of vaccinated mice prior to challenge, we noted higher levels of F1-V specific IgA in the BALF after 4 weeks of challenge (Fig. 10h). Antigen specific IgA antibodies, especially present in the airway, are important against respiratory infections, and immunization of animals *via* intranasal route is believed to facilitate the stimulation of mucosa immunity.

However, it is important to note that the role of IgA during pneumonic plague is not clear. In a study by Singh *et al.*, IgA seemed dispensable in protecting mice against pneumonic plague(61). In these studies, YopE-LcrV was produced from an attenuated strain of *Y. pseudotuberculosis*, and animals were immunized by the oral route. Our future studies will fully explore the role of IgA in protection using rAd5-YFV vaccine against pneumonic plague.

In addition to the induction of high-levels of antibodies during the long-term study with the 2-dose vaccination regimen, we also observed significant T- and B- cell proliferation along with higher percentages of CD4<sup>+</sup> IFN $\gamma$ <sup>+</sup> and CD8<sup>+</sup> IFN $\gamma$ <sup>+</sup> cells in mice both after immunization and post-challenge (Fig. 11). These data confirmed that both humoral and cell-mediated immune responses generated were robust and long-lived, and these data were further supported by the splenocyte cytokine and chemokine profiles (Fig. 12) and the rapid clearance of the invaded pathogen (Fig. 10c&f).

In control animals, we noted a significant increase in pro-inflammatory cytokines (IL-1 $\alpha$ , IL-1 $\beta$ , IL-6 and TNF- $\alpha$ ), and chemokines (RANTES/CCL5 and CXCL1) coupled with the surge of G-CSF in response to infection (Fig. 12). This proinflammatory cytokine storm is a typical result of host neutrophil-macrophage interaction in recognition of invading pathogens(71) and corresponds to the characteristic highly proinflammatory state of pneumonic plague (48-72 h p.i.), which leads to animal death if unresolved(4, 72).

The overwhelming proinflammatory cytokine storm is also the main cause of death for current COVID-19 patients, and the anti-inflammatory mediators, especially anti-RANTES, have been preferred for therapeutic intervention(73). Importantly, this proinflammatory cytokine storm was prevented in rAd5-YFV vaccine-immunized mice after *Y. pestis* challenge, as all aforementioned cytokines and chemokines were largely unchanged when compared to their levels before infection (Fig. 12). The excessive level of IL-10 in infected control mice (Fig. 12) overall suppressed the immune response with a much-reduced level of Th1 and Th2 cytokines (Fig. 12). In contrast, the level of IL-10 remained low in immunized and challenged animals compared to that in control and infected mice (Fig. 12) with concomitant higher levels of Th1 and Th2 cytokines post-challenge (Fig. 12).

CXCL1 is an important chemoattractant for neutrophils. High levels of neutrophils are observed in uncontrolled plague infection which correlate with the inflammatory cytokine storm. The latter results in immune-mediated damage to the lungs, contributing to the pathology seen during pneumonic plague(74). On the other hand, we noted increased levels of monocyte/macrophage associated chemokines CCL2/MCP1 and CCL4/MIP1 $\beta$  in rAd5-YFV vaccine-immunized mice that were not seen in controls in response to CO92

infection (Fig. 12). Influx of activated monocytes/macrophages to the infection site is important for controlling infection, clearing dead cells, and reconstituting damaged tissue structures. Beyond chemotaxis, both CCL2 and CCL4 are also involved in modulating host immune response. It has been reported that CCL2 influences myeloid cell behavior which leads to enhance host defense, cellular cleanup, allergic responses, as well as prime monocytes and macrophages in response to subsequent infections(75).

Likewise, CCL4 plays a central role in the normal initiation of T-cell and humoral responses by recruiting CD4<sup>+</sup>CD25<sup>+</sup> T-cell population(76). In addition, we observed higher level of GM-CSF in rAd5-YFV vaccine-immunized mice than in controls (Fig. 12). Unlike G-CSF, which was increased in control mice in response to *Y. pestis* challenge to prolong neutrophil survival (Fig. 12), GM-CSF is a growth and differentiation factor for both granulocyte and macrophage populations(77). Interestingly, GM-CSF has been reported to be involved indirectly in the induction of immunological tolerance and anti-inflammatory responses. More specifically, GM-CSF has been shown to facilitate T-cell-mediated tolerance by inducing “tolerogenic” dendritic cells (DCs)(77, 78). Therefore, the cytokines and chemokines elicited in rAd5-YFV vaccine-immunized mice obviously orchestrated a strong but controlled immune response to combat *Y. pestis* infection, while avoiding tissue damage, which correlated with the clearance of *Y. pestis* with no signs of disease, such as ruffled fur, lethargy, hunched posture, or lack of grooming. Our previous studies have shown that rAd5-YFV vaccinated NHPs did not show any histopathological lesions in any of the examined organs(40).

In conclusion, rAd5-YFV vaccine with a 2-dose regimen induced humoral, mucosal, and cell-mediated immune responses that protected mice against pneumonic



plague caused by parental *Y. pestis* CO92 and its F1-minus mutant. In the future, we will continue to investigate the importance of IgA antibodies and their role in protection from pneumonic plague as well as the potential for the rAd5-YFV vaccine to protect against *Y. pestis* strains with non-cross-reactive LcrV variants. In addition, we will perform a more comprehensive comparison between rAd5-YFV and rAd5-LcrV vaccines (*e.g.*, comparative expression of the *lcrV* gene, kinetics of the immune responses generated), and the individual contribution of YscF and F1 against protection.

# **Chapter 4: Combinatorial Viral Vector-Based and Live Attenuated Vaccines without an Adjuvant to Generate Broader Immune Responses to Effectively Combat Pneumonic Plague**

The following chapter was reproduced with permission from:

Kilgore PB, Sha J, Hendrix EK, Motin VL, Chopra AK. Combinatorial Viral Vector-Based and Live Attenuated Vaccines without an Adjuvant to Generate Broader Immune Responses to Effectively Combat Pneumonic Plague. *mBio*. 2021 Dec 21;12(6):e0322321. doi: 10.1128/mBio.03223-21. Epub 2021 Dec 7. PMID: 34872353; PMCID: PMC8649767.

## **INTRODUCTION**

Like other live-attenuated vaccines, one of the major advantages of LMA is that it delivers a large array of antigens in their native state, closely mimicking natural infection, and such vaccines are expected to provide protection against all circulating *Y. pestis* variants in the nature (19, 45, 58, 61, 79). While the viral vector-based vaccines, especially the replication deficient ones such as Ad5-YFV, are much safer than the live-attenuated vaccines in general, both types of vaccines have their own disadvantages. The most obvious limitation of live-attenuated vaccines is the safety profile, especially in immunocompromised individuals, and the potential concern for reversion (80–82). However, the LMA mutant was rationally designed with complete deletion of three genes located at different locations on the bacterial genome (34). Because of its high level of virulence attenuation and rapid clearance (within 12-24 h) while retaining immunogenicity in animals (42), LMA vaccine was excluded from the Centers for Disease Control and Prevention (CDC) select agent list (<https://www.selectagents.gov/sat/exclusions/hhs.html>).

The Ad5-YFV vaccine only incorporates three plague antigens: F1, LcrV and YscF, and the F1-minus strains of *Y. pestis* have been isolated from humans/animals and are as virulent as the wild-type (WT) plague bacterium (10, 11). In addition, hypervariable

regions within the LcrV protein have been described and antibody responses to these LcrV variants are not cross-protective (57). Therefore, we have successfully added a third protective antigen YscF in this vaccine to circumvent disadvantages of F1-V-based vaccines (40, 59). However, it is still plausible that the Ad5-YFV vaccine alone may not be efficacious against all circulating *Y. pestis* variants, although it is shown to be protective (100%) against CAF<sup>-</sup> mutant of CO92 (41). Importantly, both of our vaccines do not require an adjuvant to boost immune responses, unlike F1-V-based vaccines which employ Alum (33, 53–55, 69, 70).

To alleviate some of the above concerns, in this study, we carried out a heterologous immunization strategy in which both LMA and Ad5-YFV vaccines were administered either simultaneously (1-dose regimen) or in a prime-boost format (2-dose regimen). Our results showed almost all the heterologous vaccination groups of mice induced robust immune responses and provided full protection against lethal challenge doses of both parental and CAF<sup>-</sup> mutant of *Y. pestis* CO92; albeit using potentially slightly different mechanisms. This is the first detailed plague vaccine study with heterologous vaccination regimens that involved a live-attenuated vaccine LMA and a viral vector-based vaccine Ad5-YFV.

## **RESULTS**

### **Virulence and immunogenic characterization of the LMA vaccine candidate in iron overloaded conventional and or in immunocompromised mice**

We have previously shown LMA mutant to be highly attenuated in conventional (immunocompetent) mice (34, 42). To further evaluate its attenuation, we tested safety of the LMA mutant during iron overload conditions in conventional mice to mimic hemochromatosis. We also tested its safety in immunocompromised Rag1 KO mice.

We demonstrated that all of the mice challenged with the LMA vaccine ( $5 \times 10^6$  CFU, more than double the vaccination dose) by the i.n. route survived irrespective of whether the animals were iron-overloaded or not (**Fig. 13A**) with a minimal loss in the body weight (**Fig. 13B**). On the contrary, mice infected with the same dose of the KIM/D27 strain died by day 5 in the presence of  $\text{FeCl}_2$ , while 80% of the animals succumbed to infection without iron-overload (**Fig. 13A**). At a lower challenge dose of  $2 \times 10^5$  CFU, 80% of the iron-overloaded mice succumbed by day 7 while only 20% of the non-iron-overloaded mice succumbed (**Fig. 13A**). In contrast to the LMA mutant, KIM/D27 strain-infected mice showed a dramatic loss in the body weight even at the lower challenge dose of  $2 \times 10^5$  CFU (**Fig. 13B**).

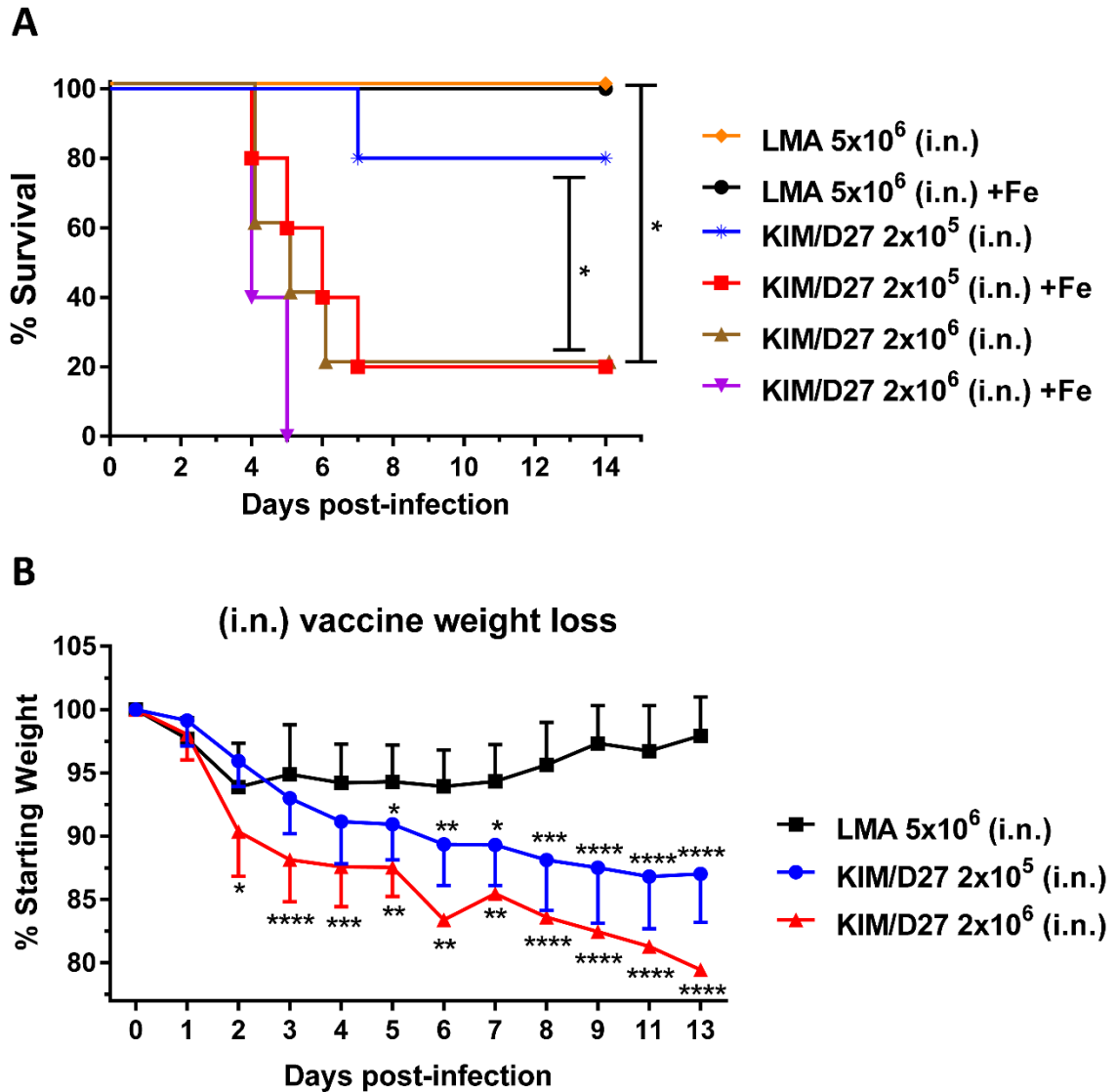


**Figure 13: Iron-overload condition does not restore virulence of the LMA vaccine.**

Swiss-Webster mice ( $n=5$ /group) were injected with  $75\mu\text{g}$  of  $\text{FeCl}_2 \cdot 4\text{H}_2\text{O}$  1h prior to infection and then infected with either the LMA vaccine or the KIM/D27 strain. Loss in body weight and mortality were monitored for 14 days; animals without iron-overload were used as controls (A and B). Kaplan-Meier analysis with log-rank (Mantel-Cox) test was used for analysis of animal survival. Two-way ANOVA with Tukey's post hoc test was used to calculate significant differences in body weight loss between vaccine groups. Asterisks represent the statistical significance between two groups indicated by a line for (A) and between LMA and the indicated dose of KIM/D27 in (B). Since absence or presence of iron did not affect animal body weight, combined data were plotted. Two biological replicates were performed. \*  $p < 0.05$ , \*\*  $p < 0.01$ , \*\*\*  $p < 0.001$  \*\*\*\*  $p < 0.0001$ .

We then infected Rag1 KO mice with 4 LD<sub>50</sub> of CO92 by either the i.n. or the i.m. route since these two routes were previously used for vaccination studies with LMA (34, 42, 43). As shown in **Fig. 14A**, 100% of mice infected by the i.n. or the i.m. route succumbed to infection by day 4-5 p.i., with up to ~20% body weight loss by day 4. We then examined bacterial burden in the lungs, liver, and spleen of these mice and found greater than 10<sup>8</sup> CFU of *Y. pestis* in both the lungs and the spleen, while a significantly higher *Y. pestis* burden, with up to a more than 10<sup>9</sup> CFU, was observed in the liver (**Fig. 14B**).

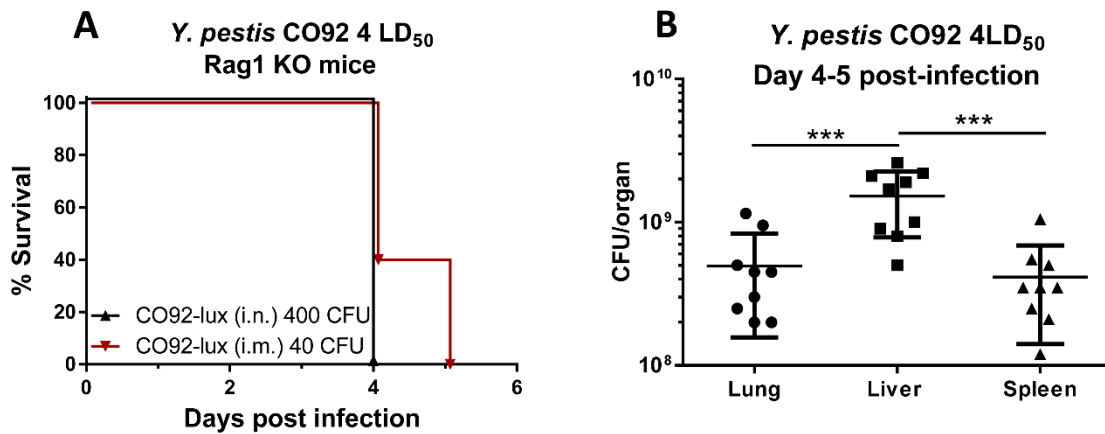


**Figure 14. Parental *Y. pestis* CO92 causes clinical disease in Rag1 KO mice.**

C57BL6 Rag1 KO mice (n=4-5 each route) were infected with 4 LD<sub>50</sub> of CO92 by either (i.n.) or (i.m.) route and the mortality of animals recorded and plotted (**A**). Lungs, liver, and spleen were removed from the moribund animals to quantify the bacterial loads (**B**). Kaplan-Meier analysis with log-rank (Mantel-Cox) test was used for analysis of animal survival (**A**). Asterisks represent the statistical significance between two groups indicated by a line and \*\*\* p<0.001 (**B**). Two biological replicates were performed, and data plotted.

We then evaluated the LMA mutant, when delivered at a vaccination dose of 2.0 x 10<sup>6</sup> CFU by both i.n. and i.m. routes, in Rag1 KO mice. Five days p.i., five mice infected with LMA from each infection route were necropsied and examined for the presence of the

mutant either at the infection site (lungs or muscle) or in the spleen as the result of systematic dissemination. As shown in **Fig. 15A**, there was no detectable LMA mutant in the spleen of mice infected by either the i.n. or the i.m. route. We also did not detect any LMA mutant at the injection site of muscle. We did enumerate 300 CFU in the lungs of one mouse that was infected by the i.n. route; however, this number was much lower than the initial infection dose of  $2.0 \times 10^6$  CFU. Further, no LMA mutant was detected in the lungs of other mice infected by the i.n. route (**Fig. 15A**). This was also indicated by the fact that all the mice infected with  $2.0 \times 10^6$  CFU of LMA survived up to 28 days p.i. (**Fig. 15B**) without any clinical signs of the disease and a minimal body weight loss similar to that shown in conventional mice (**Fig. 13B**).

These surviving mice were then challenged with 6 LD<sub>50</sub> of CO92. As expected, all LMA infected Rag1 KO mice succumbed to CO92 challenge with an overall  $>10^8$  CFU of *Y. pestis* CO92 present in the lungs (**Fig. 15C**) with ~15% loss in body weight over time. Further, there were no F1-V specific IgG antibodies in the sera of LMA (pooled from i.n. and i.m. infected) Rag1 KO mice on day 3 post CO92 challenge as compared to naïve Rag1 KO mice. However, a significantly higher level of F1-V IgG antibodies was generated in the LMA-immunized conventional (immunocompetent) mice (pooled sera from i.n. and i.m. infected) from a parallel independent study (**Fig. 15D**).

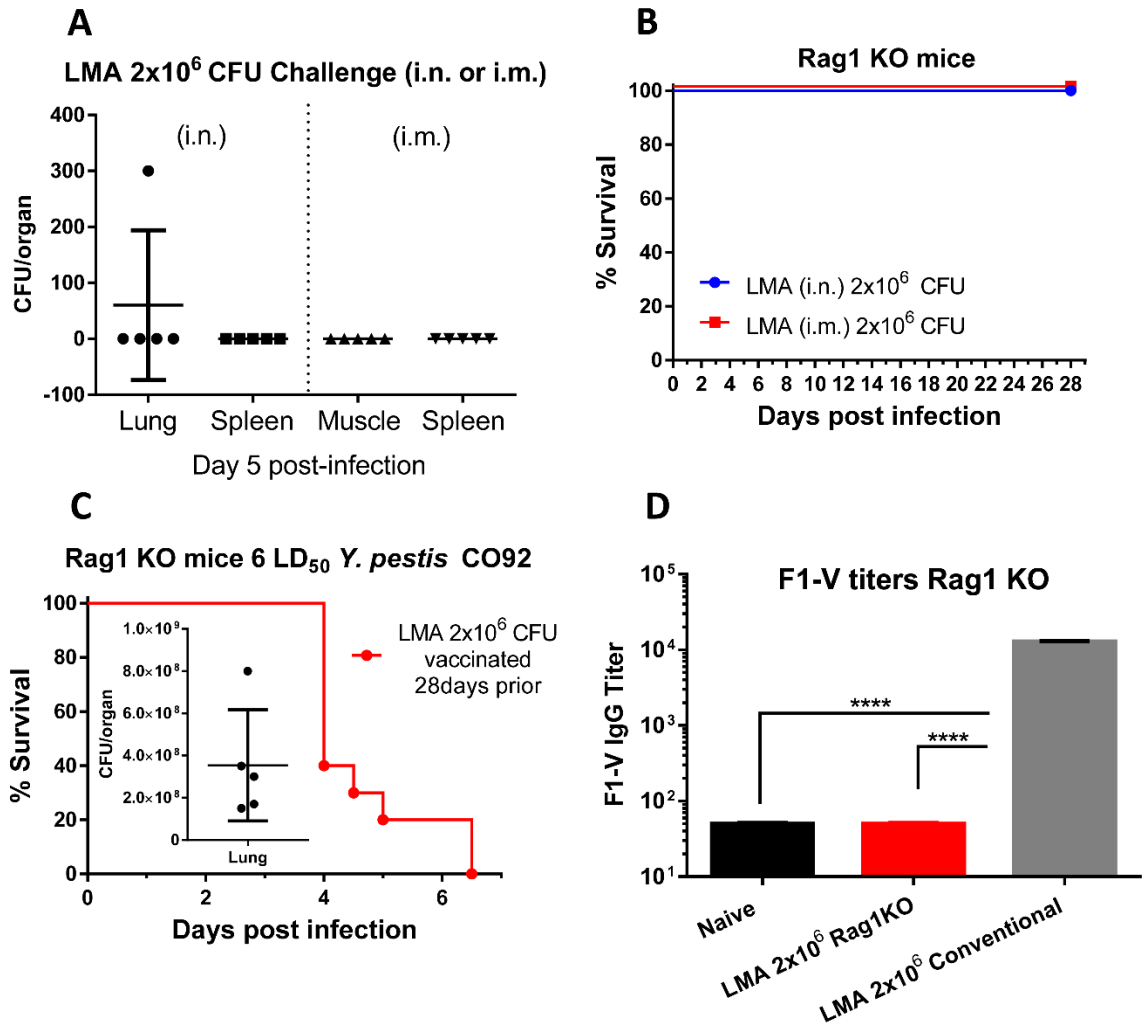


**Figure 15: Attenuation and immunologic characterization of LMA vaccine in Rag1 KO mice.**

C57BL6 Rag1 KO mice were infected with  $2.0 \times 10^6$  CFU of LMA by either the i.n. or the i.m. route (n=10 each route). On day 5 p.i., 5 animals from each infection route were euthanized and spleen, lungs or muscle (depending on the infection route) were collected to quantify the number of LMA (A). The survival of the remaining LMA infected animals (5 from each route) were monitored for up to 28 days p.i. (B). After 28 days of LMA infection, all surviving mice (n=10) were challenged with 6 LD<sub>50</sub> of CO92. The mortality of animals was recorded and bacterial loads in the lungs from 5 moribund animals (inset) were enumerated (C). F1-V specific IgG titers were evaluated by ELISA from sera collected at day 3 post CO92 challenge. Sera collected from uninfected naïve Rag1 KO mice and conventional mice immunized with LMA ( $2.0 \times 10^6$  CFU i.m.) served as negative and positive controls, respectively (D). One-way ANOVA was used to determine significance between groups for bacterial burdens and antibody titers. Kaplan-Meier analysis with log-rank (Mantel-Cox) test was used for analysis of animal survival.



Asterisks represent the statistical significance between two groups indicated by a line and \*\*\*  $p < 0.001$ . Two biological replicates were performed, and data plotted.

**Strong immune responses were elicited in conventional mice by heterologous vaccination with either a 1- or 2-dose (prime-boost) regimen**

Mice were immunized with Ad5-YFV and LMA vaccines in either a 1- or 2-dose regimen. In a 1-dose regimen, both Ad5-YFV and LMA vaccines were administered simultaneously, while in a 2-dose regimen, Ad5-YFV and LMA vaccines were delivered 21 days apart in various order and route combinations (**Fig. 16A**). The immunization schedule for either 1- or 2- dose regimens is depicted in **Fig. 16B**). Three weeks after completion of the vaccinations, the immunized and control mice were challenged with 100 LD<sub>50</sub> of either CO92 or its F1 deletion mutant CAF<sup>-</sup>. As shown in **Fig. 16C and D**, all of 2-dose heterologous prime-boost vaccinated mice, regardless of the order in which the vaccines were administered or the route of vaccination by which LMA was delivered, were 100% protected from both CO92 and its CAF<sup>-</sup> strain challenge with no body weight loss and other clinical symptoms of the disease. A 100% protection was also observed for mice simultaneously immunized with Ad5-YFV (i.n.) and LMA (i.m) during CO92 and CAF<sup>-</sup> challenges. However, when both Ad5-YFV and LMA vaccines were simultaneously administered i.n., the immunized mice had 50% (during CAF<sup>-</sup> strain challenge) and 63% (during CO92 challenge) survival rates (**Fig. 16E and F**).

**A**

| Groups                    | Vaccine and route of delivery                      | Doses given | Group size | Challenge strain (100 LD <sub>50</sub> , i.n.) |
|---------------------------|--|-------------|------------|--|
| Control                   | PBS (i.n.)   | 2 doses     | 10         | WT CO92  |
| Heterologous Prime-Boost  | Ad5-YFV(i.n.)—LMA(i.n.)                            | 2 doses     | 8          |  |
|                           | LMA(i.n.)—Ad5-YFV(i.n.)                            |             |            |  |
|                           | Ad5-YFV(i.n.)—LMA(i.m.)                            |             |            |  |
| Heterologous Simultaneous | Ad5-YFV(i.n.)+LMA(i.n.)<br>Ad5-YFV(i.n.)+LMA(i.m.) | 1 dose      | 8          |  |
| Control                   | PBS (i.n.)   | 2 doses     | 10         | CAF <sup>-</sup> mutant of CO92                |
| Heterologous Prime-Boost  | Ad5-YFV(i.n.)—LMA(i.n.)                            | 2 doses     | 8          |  |
|                           | LMA(i.n.)—Ad5-YFV(i.n.)                            |             |            |  |
|                           | Ad5-YFV(i.n.)—LMA(i.m.)                            |             |            |  |
| Heterologous Simultaneous | Ad5-YFV(i.n.)+LMA(i.n.)<br>Ad5-YFV(i.n.)+LMA(i.m.) | 1 dose      | 8          |  |

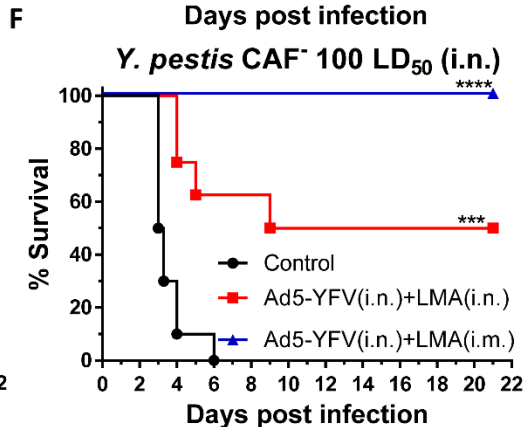
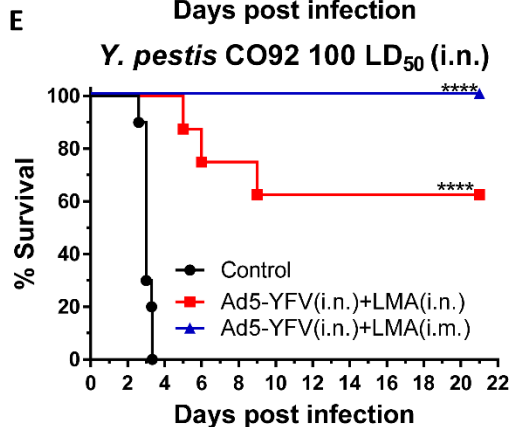
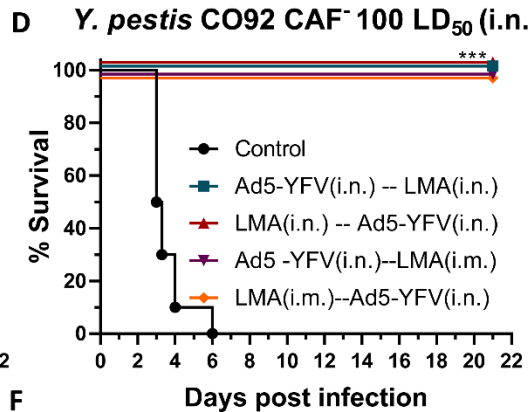
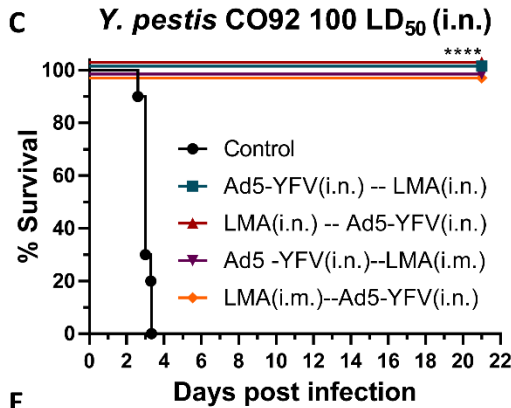
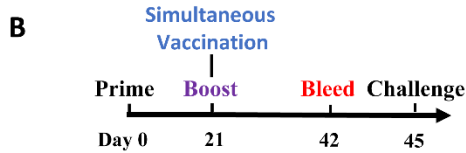


**Figure 16: Short-term heterologous vaccination study with conventional mice.**

Mice (n=8-10 per group) were immunized heterologously with Ad5-YFV and LMA vaccines in either a 1- or a 2-dose regimen. In 1-dose regimen, both Ad5-YFV and LMA vaccines were delivered simultaneously, while in a 2-dose regimen, Ad5-YFV and LMA vaccines were administered 21 days apart in various order and combinations. Mice receiving PBS were used as controls. The composition of the groups and the experiment time course are depicted in panels **A** and **B** respectively. Three weeks after completion of the vaccination schedule, mice were challenged with 100 LD<sub>50</sub> of either CO92 (**C** and **E**) or its F1 deletion mutant CAF<sup>-</sup> (**D** and **F**) and observed for morbidity and mortality for 21 days. Kaplan-Meier analysis with log-rank (Mantel-Cox) test was used for analysis of animal survivals. Asterisks represent the statistical significance between the indicated groups to the naïve control mice. \*\*\* p<0.001 , \*\*\*\*p<0.0001. Two biological replicates were performed, and data plotted.

We then measured IgG antibody titers to rF1-V fusion protein in sera of immunized mice collected on day 42 prior to the challenges. In general, all vaccinated groups of animals had notable increases in antibody titers which were 2-3 logs higher compared to that of the naïve controls (**Fig. 17A**). Among the immunized mice, relatively lower F1-V antibody titers were noted in animals immunized with either a 2-dose regimen of Ad5-YFV (i.n.)-LMA (i.m) or a 1-dose regimen of Ad5-YFV (i.n.) + LMA (i.n.). However, a significant difference was only observed between the 2 simultaneously immunized groups of mice (**Fig. 17A**, red versus blue bars).

We also examined the isotypes of F1-V IgG antibodies to gauge Th1 versus Th2 bias. In general, all vaccinated groups of mice had significantly higher levels of F1-V specific IgG1 and IgG2a as compared to those of the naïve animals. For simultaneously vaccinated groups of mice, there were generally higher levels of F1-V specific IgG2a over IgG1; however, a significant difference was only observed for animals that received Ad5-YFV (i.n.) and LMA (i.m.) (**Fig 17B**). For the 2-dose vaccinated groups of mice, when Ad5-YFV was administered first (teal and purple bars), there were always higher levels of

IgG2a over IgG1, while the difference was only significant in the Ad5-YFV (i.n.)-LMA (i.m.) immunized group of mice as shown in purple bars (**Fig. 17B**). In contrast, when the LMA vaccine was delivered as the first dose (crimson and orange bars), higher levels of IgG1 over IgG2a were observed but again these differences were only significant when LMA was administered by the i.m. route as shown in orange bars (**Fig. 17B**).

We next examined cell-mediated immune responses in immunized mice from the groups which showed 100% protection during the *Y. pestis* challenges (**Fig. 16C-F**). In a separate experiment, splenocytes were isolated from vaccinated mice 21 days after the last vaccination dose and stimulated with PMA and Ionomycin. All vaccination groups had significantly higher populations of CD4<sup>+</sup> IFN $\gamma$ <sup>+</sup>, CD8<sup>+</sup> IFN $\gamma$ <sup>+</sup> and CD4<sup>+</sup> IL-17<sup>+</sup> cells than those of naive mice (**Fig 17C-E**). Among the vaccinated groups, mice i.n. immunized with either LMA or Ad5-YFV first in a 2-dose regimen (teal and crimson bars) showed slightly higher percentages of IFN $\gamma$  producing CD4<sup>+</sup> and CD8<sup>+</sup> T cells than all other groups of immunized mice; however, no significant differences were observed (**Fig. 17C and D**).

On the other hand, notably higher population of IL-17 producing CD4<sup>+</sup> T cell was noticed in the group of mice simultaneously immunized with Ad5-YFV (i.n.) and LMA (i.m.) as compared to all the 2-dose regimen immunized groups of mice (**Fig. 17E**, blue bar). Interestingly, although it did not reach significant level, mice i.n. immunized with either LMA or Ad5-YFV first in a 2-dose regimen (teal and crimson bars) showed slightly higher percentages of IL-17 producing CD4<sup>+</sup> T cells than all other 2-dose regimen immunized groups of animals. A similar trend (to IL-17) was also observed for the IFN $\gamma$  producing CD4<sup>+</sup> and CD8<sup>+</sup> T cells (**Fig. 17C and D**).

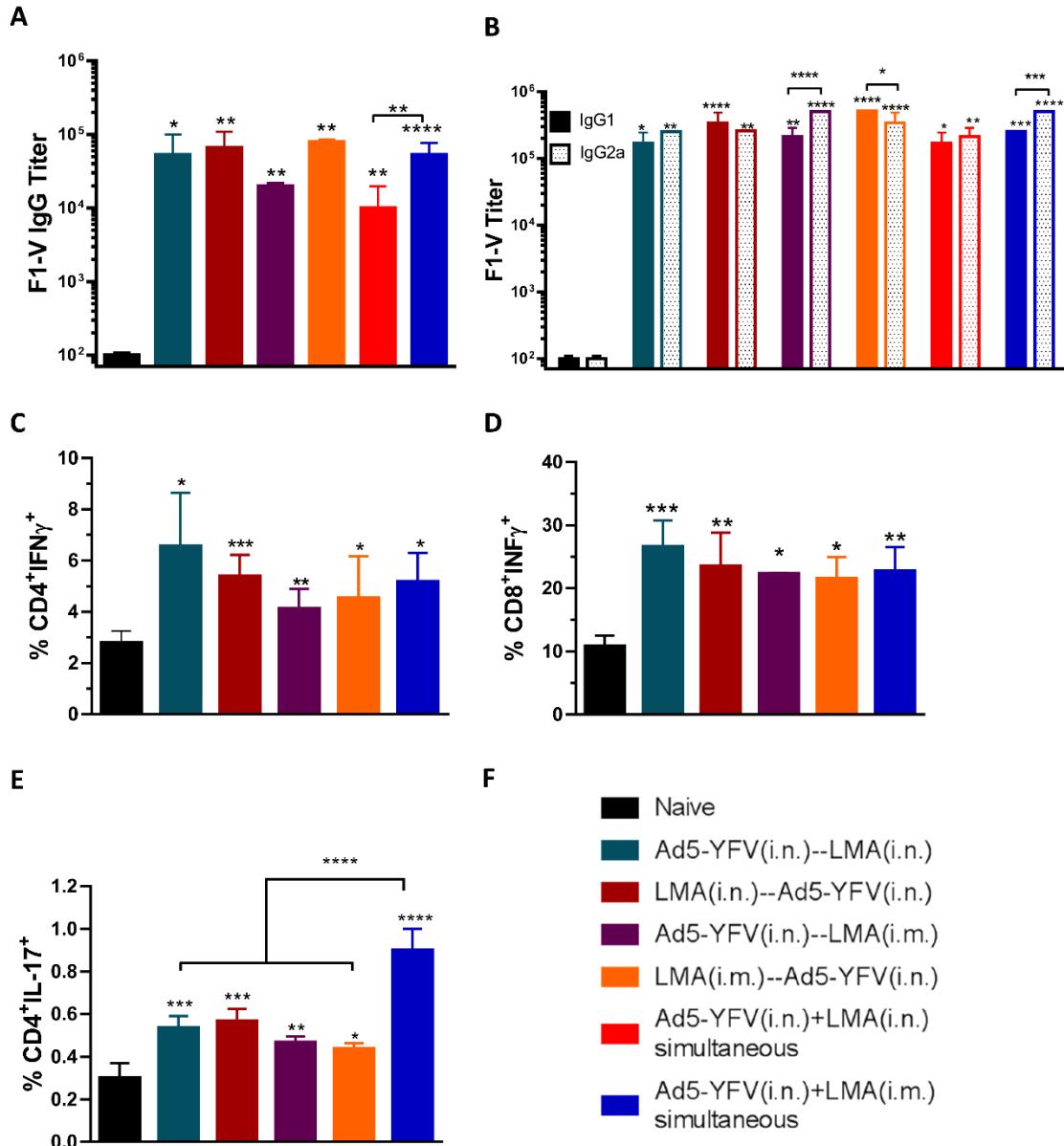


**Figure 17: Humoral and cell-mediated immune responses during short-term heterologous vaccination study.**

Sera were collected 21 days after the last immunization from both immunized and naïve control mice as described in Fig. 16. ELISA was performed to evaluate specific F1-V total IgG titers (A) as well as its isotype IgG1 and IgG2a titers (B). In a separate experiment, mice (n=5) were similarly immunized as described in Fig. 16, however, the group in which mice were simultaneously immunized with LMA and Ad5-YFV i.n. was excluded. Twenty-one days after completion of the vaccination course, spleens were harvested. Splenocytes were isolated and stimulated with PMA, Ionomycin, and Brefeldin A. Subsequently, splenocytes were surface stained for CD3, CD4, and CD8 followed by

intracellular staining for IFN $\gamma$  (C,D) and IL-17A (E). Different groups of mice used are depicted in F. Statistical analysis was performed using One-way ANOVA with Tukey's post-hoc test (A, C, D, E) or Two-way ANOVA with Tukey's post-hoc test (B) to determine significance. Asterisks directly above bars indicated significance compared to control group while asterisks with comparison bars denoted significance between the indicated groups. \* $p < 0.05$ , \*\* $p < 0.01$ , \*\*\* $p < 0.001$ , \*\*\*\* $p < 0.0001$ . Two biological replicates were performed, and data plotted. *In vitro* studies had 3 replicates.

### **Robust immune response was sustained in conventional mice with a 2-dose regimen vaccination during a long-term study**

After examining the above survival data and immune responses from both 1- and 2- dose heterologous vaccination regimens, we chose to focus on the 2-dose regimen for further evaluation in a long-term vaccination study. The sole reason for this was to develop a needle-free vaccination protocol although comparisons were also made with the i.m. vaccinated animals. During the long-term study, we examined humoral and cell-mediated responses at 42 days after the 2<sup>nd</sup> dose of vaccination as well as at 3 days post CO92 challenge. The details of immunization regimens and schedules of the study are shown in **Figs. 18A and B**.

As shown in **Fig. 18C**, a similar levels of F1-V specific antibodies were detected in the sera across all vaccinated groups of mice and were all significantly higher (>2 logs) than that of naïve control animals (**Fig. 18C**). Further, antibody isotype analysis revealed a generally balanced level of IgG1 and IgG2a in the immunized mice except for animals immunized first with Ad5-YFV (teal and purple bars) which had higher levels of IgG2a over IgG1. However, the difference was only significant in mice immunized with Ad5-YFV (i.n.)-LMA (i.n.) (**Fig. 18D**, teal bars).

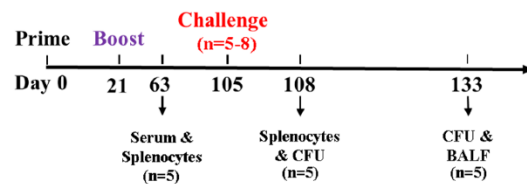
To further dissect the antibodies elicited by the vaccination, we evaluated antibody titers to each individual plague antigen F1, LcrV, and YscF that were the components of Ad5-YFV vaccine. As shown in **Fig. 18E**, all immunized mice produced a similar level of

IgG against each individual antigen and they were all significantly higher than that of naive control mice. To be more specific, antibody titers against F1 and YscF were comparable among all vaccinated groups of mice. However, antibody titers against LcrV were significantly higher in mice immunized with Ad5-YFV (i.n.)-LMA (i.n.) (teal bar) as compared to mice vaccinated with either LMA (i.n.)-Ad5-YFV (i.n.) (crimson bar) or LMA (i.m.)-Ad5-YFV (i.n.) (orange bar) (Fig. 18E).

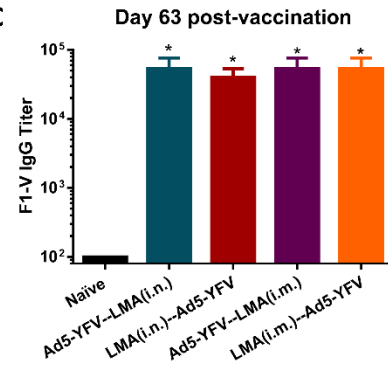
**A**

| Groups                   | Vaccine and route of delivery | Doses given | Group size | Challenge strain (100 LD <sub>50</sub> i.n.) |
|--------------------------|-------------------------------|-------------|------------|--|
| Control                  | PBS (i.n.)                    | 2 doses     | 15         | WT CO92                                      |
| Heterologous Prime-Boost | Ad5-YFV(i.n.)—LMA(i.n.)       | 2 doses     | 18         |  |
|                          | LMA(i.n.)—Ad5-YFV(i.n.)       |             |            |  |
|                          | Ad5-YFV(i.n.)—LMA(i.m.)       |             |            |  |
|                          | LMA(i.m.)—Ad5-YFV(i.n.)       |             |            |  |
| Control                  | PBS (i.n.)                    | 2 doses     | 5          | CAF <sup>-</sup> mutant of CO92              |
| Heterologous Prime-Boost | Ad5-YFV(i.n.)—LMA(i.n.)       | 2 doses     | 8          |  |
|                          | LMA(i.n.)—Ad5-YFV(i.n.)       |             |            |  |
|                          | Ad5-YFV(i.n.)—LMA(i.m.)       |             |            |  |
|                          | LMA(i.m.)—Ad5-YFV(i.n.)       |             |            |  |

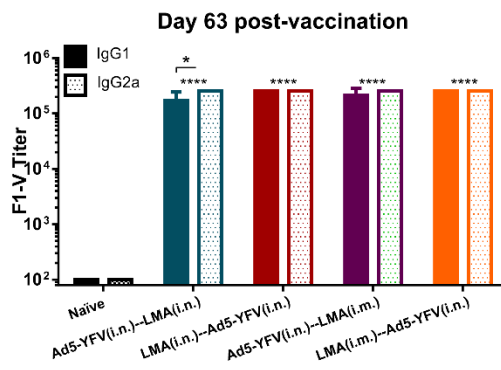
**B**



**C**



**D**



**E**

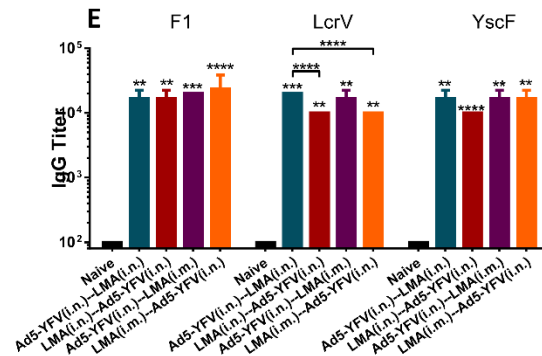


**Figure 18: Antibody responses during long-term heterologous prime-boost vaccination study.**

Mice were immunized with Ad5-YFV and LMA vaccines in 2-dose (prime-boost) regimens in which Ad5-YFV and LMA were administered 21 days apart in various combinations. The composition of the groups and the experiment time course are depicted in panels **A** and **B**, respectively. Sera were collected on day 63 of the study which was 42 days after the 2<sup>nd</sup> vaccination dose. The total IgG and its isotypes IgG1/IgG2a titers specific to F1-V were determined by ELISA and displayed in (**C**) and (**D**), respectively, while, the total IgG titers specific to individual antigens F1, LcrV, and YscF were shown in (**E**). Statistical significance was determined by One-way ANOVA with Tukey's post-hoc test (**A**, **C**, **D**) and by Two-way ANOVA with Tukey's post-hoc test (**B**). Asterisks directly above bars indicated significance compared to control group while asterisks with comparison bars denoted significance between the indicated groups. \* $p < 0.05$ , \*\* $p < 0.01$ , \*\*\* $p < 0.001$ , \*\*\*\* $p < 0.0001$ . Two biological replicates were performed, and data plotted. *In vitro* studies had 3 replicates.

The isolated splenocytes from mice 42 days post 2<sup>nd</sup> dose of vaccine were stimulated with *Y. pestis* specific rF1-V fusion antigen (100  $\mu\text{g/ml}$ ) to induce cell proliferation by measuring incorporation of BrdU in the newly synthesized chromosomal DNA (83). As shown in **Fig. 19**, a significant T- and B- cell proliferation was generally noticed in all of the vaccinated groups as compared to the naïve controls. Interestingly, a much stronger T- and B- cell proliferation was achieved in mice which were first vaccinated with Ad5-YFV (teal and purple bars) than those mice which were first immunized with LMA (crimson and orange bars) regardless of the route by which LMA was administered (**Fig. 19**). It is plausible that administration of LMA first might have somewhat of a toxic effect on T- and B- cells, an effect not observed when Ad5-YFV was delivered first and could account for less T- and B- cell proliferation. Important to note is that antibody titers to LcrV (**Fig. 18E**) were also lower when LMA was used first followed by Ad5-YFV for vaccination of mice. We suspect that antibodies to YscF, the third



component in the Ad5-YFV vaccine, compensates for this lower LcrV antibody titers in protection.

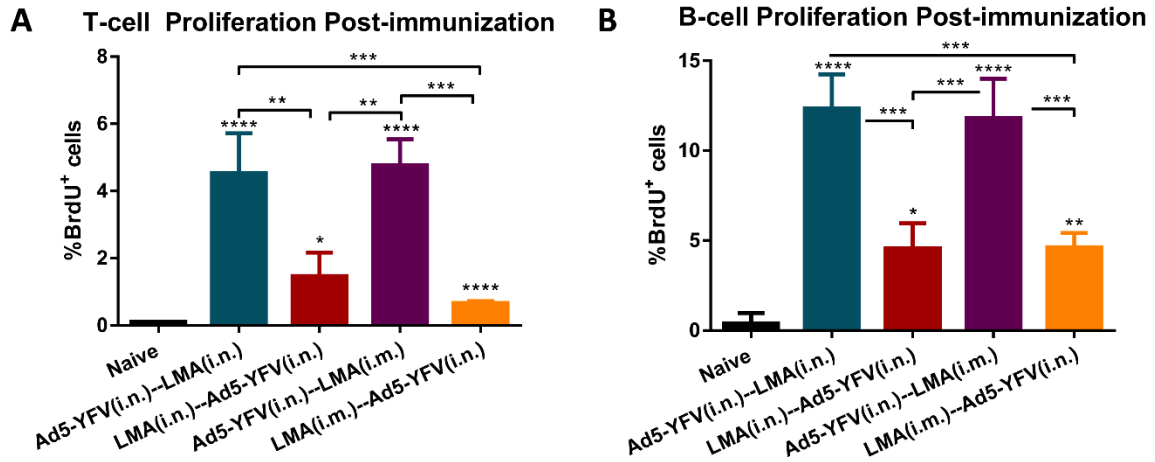


**Figure 19: T- and B-cell proliferation in response to heterologous prime-boost vaccination during long-term study.**

Spleens were collected 21 days after the last vaccination dose from a cohort (n=5 per group) of immunized and naïve control mice as described in Fig. 18. The isolated splenocytes were stimulated with rF1-V (100 µg/ml) for 72 h 37° C and then BrdU was added at a final concentration of 10 µM during the last 18 h of incubation with rF1-V to be incorporated into newly synthesized DNA of the splenocytes. Subsequently, the BrdU-labeled splenocytes were surface stained for T- and B- cell markers followed by BrdU and 7-AAD staining. The splenocytes were then subjected to flow cytometry, and the percent of BrdU positive cells in CD3 (A) and CD19 (B) positive populations were calculated using FACSDiva software. Statistical significance was determined using One-way ANOVA with Tukey’s post-hoc test. Asterisks above columns represented comparison to the control group while asterisks with comparison bars denoted significance between the indicated groups. \*p<0.05, \*\*p<0.01, \*\*\*p<0.001, \*\*\*\* p<0.0001. Two biological replicates were performed, and data plotted. *In vitro* studies had 3 replicates.

**Conventional mice vaccinated with the 2-dose regimen were fully protected from CO92 and CAF<sup>-</sup> challenges during a long-term study**

The immunized mice along with naïve controls were then i.n. challenged with 100 LD<sub>50</sub> of either CO92 or its CAF<sup>-</sup> strain. As expected, all mice in vaccinated groups survived (with no clinical symptoms of the disease), while 100% of naïve control animals succumbed to infection (Fig. 20A and B, with up to 20% body weight loss). In addition,

high plague bacilli ( $10^9$ - $10^{10}$  cfu/organ) were detected in various organs of diseased naïve control mice. In contrast, the inoculated *Y. pestis* was completely cleared from infected lungs of all the vaccinated mice after 28 days of the challenge (**Fig. 20C**). We have previously shown that mice vaccinated with either 2 doses of LMA or Ad5-YFV cleared the invading pathogen within 3 days p.i. (41, 42). At the end of the study (day 28 post-challenge), we collected BALF from all surviving mice, and all vaccinated and challenged animals had a significant level of F1-V specific IgA compared to PBS controls. (**Fig. 20D**).

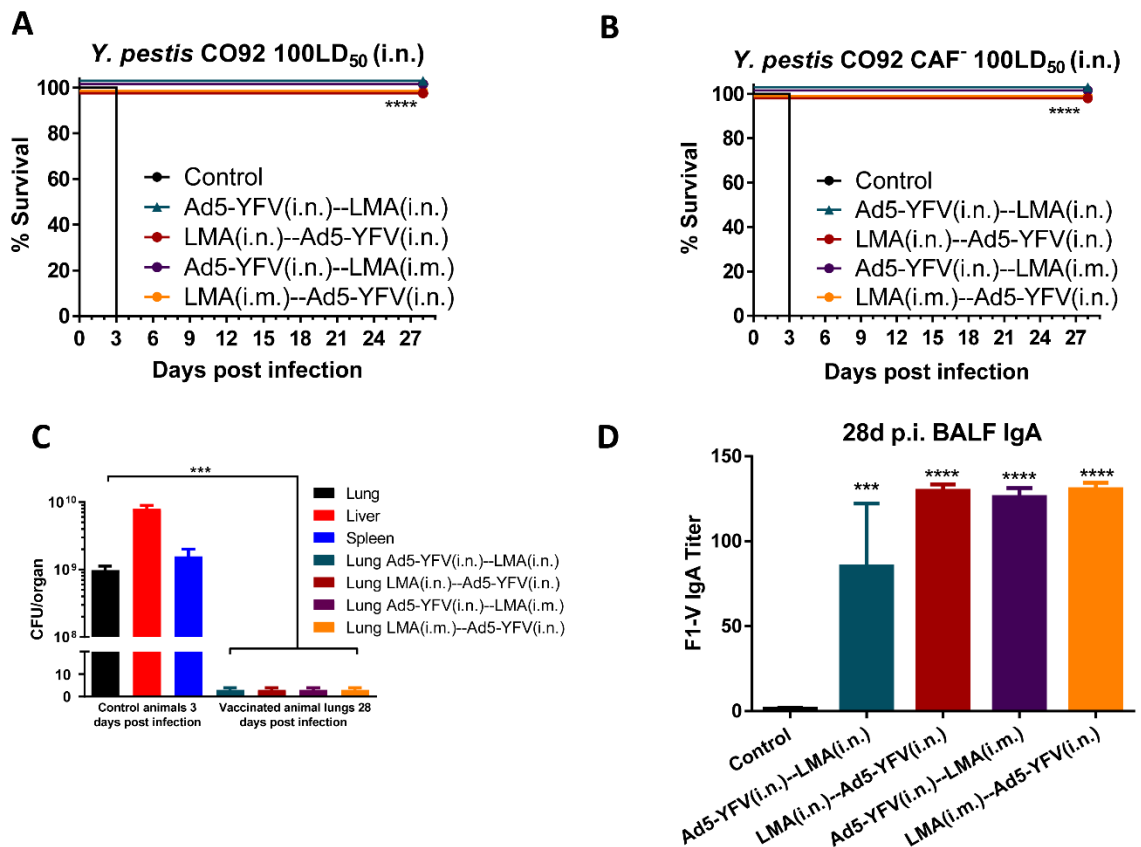


**Figure 20: Heterologous prime-boost vaccinations provide protection to immunized mice in long-term study.**

A cohort (n=5-8 per group) of immunized and naïve control mice as described in Fig. 18. were challenged on day 105 of the study (84 days after 2<sup>nd</sup> vaccination) with 100 LD<sub>50</sub> of either CO92 (**A**) or its CAF<sup>-</sup> strain (**B**) and monitored for morbidity and mortality for 28 days. On day 3 p.i., lungs, liver, and spleen were excised from all moribund mice to

quantify bacterial load (C). At the end of the study (on day 28), BALFs and lungs were collected from the terminated animals. Lung homogenates were plated to determine the clearance of *Y. pestis* from the surviving animals (C). The collected BALFs were evaluated for IgA titers specific to F1-V by ELISA, and PBS-injected mice were used as controls (D). One-way ANOVA was used to determine significance between groups for bacterial burdens and antibody titers. While, Kaplan-Meier analysis with log-rank (Mantel-Cox) test was used for analysis of animal survivals. Asterisks represented the statistical significance compared to the control group or between the two groups indicated by a line. \*\*\* $p < 0.001$ , \*\*\*\* $p < 0.0001$ . Two biological replicates were performed, and data plotted. *In vitro* studies had 3 replicates.

We then examined sera of mice for IgA post vaccination and post challenge with CO92, and no differences in titers were noted (**Fig. 21**), suggesting infection did not further enhance serum IgA levels. A similar study will be performed in the future assessing IgA levels in BALF post vaccination and post challenge. Mice from the Ad5-YFV (i.n.)-LMA (i.n.) vaccinated group had slightly lower level of IgA than the other heterologous prime-boost vaccinated groups of animals, although this differences were not significant (**Fig. 20D**). Although it is expected that in pneumonic plague, IgA would be significantly contributing to host protection, some studies indicated minimal protective role of IgA (61, 84). However, whether the immune status of the host could be a contributing factor in IgA-associated protection is unclear and needs further investigation.

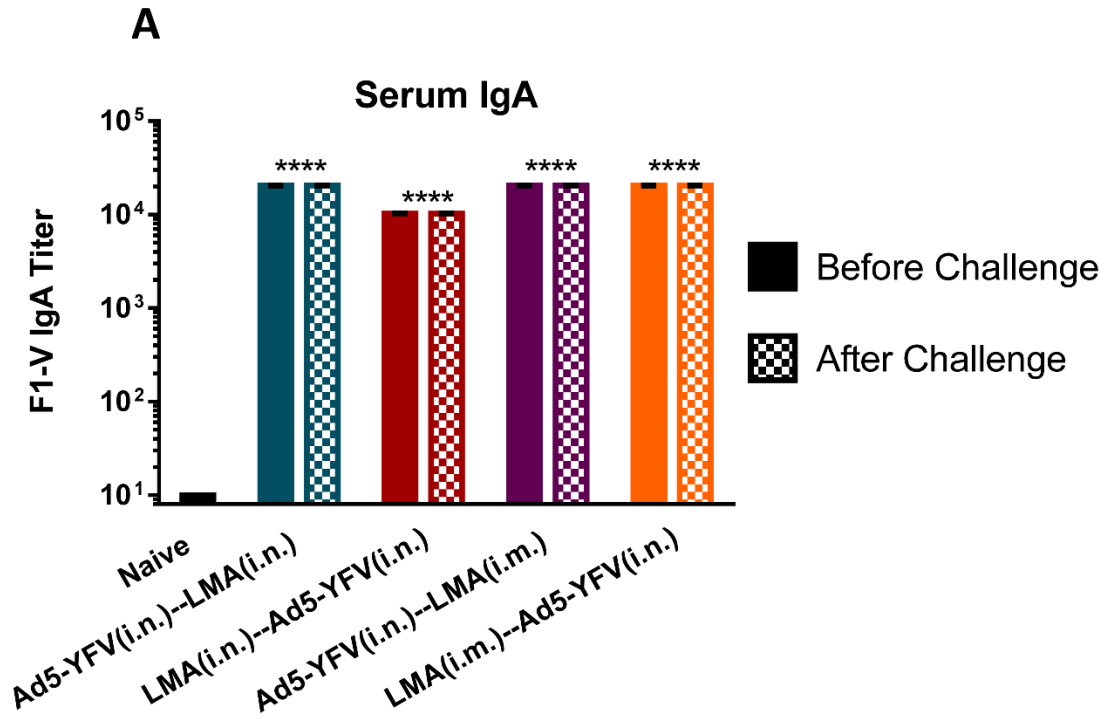


**Figure 21. No significant differences in F1-V specific serum IgA are observed in vaccinated mice before and after infection.**

Mice were immunized with Ad5-YFV and LMA vaccines in 2-dose (prime-boost) regimens in which Ad5-YFV and LMA were administered 21 days apart in various combinations (Fig 18A). Serum was collected 42 days after the 2<sup>nd</sup> vaccination as well as 28 days post-infection. F1-V specific IgA was determined by ELISA. Titers were determined in triplicate. One-way ANOVA with Tukey's post hoc test was used to determine significant differences between groups. Asterisks indicate significance compared to naïve serum. \*\*\*\*  $p < 0.0001$ .

To gauge cell-mediated immunity of vaccinated mice in response to CO92 challenge, on day 3 p.i., splenocytes were isolated from both immunized and control animals and subjected to flow analysis after PMA/Ionomycin stimulation. We noted statistically higher IFN $\gamma$  producing CD4<sup>+</sup> and CD8<sup>+</sup> T- cell populations across all of the vaccinated mice as compared to that of naïve control animals (**Fig. 22A and B**), and a similar trend was observed for the IL-17 producing CD4<sup>+</sup> T-cells (**Fig. 22C**).

More specifically, a significantly higher level of CD4<sup>+</sup> IFN $\gamma$ <sup>+</sup> population was observed for mice immunized (purple bar) with Ad5-YFV (i.n.)-LMA (i.m.) in comparison to mice vaccinated (teal bar) with Ad5-YFV (i.n.)-LMA (i.n.) (**Fig. 22A**). On the other hand, a significant difference in CD8<sup>+</sup> IFN $\gamma$ <sup>+</sup> population was only noticed between Ad5-YFV (i.n.)-LMA (i.m.) immunized group (purple bar) when compared to Ad5-YFV (i.n.)-LMA (i.n.) (teal bar) or LMA (i.m.)-Ad5-YFV (i.n.) vaccinated groups of mice (crimson bar) (**Fig. 22B**).

In terms of CD4<sup>+</sup> IL-17<sup>+</sup> population, mice immunized first with LMA either by the i.n. or the i.m. route generally revealed better levels than mice immunized with Ad5-YFV vaccine first. Significant differences were observed between LMA (i.n.)-Ad5-YFV (i.n.) immunized group (crimson bar) of mice when compared to groups vaccinated with either Ad5-YFV (i.n.)-LMA (i.n.) (teal bar) or Ad5-YFV (i.n.)-LMA (i.m.) (purple bar) as well as between groups immunized with LMA (i.m.)-Ad5-YFV (i.n.) (orange bar) and the group vaccinated with Ad5-YFV (i.n.)-LMA (i.m.) (purple bar) (**Fig. 22C**).

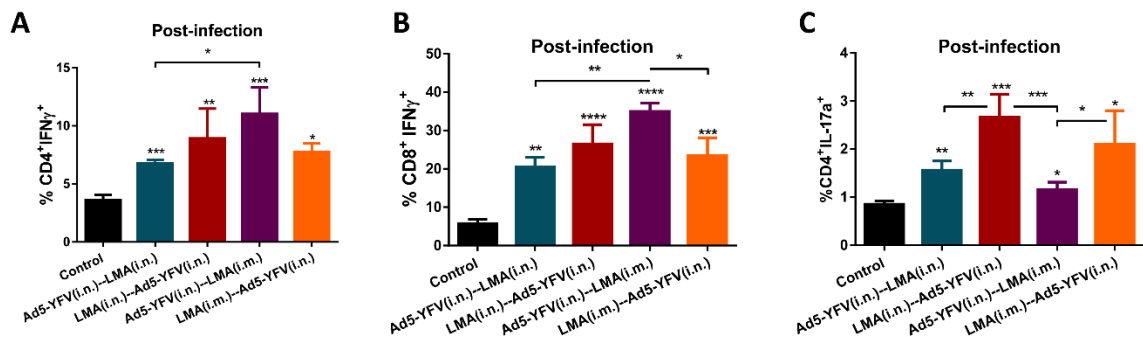


**Figure 22: T-cell responses to CO92 challenge during long-term heterologous prime-boost vaccination study.**

A cohort (n=5 per group) of immunized and naïve control mice as described in Fig. 18. were challenged on day 105 of the study (84 days after 2<sup>nd</sup> vaccination) with 100 LD<sub>50</sub> of CO92. Spleens were harvested on day 3 p.i., and the isolated splenocytes were then stimulated with PMA, Ionomycin, and Brefeldin A. Cells were stained with T-cell surface

markers CD3, CD4, and CD8 followed by intracellular IFN $\gamma$  and IL-17A staining. Percentages of CD4<sup>+</sup> IFN $\gamma$ <sup>+</sup> (A) and CD8<sup>+</sup> IFN $\gamma$ <sup>+</sup> (B) and CD4<sup>+</sup> IL-17<sup>+</sup> cells (C) were shown. Cells were then analyzed by flow cytometry. Statistical significance was determined using One-way ANOVA with Tukey's post-hoc test as well as Student's t-test. Asterisks above columns represented comparison to the control group while asterisks with comparison bars denoted significance between other indicated groups. \*p<0.05, \*\*p<0.01, \*\*\*p<0.001, \*\*\*\* p<0.0001. Two biological replicates were performed, and data plotted. *In vitro* studies had 3 replicates.

### **Characterization of mice splenic cytokine and chemokine profiles in response to vaccination and CO92 challenge**

To further evaluate cell-mediated immunity of mice in response to vaccination and infection, splenocytes collected from either post-immunization or post-challenge (**Fig. 18B**) were stimulated with rF1-V to examine cytokine/chemokine production. We divided up the cytokine/chemokine analysis into 3 panels: proinflammatory/anti-proinflammatory cytokines, Th1/Th2/Th17 associated cytokines, and chemokines. At post-vaccination time point, the overall proinflammatory cytokines in immunized mice were either slightly elevated (IL-6) or remained at the comparable levels (IL-1 $\alpha$  and IL-1 $\beta$ ) to those of naïve control mice (**Fig. 23**). However, in response to *Y. pestis* infection, significantly increased proinflammatory cytokines were observed only in naïve control mice, while the levels of these cytokines were low and almost unchanged in vaccinated animals (**Fig. 23**). For the anti-proinflammatory cytokine IL-10, a significant increase was generally observed in all of the immunized mice as compared to that of naïve controls at the post-immunization time point. In response to *Y. pestis* infection, the level of IL-10 was significantly elevated in both naïve control mice and in animals immunized first with LMA (crimson and orange bars); however, it remained unchanged in mice immunized first with Ad5-YFV (teal and

purple bars), and was significantly lower than that of naïve control at the post challenge time point (Fig. 23).

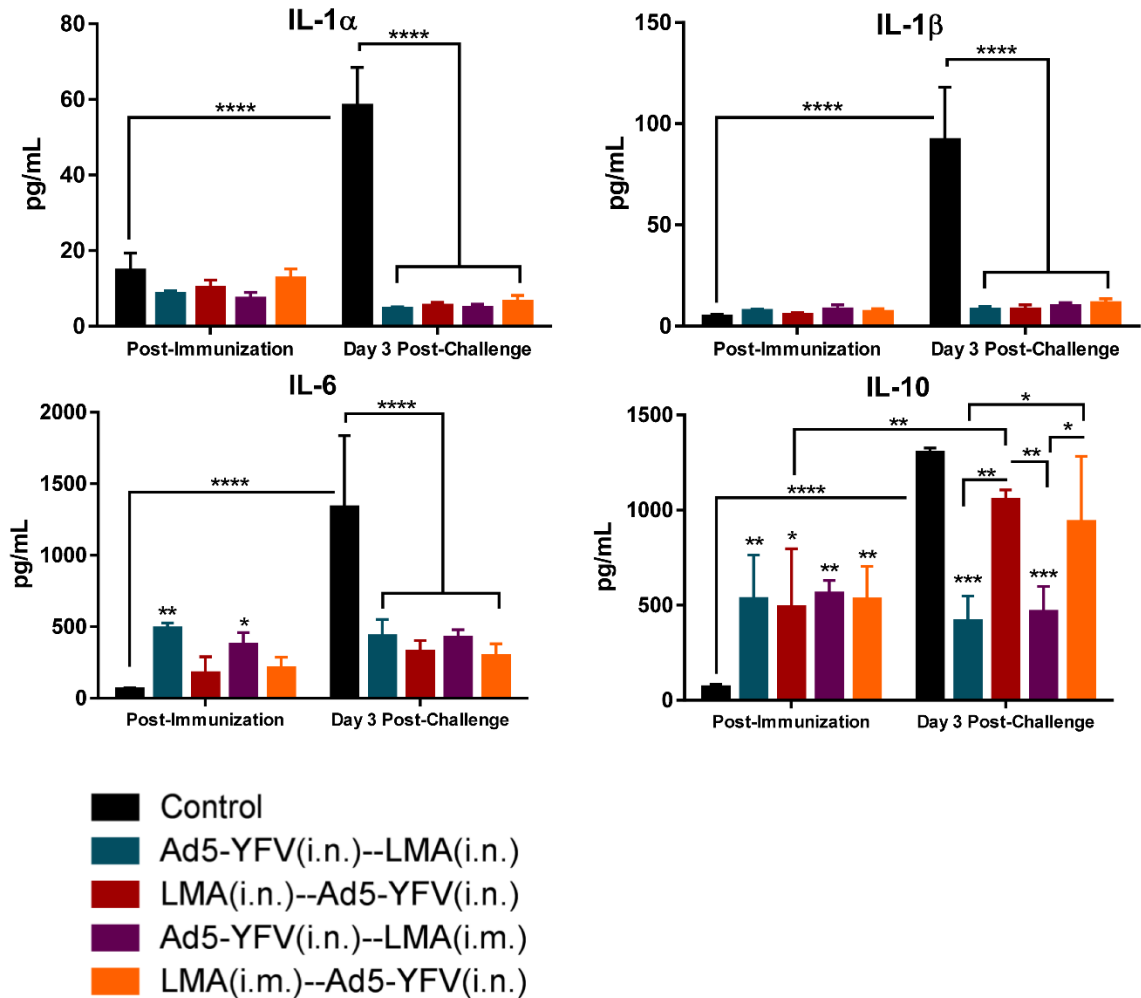


**Figure 23: Splenocyte proinflammatory and anti-proinflammatory responses during long-term heterologous prime-boost vaccination study.**

The splenocytes isolated from mice described in Fig. 19 (post immunization) and Fig. 22 (post CO92 challenge) were further stimulated with rF1-V (100  $\mu$ g/mL) for 3 days. The cytokines in the culture supernatants were analyzed by using Bioplex-23 assay and expressed as the arithmetic means  $\pm$  standard deviations. The proinflammatory and anti-proinflammatory cytokines are shown. Statistical significance was determined using Two-way ANOVA with Tukey's *post hoc* test to compare multiple time-points or student t-test to compare 2 groups within the same time-point. Asterisks above columns represented comparison to the control group, while horizontal bars represented differences between test groups. \*p<0.05, \*\*p<0.01, \*\*\*p<0.001, \*\*\*\* p<0.0001. Two biological replicates were performed, and data plotted. *In vitro* studies had 3 replicates.

In contrast to proinflammatory cytokines, the Th1- and Th2- related cytokines such as IL-2, IL-12(p70), IFN $\gamma$ , IL-4, IL-5, and IL-13 were generally increased in all immunized mice as compared to that of naïve controls at the post-immunization time point (**Fig. 24**). On the other hand, IL-2, IL-12(p70), IFN- $\gamma$  and IL-4 levels were sustained at higher levels in all immunized groups in response to CO92 challenge. The levels of IL-5 and IL-13 were only maintained higher in mice first immunized with LMA (crimson and orange bars) but subsided to the level of naïve controls in mice first vaccinated with Ad5-YFV (teal and purple bars) at the post-challenge time point (**Fig. 24**). The decline of Th2 cytokines IL-5 and IL-13 in mice immunized first with Ad5-YFV at post-challenge time point might reflect its Th1 bias as also shown above in analysis of IgG isotyping (**Fig. 17B and Fig. 18D**).

For Th17 response, slight increases in the levels of IL-17 were only observed in mice immunized first with LMA (crimson and orange bars) as compared to that of the naïve controls at post-immunization. In addition, the IL-17 level in these mice was further elevated in response to *Y. pestis* challenge. However, the IL-17 levels were consistently maintained at a low level and was comparable with that of naïve controls at both time points (post immunization and post challenge) in mice vaccinated first with Ad5-YFV (teal and purple bars) (**Fig. 24**). It should be mentioned that it is difficult to precisely correlate percentage of T cells positive for IL-17 as assessed by flow cytometry and IL-17 secreted by these cells based on Bioplex as the cells were stimulated with different agents, namely PMA or F1-V; however, a correlative trend should be expected as shown in **Figs. 22C and 24**.



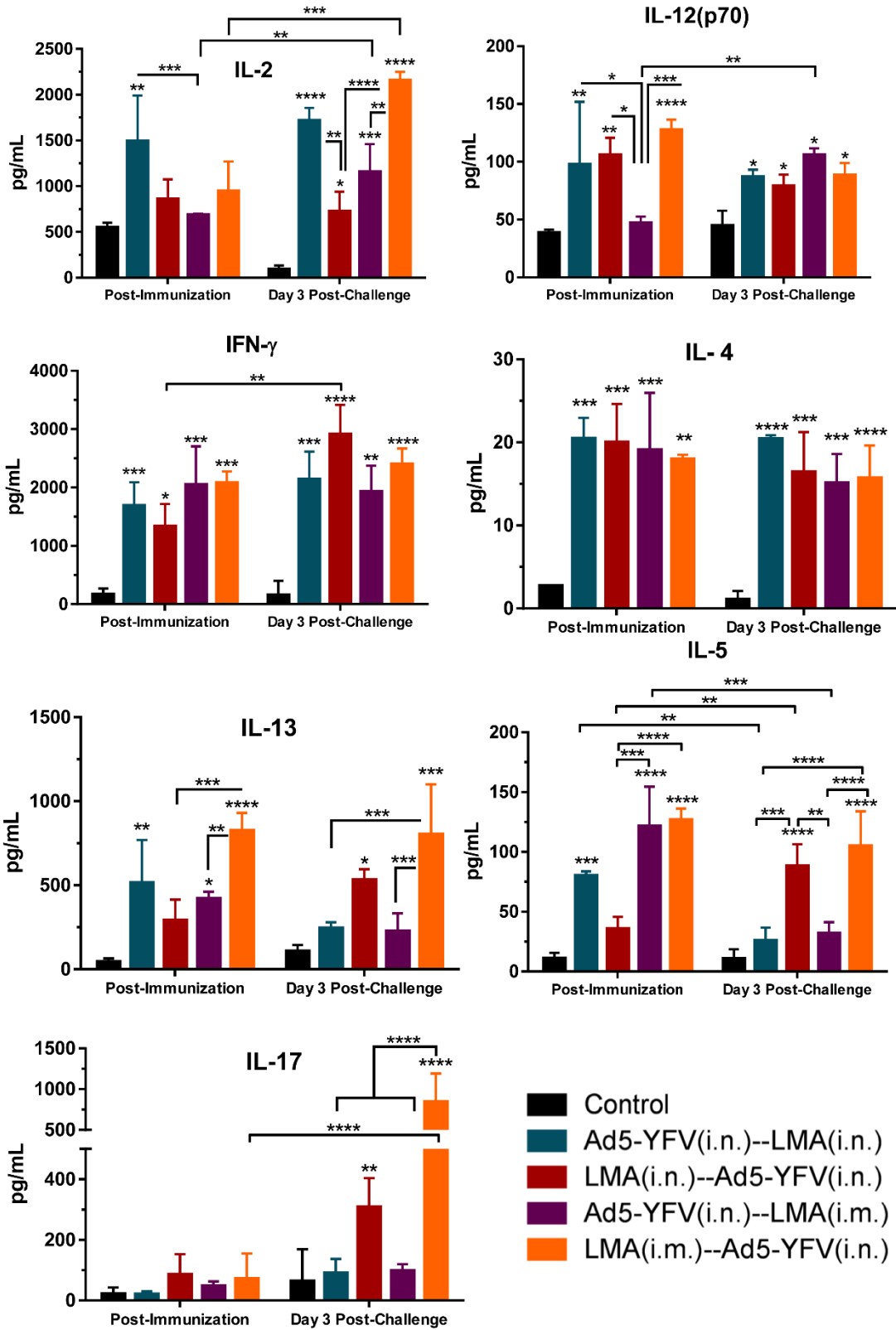


**Figure 24: Splenocyte Th1/Th2/Th17 cytokine responses during long-term heterologous prime-boost vaccination study.**

Cytokine analysis was performed as described in Figure 23. Th1/Th2/Th17 cytokine responses are shown. Statistical significance was determined using Two-way ANOVA with Tukey's *post hoc* test to compare multiple time-points or student t-test to compare 2 groups within the same time-point. Asterisks above columns represented comparison to the control group, while horizontal bars represented differences between test groups. \* $p < 0.05$ , \*\* $p < 0.01$ , \*\*\* $p < 0.001$ , \*\*\*\*  $p < 0.0001$ . Two biological replicates were performed, and data plotted. *In vitro* studies had 3 replicates.

In analysis of chemokine production, the overall level of chemokines in all immunized mice were low and comparable with their corresponding naïve controls at the post immunization time point except the GM-CSF which was significantly elevated (**Fig. 25**). In response to *Y. pestis* infection, the CXCL1, RANTES, and G-CSF behaved similarly to proinflammatory chemokines and were significantly increased only in naïve control mice but were at low levels and largely unchanged in all immunized and challenged animals (**Fig. 25**). In contrast, CCL2, CCL4, and GM-CSF had generally elevated levels in all immunized mice as compared to that of naïve control at post-challenge time point. The exception being CCL4 in mice immunized with LMA i.m. (purple and orange bars) which were at a similar level to that of naïve control challenged mice (**Fig. 25**).

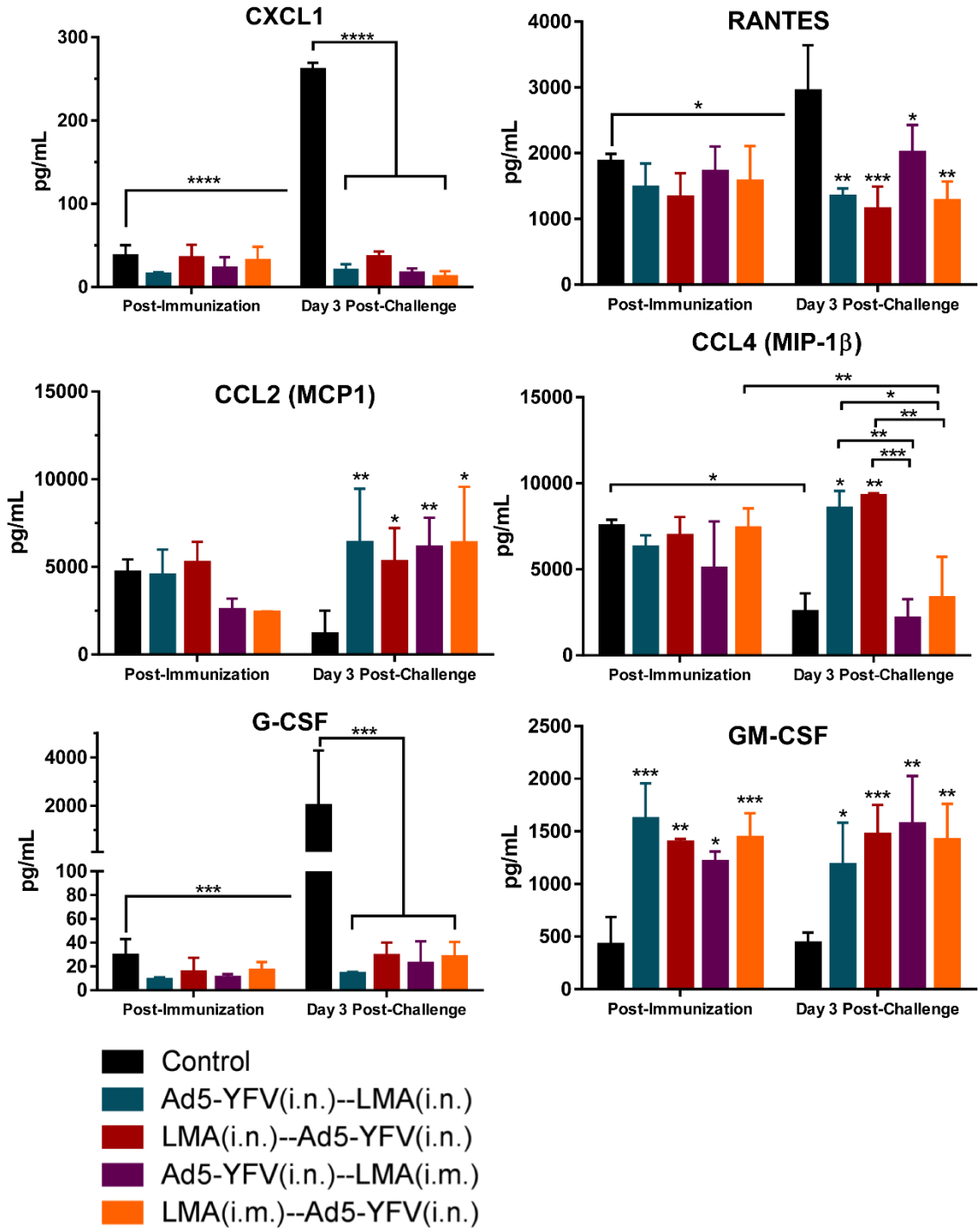


**Figure 25: Splenocyte chemokine responses during long-term heterologous prime-boost vaccination study.**

Chemokine analysis was performed as described in Figure 23. Chemokine responses are shown. Statistical significance was determined using Two-way ANOVA with Tukey's *post hoc* test to compare multiple time-points or student t-test to compare 2 groups within the same time-point. Asterisks above columns represented comparison to the control group, while horizontal bars represented differences between test groups. \* $p < 0.05$ , \*\* $p < 0.01$ , \*\*\* $p < 0.001$ , \*\*\*\* $p < 0.0001$ . Two biological replicates were performed, and data plotted. *In vitro* studies had 3 replicates.

**DISCUSSION**

After the 2017 outbreak of plague in Madagascar, the WHO released a target product profile that outlined the desired characteristics for a potential plague vaccine (50). These characteristics included: at most 2-dose vaccination schedule, long-lasting protection with humoral and cell-mediated responses, possibility of a needle-free administration, and a robust safety profile including potential use in pregnant women, children, and immuno-compromised individuals (50).

We recently have developed two plague vaccine candidates: a live-attenuated vaccine LMA and an Ad5 viral vector-based vaccine Ad5-YFV; individually both of them provided complete protection to immunized animals against challenge with CO92 (40–43). In response to the WHO requirements, here, we first further investigated the safety of the LMA vaccine in an iron-overload condition and then in Rag1 KO mice (85). In live-attenuated plague strains that rely on pigmentation locus mutations such as KIM/D27 and EV76, hereditary hemochromatosis has been shown to restore bacterial virulence (28). While the LMA mutant has intact pigmentation locus with functional T3- and T6- secretion systems (34) (data not shown).

Unlike KIM/D27 strain which exhibited more virulence under an iron-overload environment, LMA vaccine was not affected by the presence of more iron in mice (Fig. 1).

The *Rag1* gene defect in humans is associated with a broad spectrum of clinical and immunological phenotypes, and is one of the major causes of human immune deficiency (PID) (86, 87). The *Rag1* KO mice receiving up to  $2.0 \times 10^6$  CFU of LMA, which is equivalent to 20,000 LD<sub>50</sub> of CO92, did not exhibit any clinical symptoms of the disease and the LMA mutant rapidly cleared from these mice (Fig. 15). These data demonstrated a high degree of attenuation imparted by the selected mutations in LMA and provided indication that the vaccine would be suitable for use in immunocompromised individuals.

We then implemented a heterologous immunization strategy in which both LMA and Ad5-YFV vaccines were delivered either simultaneously (1-dose regimen) or in a prime-boost format (2-dose regimen), as we hypothesized such a strategy would have several advantages. First, the use of two rationally-designed vaccines, which are based on different principles, would complement each other from their own potential disadvantages such as limited plague antigens in the Ad5-YFV vaccine versus the LMA vaccine which would provide immune responses to plethora of antigens. Second, the use of an Ad5-YFV vaccine as the first dose would negate any safety concerns of employing LMA as the second booster dose. Third, the heterologous immunization scheme is expected to mount unique and durable immune responses by integrating characteristics of each of the two vaccines, and thus, leading to superior protection in a broader human population. Fourth, the 1-dose regimen would shorten the immunization course and considered ideal to be used in emergency situations such as a plague outbreak or during a bioterrorist attack.

Indeed, all our heterologous immunizations (irrespective of the order of vaccine delivery and the routes of administration) induced robust immune responses in mice and provided full protection to animals against the lethal challenges of both CO92 and its CAF<sup>r</sup>

mutant. The exception was the group of mice that received Ad5-YFV and LMA vaccines simultaneously by the i.n. route and had 50 to 63% survival rates during CO92 or its CAF<sup>-</sup> strain challenges (Fig. 16). This relatively lesser protection rate in mice was correlated well with lower F1-V specific antibody titers in mouse serum as compared to animals simultaneously immunized with Ad5-YFV and LMA *via* different routes, *i.e.*, i.n. and i.m., respectively (Fig. 17A). Further, there could be interference in triggering protective immune responses when both LMA and Ad5-YFV vaccines were delivered simultaneously in the lungs. It is also plausible that a stronger innate immunity developed in the lungs due to administration of two vaccines simultaneously, resulted in their respective rapid clearance, thus decreasing overall immunogenicity. Similar results were reported in a study in which tuberculosis vaccine BCG was used in combination with other TB subunit vaccines (*e.g.*, 85A, E6, and TB10.4) in a heterologous format. Simultaneous administration of them *via* different routes (pulmonary and parental) induced both pulmonary and systemic immunities resulting in better protection compared to animals that were simultaneously vaccinated *via* the same route (88). Interestingly, the Ad5-YFV (i.n.) and LMA (i.m.) simultaneous vaccination combination also exhibited immune response characteristics of both Ad5-YFV (Th1) and LMA (Th17) vaccines (Fig. 17B and E) with complete protection of mice against challenges with CO92 and its CAF<sup>-</sup> mutant (Fig. 16E and F). Thus, 1-dose regimen of two vaccines provided us with an excellent tool to combat plague during emergency situations.

It is difficult to discern which ones of our 2-dose heterologous regimens were better as all of them provided full protection to the immunized animals with comparable levels of F1-V specific antibodies and an overall similar cytokine profiles. However, an intriguing

phenomenon emerged in that the immune profile of 2-dose immunization was likely dictated by the vaccine which was administered first.

More specifically, when the Ad5-YFV vaccine was delivered first, Th1 immune response was more pronounced based on F1-V specific IgG2a/IgG1 antibody ratio (Fig. 17B) and the splenic cytokine profiles (Fig. 24). Likewise, when LMA vaccine was administered first followed by that of Ad5-YFV, the Th2 immune response was favored (Fig. 16B and Fig. 22C) along with that of Th17 (Fig. 22C and Fig. 24) response. Further, clear differences were noted in terms of T- and B- cell proliferation when mice were immunized first with the Ad5-YFV vaccine in response to stimulation with rF1-V and had higher LcrV antibody titers when compared to animals receiving LMA vaccine first during the long-term study (Fig. 18E and Fig. 19). Therefore, in this regard, delivering the Ad5-YFV vaccine first followed by that of LMA vaccine would be preferred, and is much more attractive based on safety and that both vaccines can be administered i.n., thus developing a more acceptable adjuvant- and needle- free administration protocol from the public health prospective.

The heterologous vaccination strategies have been previously used for diseases in which cell-mediated responses were particularly important for protection such as in patients with HIV and malaria (89). Recently, during the COVID-19 pandemic, the heterologous prime-boost vaccination has been emphasized mainly due to the shortage of available COVID-19 vaccines (90). The intentional design has also been reported in the Russian Sputnik vaccines which use two different adenovirus vectors (type 5 and type 26), and thus far, this is the only heterologous prime-boost vaccine to be licensed for human use (91–93). Further, with many COVID-19 vaccines under development based on

different platforms and strategies, and the likely need for additional boosters due to the emerging COVID-19 variants, have led to more enthusiasm in investigating the advantages of heterologous prime-boost approach over homologous boost strategy.

Indeed, it was shown that using a heterologous boost of either adenoviral-vectored vaccine or mRNA-based COVID-19 vaccines improved neutralizing antibody titers with induction of stronger Th1 responses than a homologous boost of inactivated SARS-CoV-2 vaccines (94). Similarly, using a mRNA based COVID-19 vaccine as a booster (BNT162b2) in a heterologous approach instead of using a homologous adenoviral booster (ChAdOx1-nCov-19) resulted in increased neutralizing antibody titers and SARS-CoV-2 specific T-cells (95). Although there is no data for direct comparison between heterologous and homologous immunization approach with LMA and Ad5-YFV vaccines; we did notice that the antibody titers to the individual antigen LcrV was the lowest among three tested antigens (LcrV, F1, and YscF) in mice immunized solely with the Ad5-YFV vaccine (41). In contrast, when mice were immunized with both LMA and Ad5-YFV vaccines in the heterologous format, a comparable level of antibodies to all three antigens was observed (Fig. 18E).

Recently, a prime and pull immunization regimen has been investigated in a variety of vaccines with success (96–98), which implicates that the immune response at a mucosal site can be triggered by the administration of an antigen to a distant mucosal site. In this strategy, a parenteral vaccination raises systemic cellular response (prime) followed by a mucosal delivery of chemokine or vaccine that directs the tissue targeting of the prime-activated circulating T cells (pull) (99). In our study, mice i.m. immunized with LMA followed by i.n. delivery of Ad5-YFV vaccine exactly fits this category and should be



further investigated. Although significant increases in splenic T cell population (both CD4 and CD8) was observed in all immunized mice as compared to the naïve controls, no significant differences among all of the immunized groups of mice was observed. In addition to the circulating T cells, the hallmark of prime-pull immunization is the elevated local T cell population, especially the resident memory T cells (TRM), at the mucosal sites (96–98). TRM occupies tissues without recirculating and provides a first response against infections and accelerates pathogen clearance (100). Therefore, it is possible that the local level (lungs) of T cells varies among our different heterologous immunized groups of animals and needs to be further studies.

A new vaccination strategy by combination of both simultaneous and prime-boost immunizations has been used for H1N1 signal minus influenza vaccine (S-FLU) in a pig model (101). During the prime-boost immunization course, the study has shown i.m. only immunized pigs generated a high titer of neutralizing antibodies but poor T cell responses, whereas aerosol solely induced powerful respiratory tract T cell responses but a low titer of antibodies. However, immunization of animals with S-FLU *via* both i.m and aerosol routes simultaneously during the prime-boost immunization course generated high antibody titers and strong local T cell responses with the most complete suppression of virus shedding and the greatest improvement in pathology (101). This strategy has been highly recommended for TB vaccines as well (88). Considering the Ad5-YFV (i.n.) and LMA (i.m.) simultaneous combination was the only one among all immunized groups that showed the immune characteristics of both Ad5-YFV (Th1) and LMA (Th17) (Fig. 17B and E), it will be exciting to carry out a similar experiment with LMA and Ad5-YFV vaccines in lieu of S-FLU in the future.

Finally, cytokine/chemokine production (*e.g.*, IL-1 $\alpha$ , IL-1 $\beta$ , and IL-6) from splenocytes of unvaccinated mice 72 h p.i. with CO92 indicated a highly inflammatory environment with neutrophil chemoattractants (CXCL1, RANTES, and G-CSF) at elevated level (Fig. 25). None of these cytokines/chemokines were elevated in any of the combinations of heterologous prime-boost vaccinated mice, indicating inability of *Y. pestis* to cause immune dysregulation during early stages of infection. Conversely, immunized and infected mice in all heterologous prime-boost groups had higher levels of CCL2, and some groups had higher CCL4, which could be essential in recruiting monocytes to clear the invading the pathogen. Importantly, mice immunized with the LMA vaccine first had the highest amount of secreted IL-17 during the post-infection time point, which combined with decrease in CXCL1, RANTES, G-CSF, and increases in CCL2, CCL4, and GM-CSF could have a critical role during productive versus non-productive stages of pneumonic plague.

In general, by using heterologous vaccination strategy, we have clearly demonstrated that the combination of vaccines, the route and timing of administration, as well as the length of the vaccination schedule are all crucial factors that affect efficiency and safety of vaccinations. It is important to reiterate that almost all our heterologous combinations offered complete protection from high-dose challenges of both CO92 and its CAF<sup>-</sup> strain, and each one of them has its own characteristics that can fit for different scenarios. Importantly, the 2-dose regimens especially the Ad5-YFV (i.n.) and LMA (i.n.) combination is ideal for the routine immunization in plague endemic regions, while the simultaneous approach with Ad5-YFV (i.n.) and LMA (i.m.) would be beneficial for vaccination in response to emergency situations.

Our future studies will address three important questions and include: **1)** comprehensively assessing potency of memory responses (T- and B- cells) that would navigate us on dosing strategies; **2)** assessing antibody potency in neutralizing *Y. pestis* infection, which would also support our heterologous prime-boost approach with two vaccines and potentially could reveal other additional differences that are important in humans; and **3)** testing heterologous prime-boost strategy in humanized mouse model and non-human primates to gauge superiority of our approach compared to competing vaccine candidates, and that our Ad5-YFV and LMA combination would be highly efficacious in humans.

## Chapter 5: Conclusion and Future Direction

Both 2-dose Ad5-YFV and heterologous prime-boost Ad5-YFV/LMA vaccination strategies were able to completely protect against pneumonic plague although they achieved this protection with different immune profiles. Two doses of Ad5-YFV induced a strong Th1 immune response and did not induce any detectable Th17 response. Interestingly the heterologous prime-boost strategy when Ad5-YFV was given as the 1<sup>st</sup> dose also induced a similar immune profile. This immune profile included: IgG2a>IgG1 titers, strong induction of IL-2, IL-4, IFN $\gamma$ , IL-12(p70), MCP-1, and GM-CSF. They also both induced the highest levels of T and B-cell expansion in response to antigen stimulation. When LMA was given as the first dose, a more balanced Th1, Th2 and Th17 response was seen. In addition to strong induction of Th1 associated cytokines: IL-2, IL-4, IFN $\gamma$ , and IL-12(p70), we also observed induction of Th2 associated cytokines: IL-10, IL-13, and IL-5 which were not observed when either Ad5-YFV was given as the first dose or in the Ad5-YFV 2-dose strategy. Only when LMA was given as the first dose did we see a strong IL-17 response. Based on these observations, it appears that whichever vaccine is given as the first dose helps shape the overall immune profile.

These studies were not able to cover every possible heterologous prime-boost combination or examine the effect of heterologous route administration of an Ad5-YFV only vaccination scheme. As discussed in the chapter 4 discussion, a push-pull vaccination method where the 1<sup>st</sup> dose is administered systemically followed by a intranasal booster dose may have advantages. Only one of the heterologous prime-pull groups, LMA(i.m.)—Ad5-YFV(i.n.) could be considered a push-pull vaccination method. This combination interestingly had the largest Th17 phenotype (Fig. 22 & 24) as well as having strong Th1

and Th2 markers (Fig. 24). For future studies, we would like to investigate this vaccination combination as well as the simultaneous vaccination of LMA(i.m.)+Ad5-YFV(i.n.). The simultaneous vaccination method is attractive in an outbreak response scenario where completing a full 2-dose vaccination scheme is not ideal and a quick onset of strong immunity is desired. In future studies we would like to investigate these 2 candidates further.

As mentioned in the Chapter 4 discussion, we would like to investigate the cross-protection conferred by our vaccines against different biovars of *Y. pestis*. LMA is based off *Y. pestis* CO92 which is from biovar orientalis. We have obtained challenge strain from other biovars antiqua and medievalis. While biovars are based off of biochemical characterization, showing cross protection against all biovars will give confidence that these vaccines can protect against future outbreak strains.

While we have investigated T-cell replication in response to antigen stimulation, we have not looked at memory T-cell phenotypes induced by immunization. All our studies so far have also been looking at immune cell derived from the spleen which is a measure of the systemic immune response. Investigating the local cell-mediated immune response in the lungs would be an important next step since pneumonic plague affects the lungs. The ultimate goal of this project is to test the most promising candidate in higher animal models such as non-human primates to prove efficacy before moving into clinical trials.

## References

1. Perry RD, Fetherston JD. 1997. *Yersinia pestis* -- Etiologic agent of plague. Clin Microbiol Rev 10:35–66.
2. Pechous RD, Sivaraman V, Stasulli NM, Goldman WE. 2016. Pneumonic Plague: The Darker Side of *Yersinia pestis*. Trends in Microbiology. Elsevier Ltd <https://doi.org/10.1016/j.tim.2015.11.008>.
3. Smiley ST. 2008. Current challenges in the development of vaccines for pneumonic plague. Expert Review of Vaccines.
4. Demeure CE, Dussurget O, Mas Fiol G, Le Guern AS, Savin C, Pizarro-Cerdá J. 2019. *Yersinia pestis* and plague: an updated view on evolution, virulence determinants, immune subversion, vaccination, and diagnostics. Genes and Immunity. Nature Publishing Group <https://doi.org/10.1038/s41435-019-0065-0>.
5. Kolodziejek AM, Hovde CJ, Minnich SA. 2022. Contributions of *Yersinia pestis* outer membrane protein Ail to plague pathogenesis. Current Opinion in Infectious Diseases 35:188–195.
6. Hotinger JA, May AE. 2020. Antibodies Inhibiting the Type III Secretion System of Gram-Negative Pathogenic Bacteria. Antibodies 9:35.
7. Pha K. 2016. *Yersinia* type III effectors perturb host innate immune responses . World Journal of Biological Chemistry 7:1.

8. Bland DM, Miarinjara A, Bosio CF, Calarco J, Hinnebusch BJ. 2021. Acquisition of yersinia murine toxin enabled *Yersinia pestis* to expand the range of mammalian hosts that sustain flea-borne plague. *PLoS Pathogens* 17.
9. Knight SD. 2007. Structure and assembly of *Yersinia pestis* F1 antigen, p. 74–87. *In Advances in Experimental Medicine and Biology*. Springer New York.
10. Sha J, Endsley JJ, Kirtley ML, Foltz SM, Huante MB, Erova TE, Kozlova E v, Popov VL, Yeager LA, Zudina I v, Motin VL, Peterson JW, DeBord KL, Chopra AK. 2011. Characterization of an F1 deletion mutant of *Yersinia pestis* CO92, pathogenic role of F1 antigen in bubonic and pneumonic plague, and evaluation of sensitivity and specificity of F1 antigen capture-based dipsticks. *J Clin Microbiol* 49:1708–15.
11. Meka-Mechenko T v. 2003. F1-negative natural *Y. pestis* Strains. *Advances in Experimental Medicine and Biology* 529:379–381.
12. Sebbane F, Uversky VN, Anisimov AP. 2020. *Yersinia pestis* plasminogen activator. *Biomolecules*. MDPI AG <https://doi.org/10.3390/biom10111554>.
13. van Lier CJ, Sha J, Kirtley ML, Cao A, Tiner BL, Erova TE, Cong Y, Kozlova E v., Popov VL, Baze WB, Chopra AK. 2014. Deletion of braun lipoprotein and plasminogen-activating protease-encoding genes attenuates *Yersinia pestis* in mouse models of bubonic and pneumonic plague. *Infection and Immunity* 82:2485–2503.
14. Vallès X, Stenseth NC, Demeure C, Horby P, Mead PS, Cabanillas O, Ratsitorahina M, Rajerison M, Andrianaivoarimanana V, Ramasindrazana B, Pizarro-Cerda J, Scholz HC, Girod R, Joseph Hinnebusch B, Vigan-Womas I,

- Fontanet A, Wagner DM, Telfer S, Yazdanpanah Y, Tortosa P, Carrara G, Deuve J, Belmain SR, D'ortenzio E, Baril L. 2020. Human plague: An old scourge that needs new answers. *PLoS Neglected Tropical Diseases* 14:1–22.
15. Barbieri R, Signoli M, Chevé D, Costedoat C, Tzortzis S, Aboudharam G, Raoult D, Drancourt M. 2021. *Yersinia pestis*: The natural history of Plague. *Clinical Microbiology Reviews*. American Society for Microbiology <https://doi.org/10.1128/CMR.00044-19>.
  16. He Z, Wei B, Zhang Y, Liu J, Xi J, Ciren D, Qi T, Liang J, Duan R, Qin S, Lv D, Chen Y, Xiao M, Fan R, Song Z, Jing H, Wang X. 2021. Distribution and characteristics of human plague cases and yersinia pestis isolates from 4 marmota plague foci, china, 1950-2019. *Emerging Infectious Diseases*. Centers for Disease Control and Prevention (CDC) <https://doi.org/10.3201/eid2710.202239>.
  17. Randremanana R, Andrianaivoarimanana V, Nikolay B, Ramasindrazana B, Paireau J, ten Bosch QA, Rakotondramanga JM, Rahajandraibe S, Rahelinirina S, Rakotomanana F, Rakotoarimanana FM, Randriamampionona LB, Razafimbiana V, de Dieu Randria MJ, Raberahona M, Mikaty G, le Guern AS, Rakotonjanabelo LA, Ndiaye CF, Rasolofo V, Bertherat E, Ratsitorahina M, Cauchemez S, Baril L, Spiegel A, Rajerison M. 2019. Epidemiological characteristics of an urban plague epidemic in Madagascar, August–November, 2017: an outbreak report. *The Lancet Infectious Diseases* 19:537–545.
  18. Nguyen VK, Parra-Rojas C, Hernandez-Vargas EA. 2018. The 2017 plague outbreak in Madagascar: Data descriptions and epidemic modelling. *Epidemics* <https://doi.org/10.1016/j.epidem.2018.05.001>.



19. Demeure C, Dussurget O, Fiol GM, le Guern AS, Savin C, Pizarro-Cerdá J. 2019. *Yersinia pestis* and plague: an updated view on evolution, virulence determinants, immune subversion, vaccination and diagnostics. *Microbes and Infection*. Elsevier Masson SAS <https://doi.org/10.1016/j.micinf.2019.06.007>.
20. Price PA, Jin J, Goldman WE. 2012. Pulmonary infection by *Yersinia pestis* rapidly establishes a permissive environment for microbial proliferation. *Proc Natl Acad Sci U S A* 109:3083–3088.
21. Pechous RD, Sivaraman V, Price PA, Stasulli NM, Goldman WE. 2013. Early Host Cell Targets of *Yersinia pestis* during Primary Pneumonic Plague. *PLoS Pathogens* 9.
22. Heitzinger K, Impouma B, Farham BL, Hamblion EL, Lukoya C, MacHingaidze C, Rakotonjanabelo LA, Yao M, Diallo B, Djingarey MH, Nsenga N, Ndiaye CF, Fall IS. 2019. Using evidence to inform response to the 2017 plague outbreak in Madagascar: A view from the WHO African Regional Office. *Epidemiology and Infection* 147.
23. Sebbane F, Lemaître N. 2021. Antibiotic therapy of plague: A review. *Biomolecules*. MDPI AG <https://doi.org/10.3390/biom11050724>.
24. Lei C, Kumar S. 2022. *Yersinia pestis* antibiotic resistance: a systematic review. *Osong Public Health and Research Perspectives*. Korea Centers for Disease Control and Prevention <https://doi.org/10.24171/j.phrp.2021.0288>.
25. Rosenzweig JA, Jejelowo O, Sha J, Erova TE, Brackman SM, Kirtley ML, van Lier CJ, Chopra AK. 2011. Progress on plague vaccine development. *Applied*

- Microbiology and Biotechnology. Springer <https://doi.org/10.1007/s00253-011-3380-6>.
26. Rosenzweig JA, Hendrix EK, Chopra AK. 2021. Plague vaccines: new developments in an ongoing search. *Applied Microbiology and Biotechnology*. Springer Science and Business Media Deutschland GmbH <https://doi.org/10.1007/s00253-021-11389-6>.
  27. Sun W, Curtiss R. 2014. Rational Considerations about Development of Live Attenuated *Yersinia pestis* Vaccines. *Current Pharmaceutical Biotechnology* 14:878–886.
  28. Quenee LE, Hermanas TM, Ciletti N, Louvel H, Miller NC, Elli D, Blaylock B, Mitchell A, Schroeder J, Krausz T, Kanabrocki J, Schneewind O. 2012. Hereditary hemochromatosis restores the virulence of plague vaccine strains. *Journal of Infectious Diseases* 206:1050–1058.
  29. Morris SR. 2007. Development of a recombinant vaccine against aerosolized plague. *Vaccine* 25:3115–3117.
  30. Fasciano AC, Shaban L, Meccas J. 2019. Promises and Challenges of the Type Three Secretion System Injectisome as an Antivirulence Target, p. 261–276. *In* Protein Secretion in Bacteria. American Society of Microbiology.
  31. Fellows P, Price J, Martin S, Metcalfe K, Krile R, Barnewall R, Hart MK, Lockman H. 2015. Characterization of a cynomolgus macaque model of pneumonic plague for evaluation of vaccine efficacy. *Clinical and Vaccine Immunology* 22:1070–1078.

32. Chu K, Hu J, Meng F, Li J, Luo L, Xu J, Yuan Z, Li Z, Chen W, Jiao L, Chang Y, Wang B, Hu Y. 2016. Immunogenicity and safety of subunit plague vaccine: A randomized phase 2a clinical trial. *Human Vaccines and Immunotherapeutics* 12:2334–2340.
33. Frey SE, Lottenbach K, Graham I, Anderson E, Bajwa K, May RC, Mizel SB, Graff A, Belshe RB. 2017. A phase I safety and immunogenicity dose escalation trial of plague vaccine, Flagellin/F1/V, in healthy adult volunteers (DMID 08-0066). *Vaccine* 35:6759–6765.
34. Tiner BL, Sha J, Kirtley ML, Erova TE, Popov VL, Baze WB, van Lier CJ, Ponnusamy D, Andersson JA, Motin VL, Chauhan S, Chopra AK. 2015. Combinational Deletion of Three Membrane Protein-Encoding Genes Highly Attenuates *Yersinia pestis* while Retaining Immunogenicity in a Mouse Model of Pneumonic Plague. *Infection and Immunity* 83:1318–1338.
35. Aliprantis AO, Yang RB, Mark MR, Suggett S, Devaux B, Radolf JD, Klimpel GR, Godowski P, Zychlinsky A. 1999. Cell activation and apoptosis by bacterial lipoproteins through Toll- like receptor-2. *Science* (1979) 285:736–739.
36. Sha J, Agar SL, Baze WB, Olano JP, Fadl AA, Erova TE, Wang S, Foltz SM, Suarez G, Motin VL, Chauhan S, Kumpel GR, Peterson JW, Chopra AK. 2008. Braun lipoprotein (Lpp) contributes to virulence of yersiniae: Potential role of Lpp in inducing bubonic and pneumonic plague. *Infection and Immunity* 76:1390–1409.

37. Rebeil R, Ernst RK, Jarrett CO, Adams KN, Miller SI, Hinnebusch BJ. 2006. Characterization of late acyltransferase genes of *Yersinia pestis* and their role in temperature-dependent lipid A variation. *Journal of Bacteriology* 188:1381–1388.
38. Sha J, Kirtley ML, van Lier CJ, Wang S, Erova TE, Kozlova E V., Cao A, Cong Y, Fitts EC, Rosenzweig JA, Chopra AK. 2013. Deletion of the braun lipoprotein-encoding gene and altering the function of lipopolysaccharide attenuate the plague bacterium. *Infection and Immunity* 81:815–828.
39. Bartra SS, Styer KL, O’Bryant DM, Nilles ML, Hinnebusch BJ, Aballay A, Plano G V. 2008. Resistance of *Yersinia pestis* to complement-dependent killing is mediated by the Ail outer membrane protein. *Infect Immun* 76:612–22.
40. Sha J, Kirtley ML, Klages C, Erova TE, Telepnev M, Ponnusamy D, Fitts EC, Baze WB, Sivasubramani SK, Lawrence WS, Patrikeev I, Peel JE, Andersson JA, Kozlova E V., Tiner BL, Peterson JW, McWilliams D, Patel S, Rothe E, Motin VL, Chopra AK. 2016. A Replication-Defective Human Type 5 Adenovirus-Based Trivalent Vaccine Confers Complete Protection against Plague in Mice and Nonhuman Primates. *Clinical and Vaccine Immunology* 23:586–600.
41. Kilgore PB, Sha J, Andersson JA, Motin VL, Chopra AK. 2021. A new generation needle- and adjuvant-free trivalent plague vaccine utilizing adenovirus-5 nanoparticle platform. *npj Vaccines* 6.
42. Tiner BL, Sha J, Ponnusamy D, Baze WB, Fitts EC, Popov VL, van Lier CJ, Erova TE, Chopra AK. 2015. Intramuscular Immunization of Mice with a Live-Attenuated Triple Mutant of *Yersinia pestis* CO92 Induces Robust Humoral and

Cell-Mediated Immunity To Completely Protect Animals against Pneumonic Plague. *Clinical and Vaccine Immunology* 22:1255–1268.

43. Tiner BL, Sha J, Cong Y, Kirtley ML, Andersson JA, Chopra AK. 2016. Immunisation of two rodent species with new live-attenuated mutants of *Yersinia pestis* CO92 induces protective long-term humoral- and cell-mediated immunity against pneumonic plague. *npj Vaccines* 1:16020.
44. Lin J-S, Kummer LW, Szaba FM, Smiley ST. 2011. IL-17 Contributes to Cell-Mediated Defense against Pulmonary *Yersinia pestis* Infection. *The Journal of Immunology* 186:1675–1684.
45. Cote CK, Biryukov SS, Klimko CP, Shoe JL, Hunter M, Rosario-Acevedo R, Fetterer DP, Moody KL, Meyer JR, Rill NO, Dankmeyer JL, Worsham PL, Bozue JA, Welkos SL. 2021. Protection elicited by attenuated live *Yersinia pestis* vaccine strains against lethal infection with virulent y. *Pestis. Vaccines (Basel)* 9:1–26.
46. Lee-Lewis H, Anderson DM. 2010. Absence of inflammation and pneumonia during infection with nonpigmented *Yersinia pestis* reveals a new role for the pgm locus in pathogenesis. *Infection and Immunity* 78:220–230.
47. Sha J, Agar SL, Baze WB, Olano JP, Fadl AA, Erova TE, Wang S, Foltz SM, Suarez G, Motin VL, Chauhan S, Kumpel GR, Peterson JW, Chopra AK. 2008. Braun lipoprotein (Lpp) contributes to virulence of yersiniae: Potential role of Lpp in inducing bubonic and pneumonic plague. *Infection and Immunity* 76:1390–1409.

48. Penit C. 1986. In vivo thymocyte maturation. BUdR labeling of cycling thymocytes and phenotypic analysis of their progeny support the single lineage model. *The Journal of Immunology* 137:2115–21.
49. Endl E, Steinbach P, Knüchel R, Hofstädter F. 1997. Analysis of cell cycle-related Ki-67 and p120 expression by flow cytometric BrdUrd-Hoechst/7AAD and immunolabeling technique. *Cytometry* 29:233–241.
50. 2018. W. H. O. Workshop. Efficacy trials of Plague vaccines: endpoints, trial design, site selection.
51. Boyer JL, Sofer-Podesta C, Ang J, Hackett NR, Chiuchiolo MJ, Senina S, Perlin D, Crystal RG. 2010. Protective immunity against a lethal respiratory *Yersinia pestis* challenge induced by V antigen or the F1 capsular antigen incorporated into adenovirus capsid. *Hum Gene Ther* 21:891–901.
52. Teigler JE, Iampietro MJ, Barouch DH. 2012. Vaccination with Adenovirus Serotypes 35, 26, and 48 Elicits Higher Levels of Innate Cytokine Responses than Adenovirus Serotype 5 in Rhesus Monkeys. *Journal of Virology* 86:9590–9598.
53. Hu J, Jiao L, Hu Y, Chu K, Li J, Zhu F, Li T, Wu Z, Wei D, Meng F, Wang B. 2018. One year immunogenicity and safety of subunit plague vaccine in Chinese healthy adults: An extended open-label study. *Human Vaccines & Immunotherapeutics* 14:1–5.
54. Heath DG, Anderson GW, Mauro JM, Welkos SL, Andrews GP, Adamovicz J, Friedlander AM. 1998. Protection against experimental bubonic and pneumonic plague by a recombinant capsular F1-V antigen fusion protein vaccine. *Vaccine* 16:1131–1137.

55. Williamson ED, Packer PJ, Waters EL, Simpson AJ, Dyer D, Hartings J, Twenhafel N, Pitt MLM. 2011. Recombinant (F1 + V) vaccine protects cynomolgus macaques against pneumonic plague. *Vaccine* 29:4771–4777.
56. Du Y, Rosqvist R, Forsberg Å. 2002. Role of fraction 1 antigen of *Yersinia pestis* in inhibition of phagocytosis. *Infection and Immunity* 70:1453–1460.
57. Daniel C, Dewitte A, Poiret S, Marceau M, Simonet M, Marceau L, Descombes G, Boutillier D, Bennaceur N, Bontemps-Gallo S, Lemaître N, Sebbane F. 2019. Polymorphism in the yersinia LcrV antigen enables immune escape from the protection conferred by an LcrV-secreting lactococcus lactis in a pseudotuberculosis mouse model. *Frontiers in Immunology* 10.
58. Demeure CE, Derbise A, Carniel E. 2017. Oral vaccination against plague using *Yersinia pseudotuberculosis*. *Chemico-Biological Interactions* 267:89–95.
59. Matson JS, Durick KA, Bradley DS, Nilles ML. 2005. Immunization of mice with YscF provides protection from *Yersinia pestis* infections. *BMC Microbiology* 5:38.
60. Swietnicki W, Powell BS, Goodin J. 2005. *Yersinia pestis* Yop secretion protein F: Purification, characterization, and protective efficacy against bubonic plague. *Protein Expression and Purification* 42:166–172.
61. Singh AK, Curtiss R, Sun W. 2019. A recombinant attenuated *Yersinia pseudotuberculosis* vaccine delivering a Y. Pestis YopENT138-LcrV fusion elicits broad protection against plague and yersiniosis in mice. *Infection and Immunity* 87.

62. Gregg KA, Harberts E, Gardner FM, Pelletier MR, Cayatte C, Yu L, McCarthy MP, Marshall JD, Ernst RK. 2018. A lipid A-based TLR4 mimetic effectively adjuvants a *Yersinia pestis* rF-V1 subunit vaccine in a murine challenge model. *Vaccine* 36:4023–4031.
63. Dinc G, Pennington JM, Yolcu ES, Lawrenz MB, Shirwan H. 2014. Improving the Th1 cellular efficacy of the lead *Yersinia pestis* rF1-V subunit vaccine using SA-4-1BBL as a novel adjuvant. *Vaccine* 32:5035–5040.
64. Abbas AK, Murphy KM, Sher A. 1996. Functional diversity of helper T lymphocytes. *Nature*. <https://doi.org/10.1038/383787a0>.
65. Rostamian M, Sohrabi S, Kavosifard H, Niknam HM. 2017. Lower levels of IgG1 in comparison with IgG2a are associated with protective immunity against *Leishmania tropica* infection in BALB/c mice. *Journal of Microbiology, Immunology and Infection* 50:160–166.
66. Zhang Y, Dominguez-Medina C, Cumley NJ, Heath JN, Essex SJ, Bobat S, Schager A, Goodall M, Kracker S, Buckley CD, May RC, Kingsley RA, MacLennan CA, López-Macías C, Cunningham AF, Toellner K-M. 2017. IgG1 Is Required for Optimal Protection after Immunization with the Purified Porin OmpD from *Salmonella* Typhimurium . *The Journal of Immunology* 199:4103–4109.
67. Bowen W, Batra L, Pulsifer AR, Yolcu ES, Lawrenz MB, Shirwan H. 2019. Robust Th1 cellular and humoral responses generated by the *Yersinia pestis* rF1-V subunit vaccine formulated to contain an agonist of the CD137 pathway do not translate into increased protection against pneumonic plague. *Vaccine* 37:5708–5716.



68. Dutta S, Sengupta P. 2016. Men and mice: Relating their ages. *Life Sciences*. Elsevier Inc. <https://doi.org/10.1016/j.lfs.2015.10.025>.
69. Anderson GW, Heath DG, Bolt CR, Welkos SL, Friedlander AM. 1998. Short- and long-term efficacy of single-dose sub unit vaccines against *Yersinia pestis* in mice. *American Journal of Tropical Medicine and Hygiene* 58:793–799.
70. Wang Z, Zhou L, Qi Z, Zhang Q, Dai R, Yang Y, Cui B, Wang H, Yang R, Wang X. 2010. Long-term observation of subunit vaccine F1-rV270 against *Yersinia pestis* in mice. *Clinical and Vaccine Immunology* 17:199–201.
71. Prame Kumar K, Nicholls AJ, Wong CHY. 2018. Partners in crime: neutrophils and monocytes/macrophages in inflammation and disease. *Cell and Tissue Research*. Springer Verlag <https://doi.org/10.1007/s00441-017-2753-2>.
72. Comer JE, Sturdevant DE, Carmody AB, Virtaneva K, Gardner D, Long D, Rosenke R, Porcella SF, Hinnebusch BJ. 2010. Transcriptomic and innate immune responses to *Yersinia pestis* in the lymph node during bubonic plague. *Infection and Immunity* 78:5086–5098.
73. Patterson BK, Seethamraju H, Dhody K, Corley MJ, Kazempour K, Lalezari JP, Pang AP, Sugai C, Francisco EB, Pise A, Rodrigues H, Ryou M, Wu HL, Webb GM, Park BS, Kelly S, Pourhassan N, Lelic A, Kdouh L, Herrera M, Hall E, Aklin E, Ndhlovu L, Sacha JB. 2020. Disruption of the CCL5/RANTES-CCR5 Pathway Restores Immune Homeostasis and Reduces Plasma Viral Load in Critical COVID-19. medRxiv 2020.05.02.20084673.

74. Stasulli NM, Eichelberger KR, Price PA, Pechous RD, Montgomery SA, Parker JS, Goldman WE. 2015. Spatially distinct neutrophil responses within the inflammatory lesions of pneumonic plague. *mBio* 6.
75. Gschwandtner M, Derler R, Midwood KS. 2019. More Than Just Attractive: How CCL2 Influences Myeloid Cell Behavior Beyond Chemotaxis. *Frontiers in Immunology*. Frontiers Media S.A. <https://doi.org/10.3389/fimmu.2019.02759>.
76. Bystry RS, Aluvihare V, Welch KA, Kallikourdis M, Betz AG. 2001. B cells and professional APCs recruit regulatory T cells via CCL4. *Nature Immunology* 2:1126–1132.
77. Bhattacharya P, Budnick I, Singh M, Thirupathi M, Alharshawi K, Elshabrawy H, Holterman MJ, Prabhakar BS. 2015. Dual Role of GM-CSF as a Pro-Inflammatory and a Regulatory Cytokine: Implications for Immune Therapy. *Journal of Interferon and Cytokine Research*. Mary Ann Liebert Inc. <https://doi.org/10.1089/jir.2014.0149>.
78. Steinman RM, Hawiger D, Nussenzweig MC. 2003. Tolerogenic dendritic cells. *Annual Review of Immunology* 21:685–711.
79. Demeure CE, Derbise A, Guillas C, Gerke C, Cauchemez S, Carniel E, Pizarro-Cerdá J. 2019. Humoral and cellular immune correlates of protection against bubonic plague by a live *Yersinia pseudotuberculosis* vaccine. *Vaccine* 37:123–129.
80. Danziger-Isakov L, Kumar D. 2019. Vaccination of solid organ transplant candidates and recipients: Guidelines from the American society of transplantation infectious diseases community of practice. *Clinical Transplantation* 33.

81. Pliaka V, Kyriakopoulou Z, Markoulatos P. 2012. Risks associated with the use of live-attenuated vaccine poliovirus strains and the strategies for control and eradication of paralytic poliomyelitis. *Expert Review of Vaccines* 11:609–628.
82. Zhou B, Meliopoulos VA, Wang W, Lin X, Stucker KM, Halpin RA, Stockwell TB, Schultz-Cherry S, Wentworth DE. 2016. Reversion of Cold-Adapted Live Attenuated Influenza Vaccine into a Pathogenic Virus. *Journal of Virology* 90:8454–8463.
83. Rocha B, Penit C, Baron C, Vasseur F, Dautigny N, Freitas AA. 1990. Accumulation of bromodeoxyuridine-labeled cells in central and peripheral lymphoid organs: minimal estimates of production and turnover rates of mature lymphocytes. *European Journal of Immunology* 20:1697–1708.
84. Arlen PA, Singleton M, Adamovicz JJ, Ding Y, Davoodi-Semiromi A, Daniell H. 2008. Effective plague vaccination via oral delivery of plant cells expressing F1-V antigens in chloroplasts. *Infection and Immunity* 76:3640–3650.
85. Mombaerts P, Iacomini J, Johnson RS, Herrup K, Tonegawa S, Papaioannou VE. 1992. RAG-1-deficient mice have no mature B and T lymphocytes. *Cell* 68:869–877.
86. Amaya-Uribe L, Rojas M, Azizi G, Anaya JM, Gershwin ME. 2019. Primary immunodeficiency and autoimmunity: A comprehensive review. *Journal of Autoimmunity* 99:52–72.
87. Delmonte OM, Schuetz C, Notarangelo LD. 2018. RAG Deficiency: Two Genes, Many Diseases. *Journal of Clinical Immunology* 38:646–655.

88. Tchilian EZ, Ronan EO, de Lara C, Lee LN, Franken KLMC, Vordermeier MH, Ottenhoff THM, Beverley PCL. 2011. Simultaneous Immunization against Tuberculosis. *PLoS ONE* 6:e27477.
89. Palgen J-L, Feraoun Y, Dzangué-Tchoupou G, Joly C, Martinon F, Le Grand R, Beignon A-S. 2021. Optimize Prime/Boost Vaccine Strategies: Trained Immunity as a New Player in the Game. *Frontiers in Immunology* 12:554.
90. Hillus D, Schwarz T, Tober-Lau P, Vanshylla K, Hastor H, Thibeault C, Jentzsch S, Helbig ET, Lippert LJ, Tscheak P, Schmidt ML, Riege J, Solarek A, von Kalle C, Dang-Heine C, Gruell H, Kopankiewicz P, Suttorp N, Drosten C, Bias H, Seybold J, Klein F, Kurth F, Corman VM, Sander LE, Al-Rim B, Bardtke L, Beheim-Schwarzbach JI, Behn K, Bergfeld L, Bethke N, Bleicker T, Briesemeister D, Brumhard S, Conrad C, Dieckmann S, Frey D, Gabelich J-A, Georg P, Gläser U, Hasler L, Hetey A, Hiller AL, Horn A, Hülso C, Kegel L, Koch W, Krannich A, Kroneberg P, Lisy M, Mackeldanz P, Maeß B, Münn F, Olk N, Peiser C, Pohl K, Hermel A, Rönnefarth M, Rubisch C, Sanchez Rezza A, Schellenberger I, Schenkel V, Schlesinger J, Schmidt S, Schwanitz G, Sinnigen A-S, Stubbemann P, Tesch J, Treue D, Wendisch D, Zvorc S. 2021. Safety, reactogenicity, and immunogenicity of homologous and heterologous prime-boost immunisation with ChAdOx1 nCoV-19 and BNT162b2: a prospective cohort study. *The Lancet Respiratory Medicine* [https://doi.org/10.1016/S2213-2600\(21\)00357-X](https://doi.org/10.1016/S2213-2600(21)00357-X).
91. Shaw RH, Stuart A, Greenland M, Liu X, Van-Tam JSN, Snape MD. 2021. Heterologous prime-boost COVID-19 vaccination: initial reactogenicity data. *The Lancet* 397:2043–2046.

92. Logunov DY, Dolzhikova I V., Zubkova O V., Tukhvatullin AI, Shcheblyakov D V., Dzharellaeva AS, Grousova DM, Erokhova AS, Kovyrshina A V., Botikov AG, Izhaeva FM, Popova O, Ozharovskaya TA, Esmagambetov IB, Favorskaya IA, Zrelkin DI, Voronina D V., Shcherbinin DN, Semikhin AS, Simakova Y V., Tokarskaya EA, Lubenets NL, Egorova DA, Shmarov MM, Nikitenko NA, Morozova LF, Smolyarchuk EA, Kryukov E V., Babira VF, Borisevich S V., Naroditsky BS, Gintsburg AL. 2020. Safety and immunogenicity of an rAd26 and rAd5 vector-based heterologous prime-boost COVID-19 vaccine in two formulations: two open, non-randomised phase 1/2 studies from Russia. *The Lancet* 396:887–897.
93. Logunov DY, Dolzhikova I V., Shcheblyakov D V., Tukhvatulin AI, Zubkova O V., Dzharellaeva AS, Kovyrshina A V., Lubenets NL, Grousova DM, Erokhova AS, Botikov AG, Izhaeva FM, Popova O, Ozharovskaya TA, Esmagambetov IB, Favorskaya IA, Zrelkin DI, Voronina D V., Shcherbinin DN, Semikhin AS, Simakova Y V., Tokarskaya EA, Egorova DA, Shmarov MM, Nikitenko NA, Gushchin VA, Smolyarchuk EA, Zyryanov SK, Borisevich S V., Naroditsky BS, Gintsburg AL. 2021. Safety and efficacy of an rAd26 and rAd5 vector-based heterologous prime-boost COVID-19 vaccine: an interim analysis of a randomised controlled phase 3 trial in Russia. *The Lancet* 397:671–681.
94. Zhang J, He Q, An C, Mao Q, Gao F, Bian L, Wu X, Wang Q, Song L, Liu P, Huo Y, Yan X, Yang J, Cui B, Liu S, Li C, Wang J, Liang Z, Xu M. 2021. Boosting with heterologous vaccines effectively improves protective immune responses of the inactivated SARS-CoV-2 vaccine. *Emerging Microbes & Infections* 1–28.

95. Barros-Martins J, Hammerschmidt SI, Cossmann A, Odak I, Stankov M V., Morillas Ramos G, Dopfer-Jablonka A, Heidemann A, Ritter C, Friedrichsen M, Schultze-Florey C, Ravens I, Willenzon S, Bubke A, Ristenpart J, Janssen A, Ssebyatika G, Bernhardt G, Münch J, Hoffmann M, Pöhlmann S, Krey T, Bošnjak B, Förster R, Behrens GMN. 2021. Immune responses against SARS-CoV-2 variants after heterologous and homologous ChAdOx1 nCoV-19/BNT162b2 vaccination. *Nature Medicine* <https://doi.org/10.1038/s41591-021-01449-9>.
96. Tregoning JS, Buffa V, Oszmiana A, Klein K, Walters AA, Shattock RJ. 2013. A “prime-pull” vaccine strategy has a modest effect on local and systemic antibody responses to HIV gp140 in mice. *PLoS ONE* 8.
97. Çuburu N, Kim R, Guittard GC, Thompson CD, Day PM, Hamm DE, Pang Y-YS, Graham BS, Lowy DR, Schiller JT. 2019. A Prime-Pull-Amplify Vaccination Strategy To Maximize Induction of Circulating and Genital-Resident Intraepithelial CD8 + Memory T Cells . *The Journal of Immunology* 202:1250–1264.
98. He Q, Jiang L, Cao K, Zhang L, Xie X, Zhang S, Ding X, He Y, Zhang M, Qiu T, Jin X, Zhao C, Zhang X, Xu J. 2020. A Systemic Prime–Intrarectal Pull Strategy Raises Rectum-Resident CD8+ T Cells for Effective Protection in a Murine Model of LM-OVA Infection. *Frontiers in Immunology* 11.
99. Shin H, Iwasaki A. 2012. A vaccine strategy that protects against genital herpes by establishing local memory T cells. *Nature* 491:463–467.
100. Schenkel JM, Masopust D. 2014. Tissue-resident memory T cells. *Immunity* 41:886–897.

101. Martini V, Paudyal B, Chrun T, McNee A, Edmans M, Atangana Maze E, Clark B, Nunez A, Dolton G, Sewell A, Beverley P, MacLoughlin R, Townsend A, Tchilian E. 2021. Simultaneous Aerosol and Intramuscular Immunization with Influenza Vaccine Induces Powerful Protective Local T Cell and Systemic Antibody Immune Responses in Pigs. *The Journal of Immunology* 206:652–663.

## Vita

Paul Blanton Kilgore was born March 2, 1992, in Dallas, Texas to David and Margaret Kilgore. He attended Trinity Christian Academy in Addison, Texas for high school. He earned a Bachelor of Science in Microbiology from the University of Georgia in Athens, Georgia. He returned to Texas to pursue a PhD in microbiology and immunology from the Department of Microbiology and Immunology from the University of Texas Medical Branch in Galveston, Texas. He has published in a variety of journals that cover topics related to microbiology and immunology including: *Npj Vaccines*, *mBio*, *Science Advances*, *PNAS*, *MSphere*, *PLoS One*, and *Journal of Bacteriology*.

## Publications

Zhu, J., Jain, S., Sha, J., Batra, H., Ananthaswamy, N., **Kilgore, P. B.**, Hendrix, E. K., Hosakote, Y. M., Wu, X., Olano, J. P., Kayode, A., Galindo, C. L., Banga, S., Drelich, A., Tat, V., Tseng, C.-T. K., Chopra, A. K., & Rao, V. B. (2022). A bacteriophage-based, highly efficacious, needle and adjuvant-free, mucosal COVID-19 vaccine. *Mbio*. e0182222. doi: 10.1128/mbio.01822-22.

**Kilgore, P. B.**, Sha, J., Andersson, J. A., Motin, V. L., & Chopra, A. K. (2021). A new generation needle- and adjuvant-free trivalent plague vaccine utilizing adenovirus-5 nanoparticle platform. *Npj Vaccines*, 6(1). <https://doi.org/10.1038/s41541-020-00275-3>

**Kilgore, P. B.**, Sha, J., Hendrix, E. K., Motin, V. L., & Chopra, A. K. (2021). Combinatorial Viral Vector-Based and Live Attenuated Vaccines without an Adjuvant to Generate Broader Immune Responses to Effectively Combat Pneumonic Plague. *MBio*, 12(6). <https://doi.org/10.1128/mBio.03223-21>

Zhu, J., Ananthaswamy, N., Jain, S., Batra, H., Tang, W. C., Lewry, D. A., Richards, M. L., David, S. A., **Kilgore, P. B.**, Sha, J., Drelich, A., Tseng, C. T. K., Chopra, A. K., & Rao, V. B. (2021). A universal bacteriophage T4 nanoparticle platform to design multiplex SARS-CoV-2 vaccine candidates by CRISPR engineering. *Science Advances*, 7(37). <https://doi.org/10.1126/sciadv.abh1547>

Zhu, J., Tao, P., Mahalingam, M., Sha, J., **Kilgore, P.**, Chopra, A. K., & Rao, V. (2019). A prokaryotic-eukaryotic hybrid viral vector for delivery of large cargos of genes and proteins into human cells. *Science Advances*, 5(8). <https://doi.org/10.1126/sciadv.aax0064>



Fernández-Bravo, A., **Kilgore, P. B.**, Andersson, J. A., Blears, E., Figueras, M. J., Hasan, N. A., Colwell, R. R., Sha, J., & Chopra, A. K. (2019). T6SS and ExoA of flesh-eating *Aeromonas hydrophila* in peritonitis and necrotizing fasciitis during mono- And polymicrobial infections. *Proceedings of the National Academy of Sciences of the United States of America*, *116*(48), 24084–24092. <https://doi.org/10.1073/pnas.1914395116>

Khakhum, N., Bharaj, P., Myers, J. N., Tapia, D., **Kilgore, P. B.**, Ross, B. N., Walker, D. H., Endsley, J. J., & Torres, A. G. (2019). *Burkholderia pseudomallei*  $\Delta$  tonB  $\Delta$  hcp1 Live Attenuated Vaccine Strain Elicits Full Protective Immunity against Aerosolized Melioidosis Infection . *MSphere*, *4*(1). <https://doi.org/10.1128/msphere.00570-18>

Lewis, E. R. G., **Kilgore, P. B.**, Mott, T. M., Pradenas, G. A., & Torres, A. G. (2017). Comparing in vitro and in vivo virulence phenotypes of *Burkholderia pseudomallei* type G strains. *PLoS ONE*, *12*(4). <https://doi.org/10.1371/journal.pone.0175983>

Miller, K. A., Phillips, R. S., **Kilgore, P. B.**, Smith, G. L., & Hoover, T. R. (2015). A Mannose Family Phosphotransferase System Permease and Associated Enzymes Are Required for Utilization of Fructoselysine and Glucoselysine in *Salmonella enterica* Serovar Typhimurium. *Journal of Bacteriology*, *197*(17), 2831–2839. <https://doi.org/10.1128/JB.00339-15>

Permanent address: 1811 32<sup>nd</sup> Street Apt Up Galveston, Texas 77550

This dissertation was typed by Paul Kilgore